Deltares

Enabling Delta Life

Modelling the 1775 storm surge deposits at the Heemskerk dunes

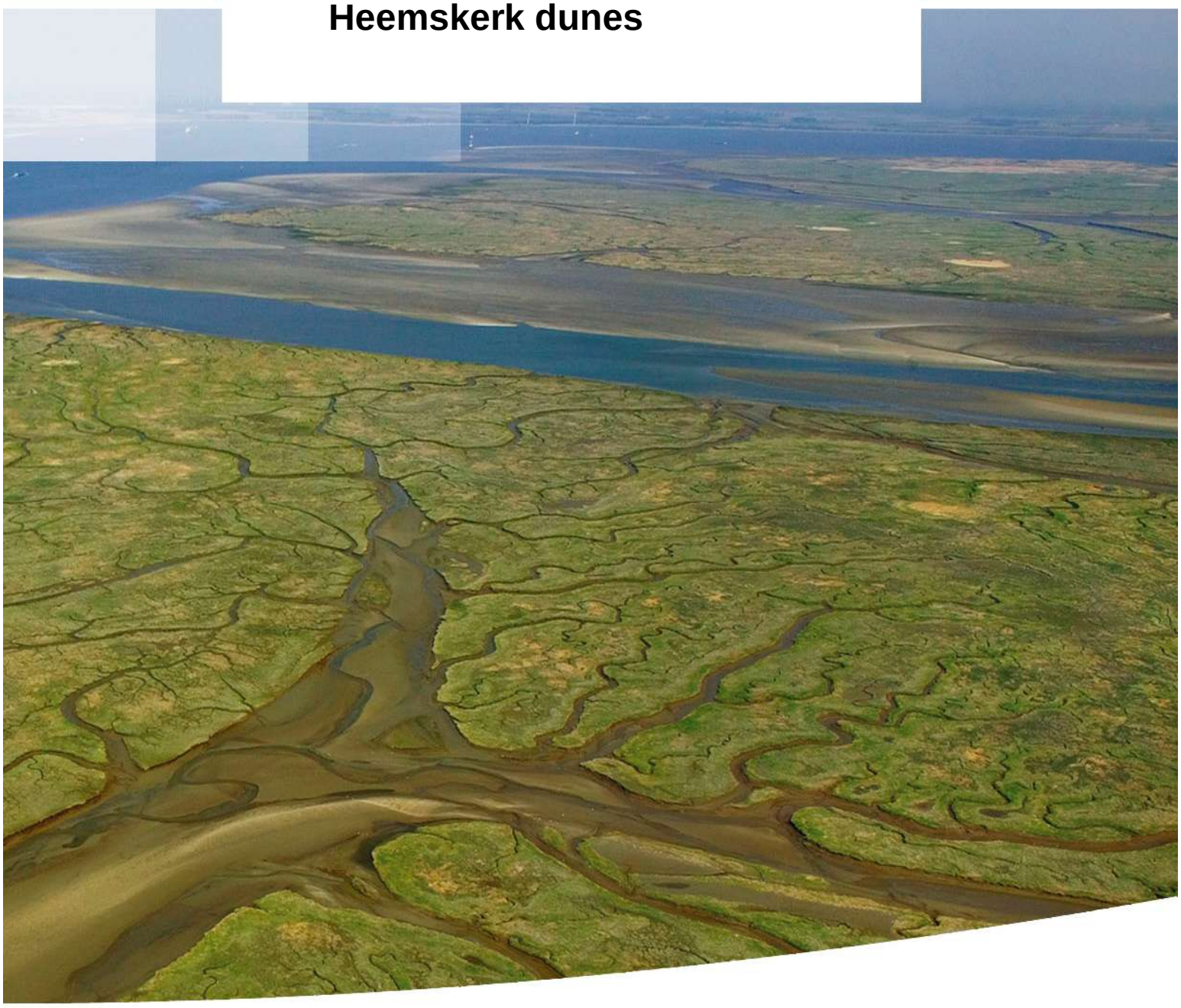

Deltares

Modelling the 1775 storm surge deposits at the Heemskerk dunes

A.D. Pool

MSc Thesis

September 2009

Supervisors:
Prof.dr.ir. M.J.F. Stive
Dr.ir. A.P. van Dongeren
Dr. S. van Heteren
Dr.ir. P.H.A.J.M. van Gelder
Dr. J.E.A. Storms

Deltares

Title
Modelling the 1775 storm surge deposits at the Heemskerk dunes

Client	Project	Pages
TU Delft	1200306-000	104

Keywords
storm surge, deposits, historical storm, 1775, dunes, dune overwash, dune breaching, dune erosion, process-based modelling, XBeach, statistics, probabilistic modelling

Summary
After a storm surge in November 2007, older storm surge deposits were discovered in the eroded dunes near Heemskerk, the Netherlands. These deposits undulate in height with a maximum elevation of over 6 m above mean sea level. Luminescence dating suggests that the layers were deposited by either the 1775 or the 1776 storm surge.
The aim of this thesis is to model the 1775 storm surge and its capability to reach the height of NAP + 6.5 m at which the deposits have been discovered. Secondary objectives are (a) to give an estimation of the probability of exceedance of the 1775 storm surge and (b) to compare the effects of this storm surge on a open dune front (historical situation) and a closed dune front (present situation).
A modelling framework has been set up to transform the available historical data into boundary conditions for the process-based model XBeach. A 1D probabilistic approach resulted in distributions for the 2% exceedance height for the storm surge level including set-up and wave run-up for six characteristic profiles. The distributions do not give reason to reject the hypothesis that, during the 1775 storm surge, the water level has reached the level of NAP + 6.5 m.
Based on the existing exceedance line for IJmuiden, the probability of exceedance of the 1775 storm surge is estimated to be $3*10^{-4}$. This is close to the existing Dutch design criteria for primary sea defences.
A comparison of several 2DH simulations with a historical dune topography containing an open dune front and the same boundary conditions with a present dune topography containing a closed dune front, give the following results:

- With the open dune front, storm surges can easily enter the dune valleys behind the first dune row, but the water is almost always stopped by the second dune row. Wave energy dissipates quickly in the dune area.
- The present situation with a closed dune front gives high erosion rates along the entire dune front, while the historical situation with an open dune front gives more variation in erosion and deposition rates. Erosion rates are generally higher in the present situation with the closed dune front.

References

Version	Date	Author	Initials	Review	Initials	Approval	Initials
1.0	2009-09-01	A.D. Pool		A. van Dongeren		T. Schilperoort	

State
final

Preface

This thesis concludes the Master of Science program at the Faculty of Civil Engineering and Geosciences at Delft University of Technology, The Netherlands. The thesis was carried out at Deltares in Delft. It is a good example of a multidisciplinary approach, which combines the fields of sedimentology, hydraulic engineering and historical research, a topic which has my interest already for a long time. The field of sedimentology was new for me, but I really enjoyed the introduction into it.

I want to thank my graduation committee for the opportunity to work with them, their support and the interesting discussions we had during the meetings. I thank prof. Marcel Stive for chairing the committee and encouraging me to start this thesis study, Ap van Dongeren for helping me with XBeach and give quick and critical feedback on my report. I thank Sytze van Heteren for his continuous efforts to explain the basics on sedimentology to me, Pieter van Gelder for his aid on the sometimes difficult probabilistic subjects and finally Joep Storms for his feedback from a geology viewpoint.

I really enjoyed working at Deltares and would like to thank all my temporary colleagues who helped me out with my questions and problems. Special thanks go out to Robert for his help on XBeach and Matlab, Gerben for his Matlab knowledge and his positive look at thinks and Kees and Fedor for their help and discussions on probabilistic and statistics. Graduating at Deltares would not have been the same without my fellow graduates: John, Johan, Renske, Marten, Claire, Anna, Thijs, Carola, Steven, Lars, Roald, Wouter, Chris, Sepehr, Evangelos, Reynald, Reinout, Pieter, Joas, Maurits and Roderik. I enjoyed the lunches, the walks, the discussions and Pancake Friday with you.

Special thanks go to my family who supported me my entire study. Most of all I want to thank Andrea for her interest, enthusiasm, encouragement and patience.

Arend Pool

Delft, September 2009

Summary

After a storm surge hit the Dutch coast at November 9, 2007, old deposits were discovered in the eroded dunes near Heemskerk, the Netherlands. These deposits consisted of one or two layers of convoluted sand and shells with occasional pieces of brick and coal. The sediment layers are 10 – 20 cm thick, and undulate in height over a distance of several hundred metres with a maximum elevation of over 6 m above mean sea level. The deposits have been recognized as evidence of one or two historical storm surges. Luminescence dating placed the storm surge layers at the end of the 18th century. From historical records, it is known that major storm surges occurred in 1775 and 1776; most likely one or both of these events are responsible for the deposition of the layers.

The aim of this thesis is to model the 1775 storm surge and its capability to reach the maximum height at which the deposits have been discovered. The modelling has been done with the numerical program XBeach, using a probabilistic approach and historical data as input. Secondary objectives are (a) to give an estimation of the probability of exceedance of the 1775 storm surge and (b) to compare the effects of this storm surge on a open dune front (historical situation) and a closed dune front (present situation).

Research into available historical data lead to three sources of useful data for this study:

- Wind force estimations at Huize Swanenburgh, 20 km south of the Heemskerk area. These observations were made three times per day; the maximum value during the 1775 storm is used as input data.
- Maximum storm surge water level recorded at Petten, 25 km north of the Heemskerk area. This value is used to compare the computed water levels with.
- Grain diameters, based on a sieve analysis of sand in the storm surge layers. The grain diameters are used as direct input to the numerical model.

A flexible modelling framework has been set-up to transform the historical data, supplemented with estimated values for missing data, into boundary and initial conditions for XBeach. XBeach is a process-based nearshore numerical model that is capable of modelling the natural coastal response during time-varying storm and hurricane conditions. This includes dune erosion, overwash and breaching.

As no historical bathymetry and topography are available, present data is used to construct a historical bathymetry/topography without the human-maintained closed dune front (‘sand dike’). Low-lying gaps in the dune front have been made to resemble the low-lying entrances presumably present in the 18th century dune front.

A probabilistic approach is used to generate 200 boundary conditions for a Monte Carlo simulation with six 1D profiles based on the constructed topography. Each simulation resulted in a $Z_{2\%}$ value, a height above NAP that is exceeded by 2% of the wave run-up peaks. For each of the six profiles the probability that $Z_{2\%}$ reached [6.0, 7.0] is calculated (NAP + 6.5 m with a margin of 0.5 m). The probabilities for all six profiles varied between 2% and 11%. These values are high enough to accept the hypothesis that the run-up levels reached the observed value of NAP + 6.5 m, based on the recorded historical data.

Based on the maximum input water levels that lead to a $Z_{2\%}$ of [6.0, 7.0] and the exceedance line for IJmuiden, the probability of exceedance of the 1775 storm surge is estimated to be $3*10^{-4}$. This is close to the Dutch design criterion for primary flood defences.

A number of 2DH simulations with both a historical topography (open dune front) and a present topography (closed dune front) have been carried out to compare the results of a storm on a natural dune system and on an artificial system with a sand dike ('zeereep'). The most obvious difference is of course the possibility with a natural dune system that the surge can enter the dune area behind the first dunes through low-lying areas/gaps. However, the fact that the surge can easily enter the dunes does not make it an unsafe situation. Energy is quickly dissipated and the water is almost always stopped by the second dune row (only in one extreme situation a larger area got flooded).

It is observed that the natural dune system experiences less erosion than the system with the human-maintained sand dike. Possible causes are gentler slopes of the natural dunes, such that less avalanching takes place and the possibility for the surge to enter the area between the dunes and bringing sediment into the dune system instead of removing sediment from it. A second effect of the low-lying areas is that the wave energy is dissipated over a larger area instead of only at the beach and the first dune row.

The model developed in this study could be improved by using air pressure data to generate wind fields instead of wind observations. The XBeach model could be improved by modelling the effects of vegetation and the infiltration of water in dry sand. A case study at 'De Kerf' in North Holland with high-resolution pre- and post-storm data could be used to validate the numerical model.

Contents

Preface i

Summary iii

List of Tables ix

List of Figures xi

List of Photographs xv

List of Symbols xvii

1 Introduction 1
1.1 Background 1
1.2 Evidence of historical storms 2
1.3 Determining age storm surge layers 5
1.4 Implications 6
1.5 Problem statement 7
1.6 Objectives 7
1.7 Methodology 7
1.8 Reader's guide 8

2 Literature study 9
2.1 The 1775 & 1776 storms 9
2.2 Other evidence of historical storm surge heights 10
2.3 Available historical data 11
2.3.1 Wind and air pressure 11
2.3.2 Surge level 13
2.4 Bathymetry & topography 14
2.4.1 Bathymetry 14
2.4.2 Topography 15

3 Model inputs 17
3.1 Available data and modelling method 17
3.2 From observed wind to potential wind over sea 19
3.2.1 Method 19
3.2.2 Potential wind 19
3.2.3 From observed wind to meso wind 19
3.2.4 From meso wind to potential wind over sea 22
3.3 From potential wind over sea to wave characteristics 23
3.4 From potential wind over sea to maximum wind setup 25
3.5 Astronomical tide 27
3.6 Storm surge duration and shape 28
3.7 Grain diameter 29
3.8 Bathymetry & cross-shore profiles 30
3.9 Monte Carlo simulation 34
3.10 Samples Monte Carlo simulation 35

3.11 Summary 38

4 XBeach 39
4.1 XBeach model description 39
4.1.1 Model functionality and numerical implementation 39
4.1.2 Coordinate system and grid 40
4.1.3 Boundary conditions 41
4.2 Test case: November 2007 storm surge 41
4.2.1 Bathymetry and topography 42
4.2.2 Water level 43
4.2.3 Wave conditions 44
4.2.4 Numerical parameters 45
4.2.5 Results 46

5 Results simulations 1775 storm 51
5.1 1D simulations 51
5.1.1 Histograms and distributions 51
5.1.2 Probability of exceedance 54
5.1.3 Regression analysis 56
5.1.4 Relation with the Irribarren number 62
5.2 2DH simulations 64
5.2.1 1775 topography 65
5.2.2 2007 topography 70
5.3 Conclusions 73
5.4 Discussion 74

6 Conclusions and recommendations 75
6.1 Conclusions 75
6.2 Recommendations 76
6.3 Closure 77

7 Literature 79

Glossary 83

Appendices

A XBeach parameter settings 85
A.1 Calibration run: November 2007storm surge (1D / 2D) 85
A.2 November 1775 storm surge (1D/2D runs) 86

B BestFit results 89
B.1 Profile 1 89
B.2 Profile 2 89
B.3 Profile 3 90
B.4 Profile 4 90
B.5 Profile 5 90
B.6 Profile 6 90

C Running XBeach on Deltares cluster 91

C.1 Compiling XBeach executable 91
C.2 Run XBeach parallel version on the cluster 91

List of Tables

Table 2.1 Overview of all floods between 1500 and 1850 as classified by Van Gelder (1996). Class A is for very severe floods, down to class D for light floods (table modified by author). 9
Table 2.2 Noppen's Wind Mill scale (Geurts and Van Engelen, 1992). Transformation from Beaufort to m/s from Wieringa and Rijkoort (1983). 12
Table 2.3 Estimated wind force during the November storms of 1775 and 1776; recorded at Huize Swanenburgh. Observation times are approximate (KNMI, 2008). 13
Table 3.1 Available (historical) data 17
Table 3.2 Required input parameters XBeach model 17
Table 3.3 Revised Davenport terrain roughness classification (taken from Wieringa (1996)) 20
Table 3.4 Parameter values transformation observed wind to meso wind 21
Table 3.5 Coefficients representing wind-wave growth in the idealised situation (from Holthuijsen (2007)) 24
Table 3.6 Values for wind speed ratio to area II and wind direction in all areas of Weenink's method. 27
Table 3.7 Statistical values of chosen distribution for the storm surge duration. 29
Table 3.8 Values of the sediment parameters used in XBeach. 30
Table 5.1 $P(Z_{2\%} \in [6.0, 7.0])$ and distribution parameters for all profiles. 53
Table 5.2 Results simple linear regression analysis. 58
Table 5.3 R^2 values multiple linear regression compared to simple linear regressions. 61
Table 5.4 Overview of relevant moments for nine selected samples: simulation time, start of overwash, moment of breaching of the sill and moment of maximum inundation (all times in hours). 70

List of Figures

Figure 1.1 Astronomical tide (blue) and measured water level (red) between 8 and 10 November, 2007 for IJmuiden (top) and Petten (bottom). Source: Rijkswaterstaat, www.actuelewaterdata.nl. 1

Figure 1.2 Isobars and air pressure on November 9th, 2007 (KNMI, source: Stormvloedflits 2007-09, www.svsd.nl). 2

Figure 1.3 Location of Heemskerk and associated dunes on the Dutch coast. 3

Figure 1.4 Luminiscence dating site Heemskerk 7 (TV site). Upper panel: location of the samples with dated year and confidence interval. Lower panel: Probability density functions of all samples with the probability density function of the shell layer in green. The three major storm surges in that period are indicated by the vertical red dashed lines (Cunningham et al, 2009). 6

Figure 2.1 Locations of Huize Swanenburgh and Petten. 12

Figure 2.2 Water levels 14-16 November 1775 in Amsterdam, Halfweg and Spaarndam (data from Van Malde, 2003). 13

Figure 2.3 Reconstructed historical depth contours (-11 m, -18 m and -20 m), close up Heemskerk area based on charts from 1853, 1859, 1863, 1897, 1909, 1921 and 1931 (Haartsen et al., 1997). 14

Figure 2.4 Reconstructed historical depth contours (-8 m and -9 m), close up Heemskerk area based on charts from 1853, 1859, 1863, 1897, 1909, 1921 and 1931 (Haartsen et al., 1997). 14

Figure 2.5 Cut-out of a map of the Holland coast with frontal views of the coast (fordunes) from Den Helder to Egmond (top right). Lower areas in the foredunes are clearly visible. Published by Waghenaer in 'Spieghel der Zeevaert' in 1584 (from Waghenaer, 1964). 15

Figure 2.6 Map of Egmond in 1718, painted by Rollerus in 1719. In the lower two subpictures the individual dunes and the low areas between them can be seen. 16

Figure 3.1 Schematization of the various modelling steps for the XBeach 1D-runs. 18

Figure 3.2 Logarithmic wind speed transformation model. A measured wind speed at reference height with a local z_0 has a certain corresponding meso wind speed; the accompanying potential wind speed can be calculated from the meso wind with the Reference z_0. For step 1 of our transformation method, the blue line is used to calculate the wind speed at blending height; for step 4, the dotted red line is used to calculate the potential wind over sea from the meso wind (from KNMI Hydra Project). 20

Figure 3.3 Huize Swanenburgh in 1702; painting by Dick Maas (from KNMI website) 21

Figure 3.4 Location of Huize Swanenburgh in 1702 on the small strip of land between the two lakes (from KNMI website) 21

Figure 3.5 The dimensionless significant wave height and period (left hand vertical axes) as a function of dimensionless fetch (horizontal axes) and depth (right-hand vertical axes) (from Holthuijsen (2007)). 24

Figure 3.6 The five subfields used in Weenink's method: the Northern Area, Area I, II and III in the Southern North Sea and the Channel. Each area has a uniform wind field (from Weenink, 1957). 26

Figure 3.7 The five subfields of Weenink's method over the wind and pressure field of February 1st, 1953 (0:00 GMT). The black numbers give the average wind speed in each subfield (adapted from Van Haaren (2005)). 27

Figure 3.8 Astronomical tide Heemskerk for the period November 1, 1775 to November 15, 1775. 28
Figure 3.9 The wind setup as a function of time (cos^2 shape) (from Vrijling and Bruinsma, 1980). 29
Figure 3.10 Sieve curve of a sand sample from the storm surge layer (TV site; HK7). 30
Figure 3.11 Detailed AHN data for the Heemskerk dune area (data from 2007; source: AHN, Rijkswaterstaat). 31
Figure 3.12 Plan view of the historic bottom with the low areas indicated by the rectangles. The six profiles are indicated by the dotted lines. 32
Figure 3.13 Bathymetry profile 1 (left panel) and detail beach and dune area profile 2 (right panel).32
Figure 3.14 Bathymetry profile 2 (left panel) and detail beach and dune area profile 2 (right panel).33
Figure 3.15 Bathymetry profile 3 (left panel) and detail beach and dune area profile 3 (right panel).33
Figure 3.16 Bathymetry profile 4 (left panel) and detail beach and dune area profile 4 (right panel).33
Figure 3.17 Bathymetry profile 5 (left panel) and detail beach and dune area profile 5 (right panel).33
Figure 3.18 Bathymetry profile 6 (left panel) and detail beach and dune area profile 6 (right panel).34
Figure 3.19 Sampled values for $U_{Zwanenburg,max}$ (left panel) and its normal distribution (right panel). 35
Figure 3.20 Sampled values for the storm surge duration D (left panel) and its lognormal distribution (right panel). 36
Figure 3.21 The variables and transformations in the grey box are used to compute the water level. 36
Figure 3.22 Maximum storm surge level for all 200 MC samples (left panel) and its (fitted) lognormal distribution (right panel). 37
Figure 3.23 Maximum H_{m0} and T_p for all 200 MC samples (left panel) and their (fitted) normal distributions (right panel). 37
Figure 4.1 XBeach coordinate system 40
Figure 4.2 Staggered grid in XBeach 41
Figure 4.3 Nine JARKUS transects in the study area; dotted lines are measured data from spring 2007 (pre-storm), solid lines are measured data from spring 2008 (post-storm). 42
Figure 4.4 Bathymetry and topography in m relative to NAP used in the XBeach November 2007 storm surge model runs. Contour lines every 5 m, starting at -20 m. 43
Figure 4.5 Water level at IJmuiden Buitenhaven between November 8th 21:00 and November 10th 12:00. 44
Figure 4.6 Significant wave height (upper panel), mean wave period (middle panel) and wave direction (lower panel), measured by the wave buoy 'IJmuiden munitiestortplaats' between November 8th 21:00 and November 10th 12:00. 45
Figure 4.7 Comparison between the Upwind scheme (default) and the Lax-Wendroff scheme (transect 147). 46
Figure 4.8 Comparison between different values of gammax, ranging from 2 to 5. Upper left panel: transect 147; upper right panel: transect 141; lower left panel: transect 178; lower right panel: transect 200). The legend for the right panels is equal to the legend of the lower left panel. 46

Figure 4.9 Comparison between two different values of eps, 0.1 and 0.01. Upper left panel: transect 147; upper right panel: transect 141; lower left panel: transect 178; lower right panel: transect 200). The legend for all panels is equal. 47
Figure 4.10 Comparison of gammax with 1D and 2D simulations for the four transects; legend: start profile 1D (solid black line), start profile 2D (dashed black line), 1D end situations (blue lines), gammax=2 (dashed blue line), gammax=3 (dashed-dotted blue line), gammax=5 (solid blue line), 2D end situations (red lines), gammax=2 (dashed red line), gammax=3 (dashed-dotted red line) and gammax=5 (solid red line). 48
Figure 4.11 Comparison of eps with 1D and 2D simulations for the four transects; legend: start profile 1D (solid black line), start profile 2D (dashed black line), 1D end situations (blue lines), eps=0.1 (dashed-dotted blue line), eps=0.01 (solid blue line), 2D end situations (red lines), eps=0.1 (dashed-dotted red line) and eps=0.01 (solid red line). 48
Figure 4.12 Comparison of gammax/eps with 1D and 2D simulations for the four transects; legend: start profile 1D (solid black line), start profile 2D (dashed black line), 1D end situations (blue lines), gammax=5 (dashed-dotted blue line), eps=0.01 (solid blue line), gammax=5 and eps=0.01 for 2D simulation (solid red line). 49
Figure 5.1 Left panel: close-up bathymetry profile 1. Right panel: histogram $Z_{2\%}$ and best-fit distribution for profile 1. 51
Figure 5.2 Left panel: close-up bathymetry profile 2. Right panel: histogram $Z_{2\%}$ and best-fit distribution for profile 2. 52
Figure 5.3 Left panel: close-up bathymetry profile 3. Right panel: histogram $Z_{2\%}$ and best-fit distribution for profile 3. 52
Figure 5.4 Left panel: close-up bathymetry profile 4. Right panel: histogram $Z_{2\%}$ and best-fit distribution for profile 4. 52
Figure 5.5 Left panel: close-up bathymetry profile 5. Right panel: histogram $Z_{2\%}$ and best-fit distribution for profile 5. 52
Figure 5.6 Left panel: close-up bathymetry profile 6. Right panel: histogram $Z_{2\%}$ and best-fit distribution for profile 6. 53
Figure 5.7 Exceedance line for Petten-Zuid, based on observations between 1933 and 1985 (Philippaert et al., 1995). The red solid line indicates the computed level; the dashed red line indicates the observed maximum level in Petten-Zuid in 1775. 55
Figure 5.8 Exceedance line for IJmuiden, based on observations between 1884 and 1985 (Philippaert et al., 1995). The red solid line indicates the computed maximum storm surge level. 55
Figure 5.9 Left panel: scatter plot of $Z_{2\%}$ vs. water level. Right panel: scatter plot of $Z_{2\%}$ vs. deep water H_{m0} (profile 1). 56
Figure 5.10 Left panel: scatter plot of $Z_{2\%}$ vs. water level. Right panel: scatter plot of $Z_{2\%}$ vs. deep water H_{m0} (profile 2). 56
Figure 5.11 Left panel: scatter plot of $Z_{2\%}$ vs. water level. Right panel: scatter plot of $Z_{2\%}$ vs. deep water H_{m0} (profile 3). 57
Figure 5.12 Left panel: scatter plot of $Z_{2\%}$ vs. water level. Right panel: scatter plot of $Z_{2\%}$ vs. deep water H_{m0} (profile 4). 57
Figure 5.13 Left panel: scatter plot of $Z_{2\%}$ vs. water level. Right panel: scatter plot of $Z_{2\%}$ vs. deep water H_{m0} (profile 5). 57
Figure 5.14 Left panel: scatter plot of $Z_{2\%}$ vs. water level. Right panel: scatter plot of $Z_{2\%}$ vs. deep water H_{m0} (profile 6). 58
Figure 5.15 $Z_{2\%}$ versus water level and deep water H_{m0} (profile 1). 59
Figure 5.16 $Z_{2\%}$ versus water level and deep water H_{m0} (profile 2). 59

Figure 5.17 $Z_{2\%}$ versus water level and deep water H_{m0} (profile 3). 60
Figure 5.18 $Z_{2\%}$ versus water level and deep water H_{m0} (profile 4). 60
Figure 5.19 $Z_{2\%}$ versus water level and deep water H_{m0} (profile 5). 61
Figure 5.20 $Z_{2\%}$ versus water level and deep water H_{m0} (profile 6). 61
Figure 5.21 $R_{2\%}$ wave run-up height as a function of the deep water Irribarren number, calculated with the dune slope at the start of the simulation (black dots), at the moment of the maximum wave attack (blue dots) and at the end of the simulation (red dots).Left panel: profile 1; right panel: profile 2. 63
Figure 5.22 $R_{2\%}$ wave run-up height as a function of the deep water Irribarren number. Data as in Figure 5.21. Left panel: profile 3; right panel: profile 4. 63
Figure 5.23 $R_{2\%}$ wave run-up height as a function of the deep water Irribarren number. Data as in Figure 5.21. Left panel: profile 5; right panel: profile 6. 64
Figure 5.24 Left panel: plan view constructed topography 1775 with the three low-lying areas indicated with dashed rectangles, numbered from bottom to top 1 to 3. Right panel: topography 2007. 65
Figure 5.25 Snapshot of water level and bed elevation for sample 053; after 23.50 hours (left panel) and after 36.25 hours (right panel). 66
Figure 5.26 Snapshot of water level and bed elevation for sample 129; after 21.50 hours (left panel) and after 43.00 hours (right panel). 66
Figure 5.27 Snapshot of water level and bed elevation for sample 184; after 20.50 hours (left panel) and after 29.75 hours (right panel). 67
Figure 5.28 Snapshot of water level and bed elevation for sample 196; after 30.25 hours (left panel) and after 44.25 hours (right panel). 67
Figure 5.29 Simulated sedimentation and erosion at the end of the simulation for sample 053. 68
Figure 5.30 Simulated sedimentation and erosion at the end of the simulation for sample 129. 68
Figure 5.31 Simulated sedimentation and erosion at the end of the simulation for sample 184. 69
Figure 5.32 Simulated sedimentation and erosion at the end of the simulation for sample 196. 69
Figure 5.33 Simulated sedimentation and erosion at the end of the simulation for sample 053 with the topography of 2007. 71
Figure 5.34 Simulated sedimentation and erosion at the end of the simulation for sample 129 with the topography of 2007. 71
Figure 5.35 Simulated sedimentation and erosion at the end of the simulation for sample 184 with the topography of 2007. 72
Figure 5.36 Simulated sedimentation and erosion at the end of the simulation for sample 196 with the topography of 2007. 72

List of Photographs

Photo 1.1	November 8, 2007 storm surge (photo by Marcel Bakker, Deltares).	1
Photo 1.2	Eroded frontal dune near Heemskerk (photo by Marcel Bakker, Deltares).	2
Photo 1.3	Shells with convex-side up (photos by Sytze van Heteren, Deltares).	4
Photo 1.4	Part of a brick found in the shell layer (photo by Marcel Bakker, Deltares).	4
Photo 1.5	Slump or loading structures, marked by white line (photo by Marcel Bakker, Deltares).	4
Photo 1.6	Air-escape structure, marked by black lines (photo by Sytze van Heteren, Deltares).	5
Photo 2.1	Eroded dunefront at Bergen aan Zee after severe storms in the 1980's (photo taken in 1990, www.BeeldbankVenW.nl, Rijkswaterstaat).	10
Photo 2.2	Layers of Younger Dunes at the Bergen site (1984). In the top-half, the single shell layer can be found (Jelgersma et al., 1995).	10
Photo 2.3	Two photos showing convolute bed layers in Plouescat, France (Photos taken by Deltares, 2008).	11

List of Symbols

Roman symbols

Symbol	Unit	Description
a_i	m	amplitude tidal component with index i
d	m	water depth
$\tilde{d}$	-	dimensionless depth
d_{50}	m	median grain size
d_{90}	m	grain size at which 90% of sample is finer
D	hours	storm surge duration
E	-	limit state value relative error
F	m	fetch length
$\tilde{F}$	-	dimensionless fetch length
g	m/s_2	gravitational acceleration
h	m	water level above reference level
h_{petten}	m	observed water level in Petten
$\tilde{H}$	-	dimensionless significant wave height
H_{m0}	m	significant wave height
k	-	level of reliability
L_0	m	deep water wave length based on peak period
n	-	number of simulations
P	-	probability
R^2	-	coefficient of determination
$R_{2\%}$	m	2% wave run-up height based on individual peaks
S	m	wind set-up
S_{max}	m	maximum wind setup during storm surge
$\tilde{T}$	-	dimensionless peak wave period
T_p	s	peak wave period
u_*	m/s	friction velocity
U_{10}	m/s	potential wind speed (at reference level of 10 m)
U_{60}	m/s	meso wind speed at blending height (60 m)
$U_{zwanenburg}$	m/s	observed wind speed at Huize Swanenburgh
V_s	cm/s	0.75 x gradient wind speed (in Weenink model)
z_0	m	roughness length
z_b	m	blending height (60 m)
$Z_{2\%}$	m	2% exceedance height relative to reference level based on individual run-up peaks

Greek symbols

Symbol	Unit	Description
α	-	slope
α_c	-	Charnock coefficient
ε	-	relative error in Monte Carlo simulation
κ	-	Von Karman coefficient
ξ_0	-	deep water Irribarren number

μ	-	mean (of a distribution)
ρ_{air}	kg/m^3	air density
σ	-	standard deviation
τ	N	surface drag
φ	-	time shift
Φ	-	standard normal distribution

1 Introduction

1.1 Background

On November 8-9, 2007, a fairly severe storm surge hit the Dutch North Sea coast (Photo 1.1 and Figure 1.1). A low-pressure area moved from Iceland to South Scandinavia, while a powerful high-pressure area was present west of Ireland. A severe storm field developed at the west side of the depression: storm depression Tilo (Figure 1.2). In the Netherlands, the weather was not different from an 'ordinary autumn storm' (KNMI, 2007).

Photo 1.1 November 8, 2007 storm surge (photo by Marcel Bakker, Deltares).

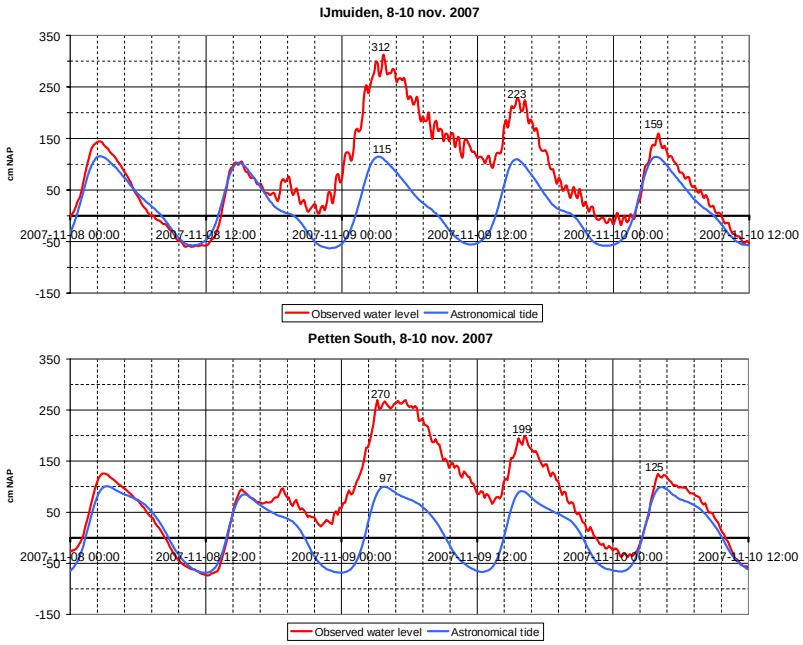

Figure 1.1 Astronomical tide (blue) and measured water level (red) between 8 and 10 November, 2007 for IJmuiden (top) and Petten (bottom). Source: Rijkswaterstaat, www.actuelewaterdata.nl.

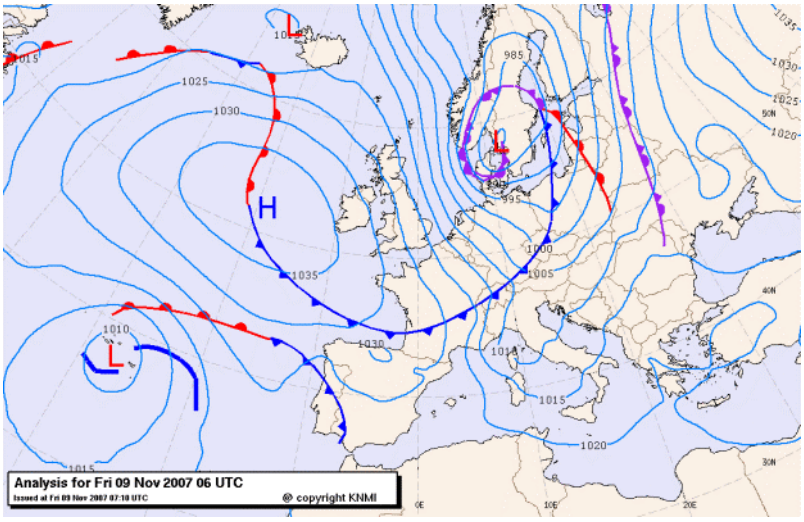

Figure 1.2 *Isobars and air pressure on November 9th, 2007 (KNMI, source: Stormvloedflits 2007-09, www.svsd.nl).*

1.2 Evidence of historical storms

In the days after the storm, shell layers were found in the frontal dune row, up to NAP + 6.5 m, near Heemskerk (Figure 1.3), which had eroded due to the storm surge and wave attack (Photo 1.2). In an area of 1 km along the coast, at least seven sites have been found were these shell layers were visible. At some sites, one layer has been found, but on other sites two layers just above each other could be seen. In contrast with most other parts of the Dutch coast, the coastal zone near Heemskerk has never been nourished. Therefore, the storm of November 2007 uncovered older, naturally formed dunes, instead of nourished sediments.

Photo 1.2 *Eroded frontal dune near Heemskerk (photo by Marcel Bakker, Deltares).*

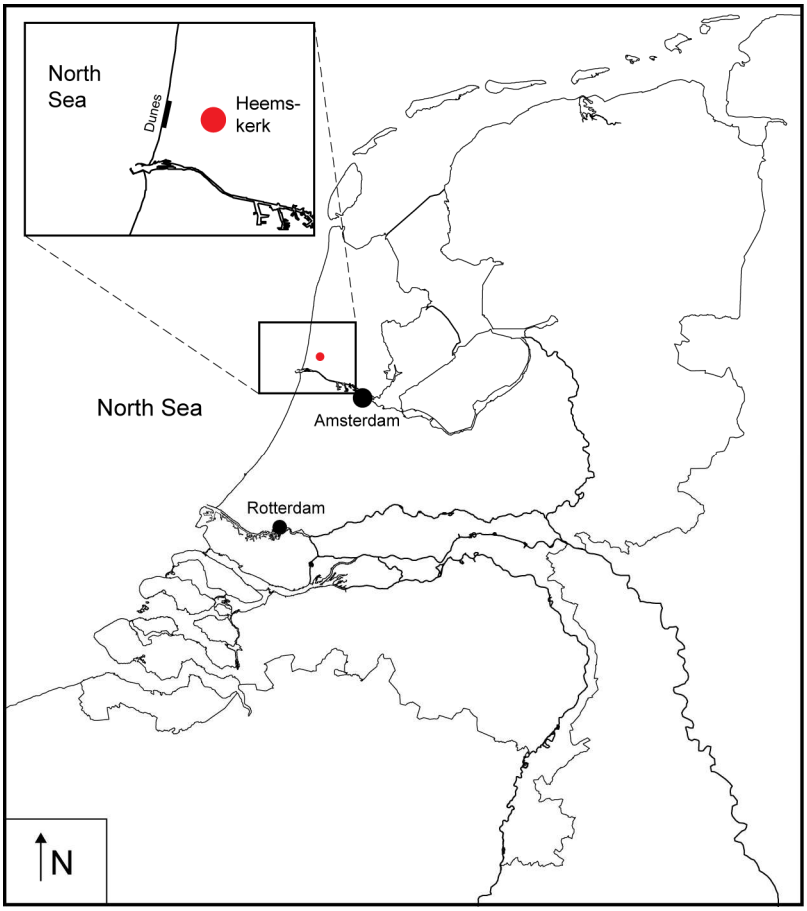

Figure 1.3 *Location of Heemskerk and associated dunes on the Dutch coast.*

The layers consist mostly of shells that are oriented convex-side up (Photo 1.3), which means that the shells have been deposited by a shallow layer of flowing water (sheetflow): only water (not wind) can deliver the force needed to turn the shells over to the convex-up orientation. Also coal fragments and parts of bricks have been found (Photo 1.4) in elevated position. Besides these materials, also slump structures (Photo 1.5) and air-escape structures (Photo 1.6) have been observed (Van Heteren *et al.*, 2008). The air-escape structures are an indication of a rapid water level rise during the storm: air gets trapped and escapes vertically, taking sand with it. This evidence leads to the conclusion that the shell-bearing beds are deposited by a storm surge, which locally has reached levels of at least 6.5 m above NAP.

Photo 1.3 *Shells with convex-side up (photos by Sytze van Heteren, Deltares).*

Photo 1.4 *Part of a brick found in the shell layer (photo by Marcel Bakker, Deltares).*

Photo 1.5 *Slump or loading structures, marked by white line (photo by Marcel Bakker, Deltares).*

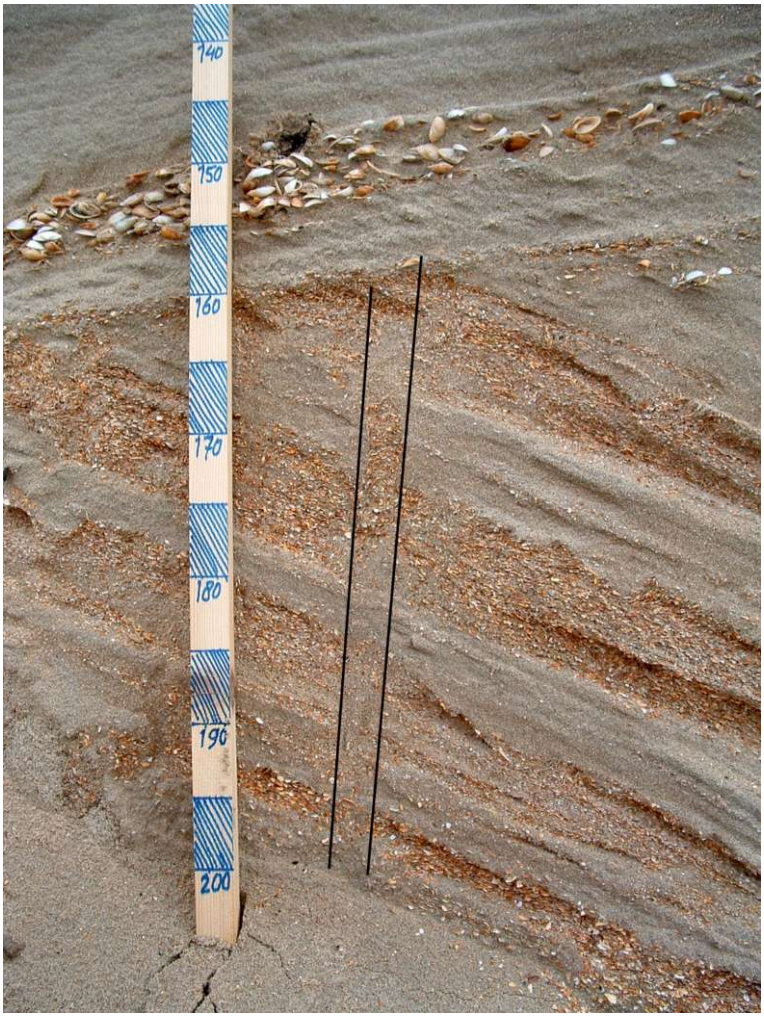

Photo 1.6 Air-escape structure, marked by black lines (photo by Sytze van Heteren, Deltares).

1.3 Determining age storm surge layers

The age of the layer of shells, coal and parts of bricks has been determined in different ways, using several indirect and direct methods. Firstly, materials made or used by humans can indicate certain periods. The bricks in the storm surge layers can originate from coastal villages that have been under attack during earlier storm surges. Brick has been used in Holland since circa 1200, but the found pink/red brick has only been used since the 15th century. The presence of coal indicates that the layers have formed after the 17th century, when coal was used as fuel for beacons, the predecessors of lighthouses (Van Heteren *et al.*, 2008).

Besides these indirect indicators, also direct dating of the storm surges layers has been done. At one place in the layer, a concentration of common cockles was found. They were still bivalved, which indicates the cockles were still alive at the time of deposition. A radiocarbon (^{14}C) dating of one of these cockles placed the shell in the period 1697 AD – 1805 AD (Van Heteren *et al.*, 2008). More accurate information about the age of the storm surge layers has been obtained by luminescence dating of the layer itself and the sand below and above it. The sand below the storm surge layer has been deposited around 1700 AD, the sand above the layer after 1800 AD. The storm surge layer itself has been deposited around 1785 AD

(Figure 1.4) (Van Heteren *et al.*, 2008; Cunningham *et al.*, 2009). The accuracy range of the dating is some decades.

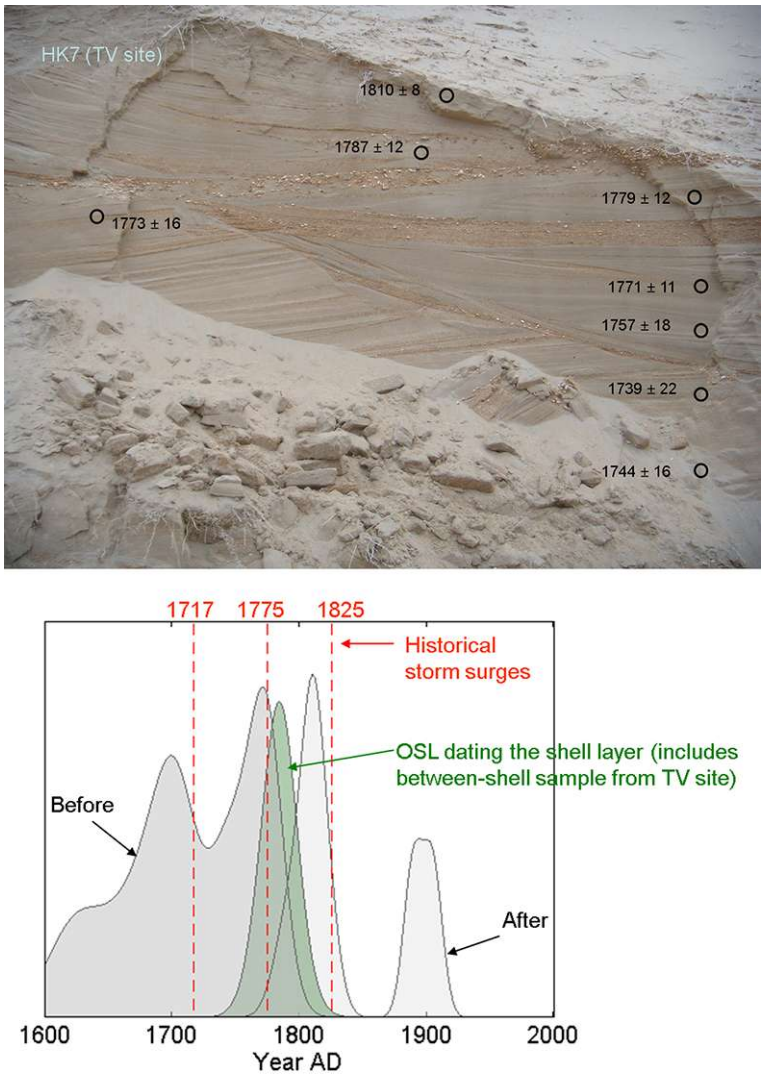

Figure 1.4 *Luminiscence dating site Heemskerk 7 (TV site). Upper panel: location of the samples with dated year and confidence interval. Lower panel: Probability density functions of all samples with the probability density function of the shell layer in green. The three major storm surges in that period are indicated by the vertical red dashed lines (Cunningham et al, 2009).*

1.4 Implications

As the storm surge layers have been determined late 18th century, they form unique records of deposits by one or two large historical storms. From historical records and research into storm surges (Van Malde, 2003), it is known that only two major storm surges took place in the end of the 18th century: in 1775 and in 1776. For both storm surges, the maximum observed water level in Petten (the location closest to Heemskerk with observations) was the same. Therefore and because the 1775 was the first of the two storms, it is decided to model the 1775 storm in this study.

Because systematic measurements on an hourly or daily basis were not made at that time, not much is known about the conditions in which the storm took place – water levels, wave

heights and wind speeds, but also local bathymetry. It is therefore also not certain which factors affected the deposition of the shell layers the most. Because of this uncertainties, a probabilistic approach in which these uncertainties can be taken into account, is useful.

The systematic measurements are only available for a relatively short period: only the last 150 years. The safety norms for the Dutch coast, that define the dunes have to withstand a 1/10.000 year event, are based on extrapolation of this short measurement series. Information about events before 1850 is only available through historical and geological archives; these can provide additional information for those long-term predictions. Additionally, the geological archive can provide information about the effect of storm surges on the coast at that time, such as the influence of low-lying areas in the coastal dunes and the depth to which the storm surge entered the dune area.

1.5 Problem statement

With luminescence dating and other dating methods, storm surge deposits near Heemskerk have been dated the last decades of the 18th century, most probably 1775 or 1776. Which combination of boundary conditions and geometry is the most probable to deposit the storm surge layers at the heights found? Is it possible to estimate a probability of occurrence for the estimated boundary conditions (water level and/or wave height)?

Based on historical information it is known that the dunes were more natural in the past (in the 18th century). What is the difference in impact of large storms on less well maintained natural dunes (historical) and artificial, well maintained “sand dikes” (present)? What can we learn for more natural, so-called “dynamical dune management” now and in the future?

1.6 Objectives

1. Set up a modelling framework to run probabilistic simulations for the 1775 storm surge and collect as much historical data as possible to use in the model.
2. Find out if the range of modelled maximum water levels, including set-up and wave run-up, corresponds with the maximum height of the discovered storm surge deposits.
3. Find the most probable combination of boundary conditions and geometry that predicts the storm surge layer height at Heemskerk for the 1775 storm surge. Make an estimate for the probability of exceedance for the 1775 storm surge in terms of water level.
4. Compare the effects of a storm on natural dunes (historical situation) with effects of a storm surge on a sand dike (present situation).

1.7 Methodology

Recently a 2DH process-based cross-shore model called XBeach has been developed (Roelvink *et al.*, accepted). With this model dune erosion, breaching and overwash during storm conditions can be simulated. Not only dune avalanching is accurately predicted, but also longshore variations in hydrodynamic and morphological processes.

XBeach is an appropriate tool to model the conditions of the 1775 storm surge, because long waves (surfbeat) are accounted for in the model and variance in the infragravity wave band dominates the hydrodynamic processes in very shallow water and dune erosion (Van Thiel de Vries *et al.*, 2008). XBeach is currently the only model that can take longshore variations in forcing, sediment transport and dune profile into account (2D). With XBeach it is possible to find out which water levels and wave heights could have caused the depositions on the dunes.

The first step is to set up a model to perform probabilistic simulations with XBeach and acquire all the necessary boundary condition data. There is some historical data available, but it has to be determined what data is useful. Historic weather data can be found at the KNMI, water level and wave data may be available at Rijkswaterstaat. Other data has to be estimated from historical documents (archives, paintings, etc.) or research that already has been carried out. For still missing data plausible values have to be estimated. Also in this step, the probability distribution functions of the various data are determined or estimated.

As a second step, a base simulation in XBeach is set-up and calibrated against the 2007 storm.

Because of the uncertainties in the boundary conditions and/or historical data, a probabilistic 1D approach is used. For each parameter, a distribution is determined (if possible) or else estimated. Therefore, the third step consists of a sensitivity analysis by doing numerous simulations with the working model (i.e. a Monte Carlo analysis).

The fourth step is a 2DH model comparison between the present dune situation with artificial dunes and the historic situation with natural dunes. This will be done for storm conditions, either for the historical storm or for the November 2007-storm.

The last step is a comparison of the model results for the 1775 storm with the present available ‘exceedance curve’ for IJmuiden to determine the probability of exceedance for the 1775 storm, e.g. was it an once-in-50-years storm or an once-in-200-years storm?

1.8 Reader’s guide

In this study the possibilities of modelling the historical storm surge of 1775 with the process-based model XBeach are explored. The context for this study has been presented in the current chapter. Chapter 2 provides more details on the context and gives an overview of all available and relevant historical data and information. Chapter 3 introduces the modelling framework and describes all inputs for the XBeach model. The XBeach model and a calibration case with the November 2007 storm surge are described in chapter 4. The results of a Monte Carlo analysis with 200 1D simulations is discussed in chapter 5, as well as the results of a number of 2DH runs that give more insight in the 2D breaching and overwash processes in the dunes. Conclusions and recommendations are found in chapter 6.

2 Literature study

2.1 The 1775 & 1776 storms

Little is known about the conditions during extreme storm surge events before the start of regular publications in 1854 AD by Rijkswaterstaat (Directorate-General for Public Works and Water Management) of the daily (sometimes hourly) measurements at the 'Rijkspeil-meetstations'. The systematic collection of water levels before that time only took place locally: since 1682 in Amsterdam (since 1700 hourly and partially semi-hourly), from 1737 until 1741 in Katwijk (hourly, see also www.waterbase.nl) and in other places daily tidal maxima and minima (Van Malde, 2003). All together, there are a number of records available with visual observations of extreme surge levels, visual observed time series of the surge level and wind speed measurements. These records however do not have much overlap, both in time and space.

In recent years, historical data about floods in the period 1500-1850 have been studied systematically (Gottschalk, 1971-1977; Jonkers, 1988; Van Malde, 2003; Buisman, 2006). For statistical analysis, Van Gelder (1996) classified all these floods into four categories based on the available water level records. An overview of these floods can be found in Table 2.1 (from class A, very severe floods, to class D, light floods). It can be seen that both the storms in 1775 and 1776 belong to the ten (major) floods in the period 1500-1850.

Table 2.1 Overview of all floods between 1500 and 1850 as classified by Van Gelder (1996). Class A is for very severe floods, down to class D for light floods (table modified by author).

Year	Class (A-D)
1570	A
1672	D
1682	D
1715	D
1717	D
1775	D
1776	C
1806	B
1808	B
1825	B

Buisman (1984) and Buisman (in prep.) made a description of the weather under which the November storm surges took place. About the 1775 storm, he says: "In the late afternoon of November, 14th and the night of November, 14th/15th a severe WNW-NW storm raged accompanied by heavy rain, hail and thunder. The sea level rises higher than every flood before, especially higher than the severe storm surges of 1682 and 1717. [..] At the North Sea coasts, much dune damage develops, e.g. near Terheyde and Scheveningen ('half of it covered by the sea'). Part of the Hondsbosse sea defence is destroyed. [..] Many ships have been wrecked, especially on the North Sea. 'Along the entire beach one saw nothing more than ship wrecks, rigging, goods and bodies being washed to the shore.' 200 ships have been lost!"

At Ter Heyde the waves erode almost 21 feet of the dunes, at Scheveningen half of the village is inundated and after the storm, the slope to the beach and the sea is vertical (which

happens almost every storm though). At Petten the Hondsbosse Zeewering is destroyed for two-thirds, while at several places along the Holland coast almost 10 ‘el’ (around 6.5 m) of dunes disappeared (Buisman, in prep.).

The area that is hit most by the 1776 storm is different from 1775. The areas that sustain the most damage, are the Wadden Islands (especially Texel) and the Zuiderzee area. No special remarks about this Holland coastal area are known (Buisman, in prep.). Maximum water levels are equal to 1775 or slightly lower (Van Malde, 2003).

Buisman (1984) says about the 1776 storm: “After days of strong SW and W winds, the catastrophical NW storm follows on November 20th/21st, which pushes up the sea water north of Amsterdam and in the Zuiderzee even higher than a year before. Different from ’75 the southwestern part of the Netherlands sustains relatively little damage. [..] On Texel the water washed over everywhere and also the other Wadden islands are in utmost distress.”

2.2 Other evidence of historical storm surge heights

The discovery of the shell layers in Heemskerk in November 2007 was special. Not very often elevated deposits are encountered; more often low-lying deposits in polder areas are found. Only the elevated deposits can tell something about the storm surge height and magnitude. Before November 2007, a small number of elevated storm surge deposits have been encountered in the Netherlands. In the 1980’s and early 1990’s shell layers were found in Bergen, where the foredunes were subject to strong and structural erosion during storm surges (Photo 2.1) until an extensive nourishment in the 1990’s covered the eroded dune front with tens of meters of sand. At this site, also a layer with a thickness of one shell, convex-up, was present (Photo 2.2). Occasionally the thickness of the layer was two shells. The deposits were present over a length of 750 m, with the elevation ranging from NAP + 5 m up to + 6.55 m (where the layer disappeared). ^{14}C-datings of the shells indicated a date around the 13th and 14th century, but the presence of a red brick indicates a later date. The storm surge level of the event at the Bergen site was estimated at NAP + 5 m (Jelgersma *et al.*, 1995).

Photo 2.1 *Eroded dunefront at Bergen aan Zee after severe storms in the 1980’s (photo taken in 1990, www.BeeldbankVenW.nl, Rijkswaterstaat).*

Photo 2.2 *Layers of Younger Dunes at the Bergen site (1984). In the top-half, the single shell layer can be found (Jelgersma et al., 1995).*

Other sites described in the article by Jelgersma *et al.* (1995) are the Bakkum dunes, where a shell rich layer and slumping structures have been found; the IJmuiden fishing harbour where various convex up shell layers have been found and sites in Velsen and along the North Sea channel, where also multiple convex up shell layers were discovered. Through radiocarbon dating it was determined that the shell layers found at different sites belonged to different storm surge events; there were at least 4 or 5 different events, dated between around 2450 BC and 1600 AD.

Also in other parts of the world evidence of historical (storm) surge events have been found. In north-western France, near Plouescat in Brittany, at an exposed part of the dune system, convolute beds were observed (Lindström, 1979; see Photo 2.3). These are distorted layers that are created by pressure differences during or just after sedimentation (De Boer, 1979).

Photo 2.3 Two photos showing convolute bed layers in Plouescat, France (Photos taken by Deltares, 2008).

2.3 Available historical data

2.3.1 Wind and air pressure

Historical wind measurements, especially from the 18th century, are rare. Only a limited number of interested individuals did systematic meteorological measurements and observations in the Netherlands before the establishment of the KNMI (Royal Netherlands Meteorological Institute) in 1854. In an extensive study in the 1980's, Geurts and Van Engelen (1992) tried to gather all remaining antique measurement series in the Netherlands. Employees of the Waterstaat at Huize Swanenburgh (Figure 2.1) recorded the largest still existing measurement series, between 1735 and 1861. This series is one of a few antique series in the Netherlands available that gives an idea of the wind speeds during the storms in 1775 and 1776. At Huize Swanenburgh, temperature, precipitation, air pressure, wind direction and wind force were measured or estimated. Wind force has been recorded on a 'Wind Mill scale', originally developed by Jan Noppen. In Table 2.2, a conversion between the wind mill scale and the Beaufort scale can be found.

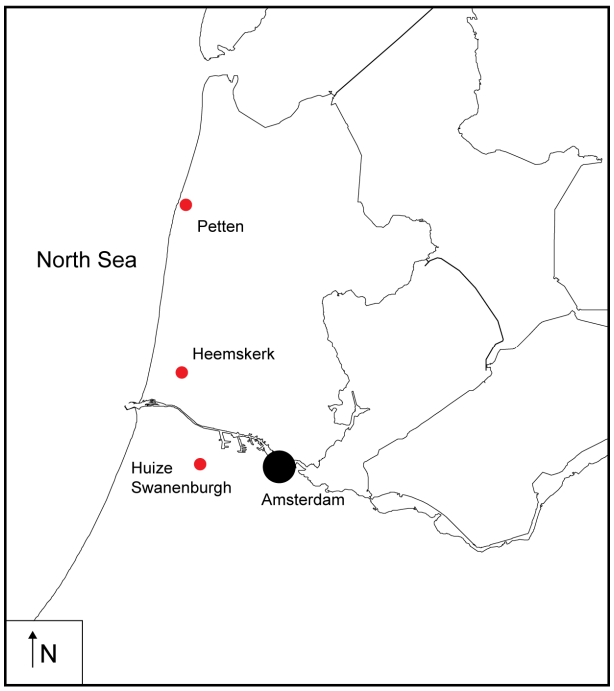

Figure 2.1 *Locations of Huize Swanenburgh and Petten.*

Other useful measurement series, containing data of the 1775 and 1776 storms, are a series by Schaaf in Amsterdam (1759-1778) and a series by Van der Muelen in Utrecht and Driebergen (1759-1810) (Geurts and Van Engelen, 1992; KNMI, 2004, 2008; Buisman, in prep.).

Meteorological measurements were not only done in the Netherlands before the 19th century. In various places in Europe temperature, wind speed, wind direction and air pressure were measured. Examples of antique series abroad are those of Hutchinson in Liverpool, United Kingdom (Woodworth, 2006), the Society of Science in Uppsala, Sweden (Bergström and Moberg, 2002) and the Royal Swedish Academy of Sciences in Stockholm, Sweden (Moberg *et al.*, 2002).

Table 2.2 *Noppen's Wind Mill scale (Geurts and Van Engelen, 1992). Transformation from Beaufort to m/s from Wieringa and Rijkoort (1983).*

Wind mill scale	Beaufort scale	m/s
0	0	0 – 0.2
1	1	0.3 – 1.5
2	2	1.6 – 3.3
3 – 4	3	3.4 – 5.4
5 – 6	4	5.5 – 7.9
7 – 8	5	8.0 – 10.7
9 – 10	6	10.8 – 13.8
11 – 12	7	13.9 – 17.1
13 – 14	8	17.2 – 20.7
15 – 16	9 – 10	20.8 – 28.4
16 +	11 – 12	≥ 28.5

The estimated wind forces during the November storms of 1775 and 1776 are given in Table 2.3.

Table 2.3 Estimated wind force during the November storms of 1775 and 1776; recorded at Huize Swanenburgh. Observation times are approximate (KNMI, 2008).

Estimated wind force on Noppen's wind mill scale			
1775		*1776*	
November 13th, 22:00	4	November 20th, 12:00	10
November 14th, 07:00	14	November 20th, 22:00	14
November 14th, 12:00	14	November 21st, 07:00	14
November 14th, 22:00	14	November 21st, 12:00	8
November 15th, 07:00	6	November 21st, 22:00	10

2.3.2 Surge level

Not much is known about the surge levels along the Dutch coast during the 1775 and 1776 storms. Data that has been observed and recorded is usually from 'water level rules' at sluices or flood marks on churches and only the highest level during a storm surge event has been recorded. The largest collection of these storm surge levels has been made by Jonkers (1989) and improved and supplemented by Van Malde (2003).

Petten (for location see Figure 2.1) is the location closest to Heemskerk that has water level data for the 1775 and 1776 storms. For both storms, the recorded maximum storm surge water level was '8 feet above Volzee'. There are different definitions for 'Volzee', but the most probable is 'mean high water' (MHW) (Van Malde, 2003). Based on tidal analysis (see paragraph 3.5), this was around NAP + 0.6 m in 1775. The length system used for measuring feet in Petten is the 'Hondsbosse foot', equal to 28.52 cm. This means that the maximum storm surge level observed in Petten in 1775 and 1776 is around NAP + 2.8 / 2.9 m.

Although no full water level records are available for locations along the coast, there are complete time series for the 1775 storm at the southern Zuiderzee, in Amsterdam and surrounding locations. These time series give an impression of the development of the water level during the 1775 storm (Figure 2.2).

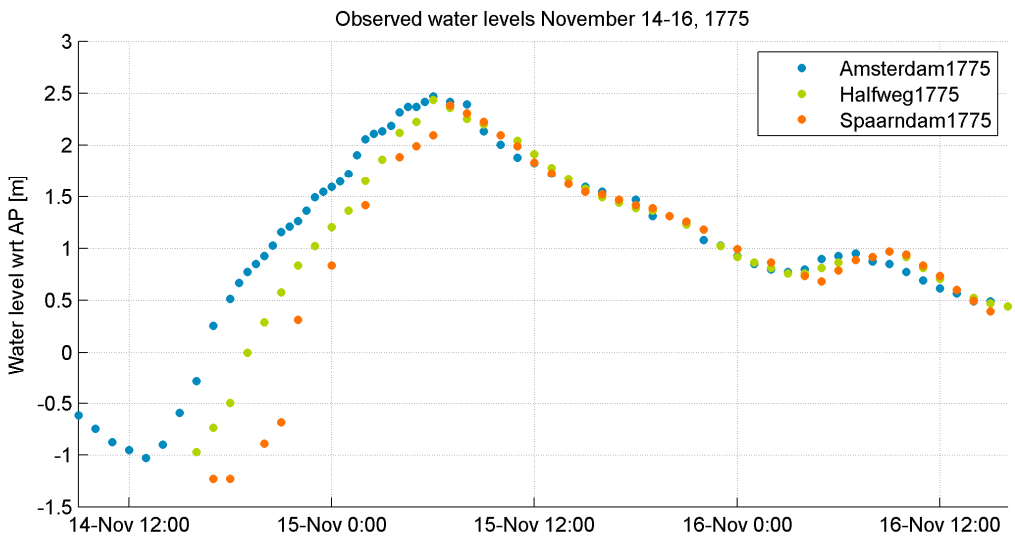

Figure 2.2 Water levels 14-16 November 1775 in Amsterdam, Halfweg and Spaarndam (data from Van Malde, 2003).

2.4 Bathymetry & topography

2.4.1 Bathymetry

Since 1964, the bathymetry of the entire Dutch coast is monitored on an annual basis and contained in the JARKUS database. Before 1964 and especially before mid nineteenth century, no systematic and regular (yearly or five-yearly) bathymetry measurements were done. This means there is little information known about the bathymetry near Heemskerk during the considered period.

Within the framework of the project 'KUST*2000', Haartsen *et al.* (1997) reconstructed historical depth contours based on old hydrographical charts. In this study old charts and maps since the 18th century have been found, but only charts from 1825 and later were useful and have been studied. It has been concluded that the accuracy of the old charts was quite good, both in horizontal and vertical direction (Haartsen *et al.*, 1997). From the available depth contour maps along the Holland coast, It can be seen that the depth contours did not change much over the course of a century, since 1859 (Figure 2.3 and Figure 2.4). The contour lines do not show a steepening or flattening of the nearshore profile. It is therefore assumed that no significant change of the depth profile (in the order of multiple degrees) took place in the period before which influences the way the waves feel the bottom significantly.

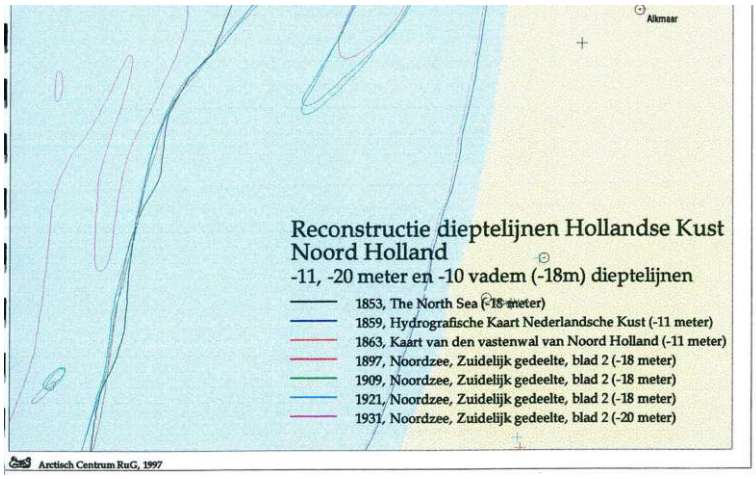

Figure 2.3 *Reconstructed historical depth contours (-11 m, -18 m and -20 m), close up Heemskerk area based on charts from 1853, 1859, 1863, 1897, 1909, 1921 and 1931 (Haartsen et al., 1997).*

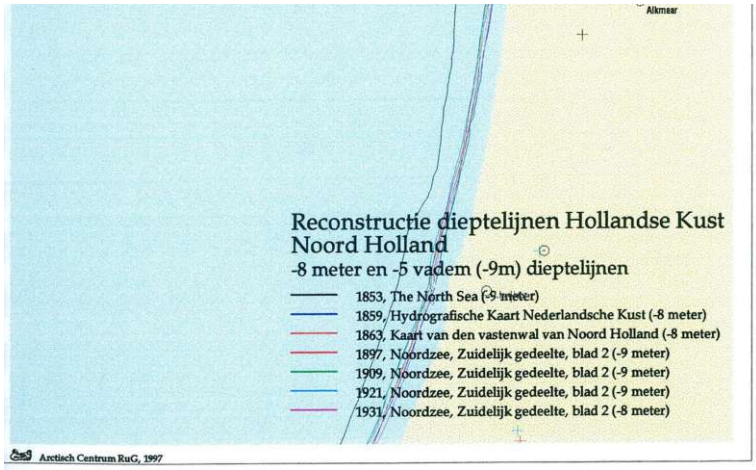

Figure 2.4 *Reconstructed historical depth contours (-8 m and -9 m), close up Heemskerk area based on charts from 1853, 1859, 1863, 1897, 1909, 1921 and 1931 (Haartsen et al., 1997).*

2.4.2 Topography

In the 18th century, the Dutch foredunes (first dunes behind the beach) were different from the sand dike (Dutch: ‘zeereep’) we know today. It consisted of high, natural sand dunes, formed and reshaped by aeolian action, alternating with low entrances to dune valleys. The low areas were frequently flooded during high water levels: spring tides and storm surges. Nowadays, the foredunes have a minimal height of NAP + 11 m and are fixated by vegetation, maintained by humans. Everywhere along the Dutch coast, these ‘sand dikes’ stop the seawater, except for a few places where this dune row is intentionally breached to give the natural processes a chance, e.g. De Kerf (Vertegaal *et al.*, 2003) or where mankind was not able to close a tidal inlet, e.g. De Slufter on Texel. De Kerf resembles the 18th century situation of the study area the most.

The only sources available that can give an indication of the (dune) topography, are old drawings (drawn maps) and old paintings. Some parts of the Holland coast have been painted extensively, such as Scheveningen, Katwijk or Egmond aan Zee. Unfortunately, this is not the case for the Heemskerk area, since it has no village at the coast. However, those old drawings and paintings give an idea what the coastal zone looked in the 18th century. On the map of Waghenaer (made in 1584) in the top right corner, a frontal view of the dunefront, with all individual dunes, from Texel to Egmond can be seen (Figure 2.5). Rollerus (1719) made a painting of Egmond in 1719 (Figure 2.6) with two views of Egmond and surrounding dunes in the bottom part of the drawing. These views show clearly the natural dunes with lower areas between them, the latter often being open to the sea. It may therefore be assumed that the 18th century coast had a more “open outlook” than the present “sand dike”.

Figure 2.5 *Cut-out of a map of the Holland coast with frontal views of the coast (fordunes) from Den Helder to Egmond (top right). Lower areas in the foredunes are clearly visible. Published by Waghenaer in ‘Spieghel der Zeevaert’ in 1584 (from Waghenaer, 1964).*

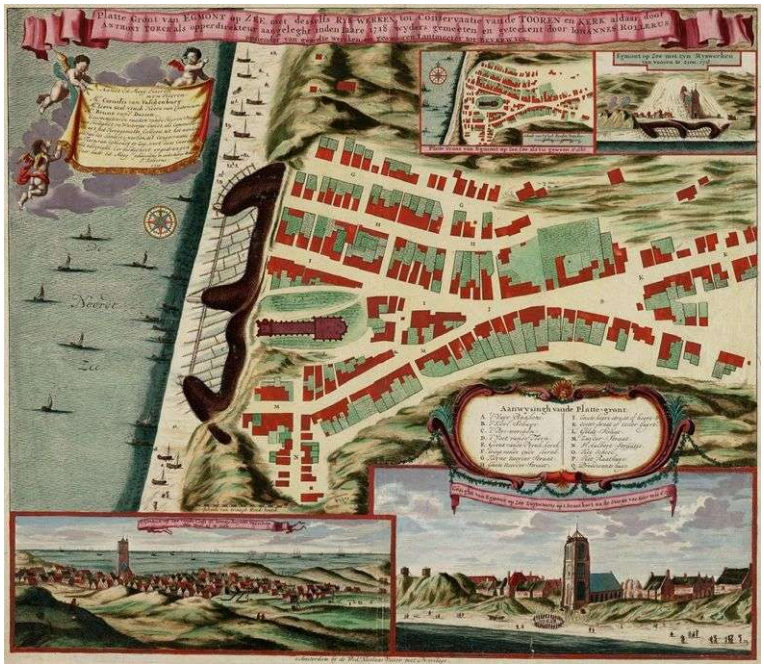

Figure 2.6 *Map of Egmond in 1718, painted by Rollerus in 1719. In the lower two subpictures the individual dunes and the low areas between them can be seen.*

3 Model inputs

To cope with the limited (historical) data available from the November 1775 storm, a probabilistic approach is used. A large number of simulations with slightly different boundary conditions are run, resulting in a large number of post-storm situations. The boundary conditions are randomly sampled from the distributions of the input parameters. This method is known as Monte Carlo simulation.

A typical full 2DH-simulation in XBeach takes 10-20 CPU hours to compute (desktop with P4 3 GHz processor and 1 GB of RAM). A large number of simulations, as required for a Monte Carlo analysis, will therefore cost thousands of CPU hours. As this is hardly possible, a full 2D probabilistic analysis will not be done. Instead, 1DH-simulations will be used for a number of characteristic cross-shore profiles. In that way, variations in longshore dimension are considered and computation time is much shorter.

3.1 Available data and modelling method

In chapter 2, the available historical data have been discussed. See Table 3.1 for an overview.

Table 3.1 Available (historical) data

Observed and measured data			
Parameter	Symbol	Type	Remarks
Wind	$U_{Zwanenburg,max}$	Estimated wind speed at Zwanenburg (observed 3x per day).	Estimated using Noppen's wind mill scale.
Water level	$h_{Petten,max}$	Highest observed water level during 1775 storm in Petten.	In feet above 'Volzee'.
Grain diameter	d_{50}, d_{90}	Grain size distribution storm surge layer.	Determined by sieving a sample from one of the Heemskerk sites.

As the above data are the only data that are actually measured (with a certain amount of uncertainty), it is necessary to estimate the other boundary conditions or calculate them using the above data. Examples are the variations in water level (surge) in time, wind field (strength, direction and duration) and fetch over the North Sea, significant wave height (in time) and the bathymetry. An overview of the required input parameters can be found in Table 3.2. The applied modelling method is visualized in Figure 3.1.

Table 3.2 Required input parameters XBeach model

Required data XBeach simulations		
Parameter	Symbol	Type
Water level	$h\ (t)$	Storm surge water level as a function of time (water level time series).
Significant wave height	$H_{m0}\ (t)$	Significant wave height as a function of time.
Peak wave period	$T_p\ (t)$	Peak wave period as a function of time.
Wave direction	-	Mean wave direction as a function of time
Grain diameter	d_{50}, d_{90}	Median and 90% grain diameters

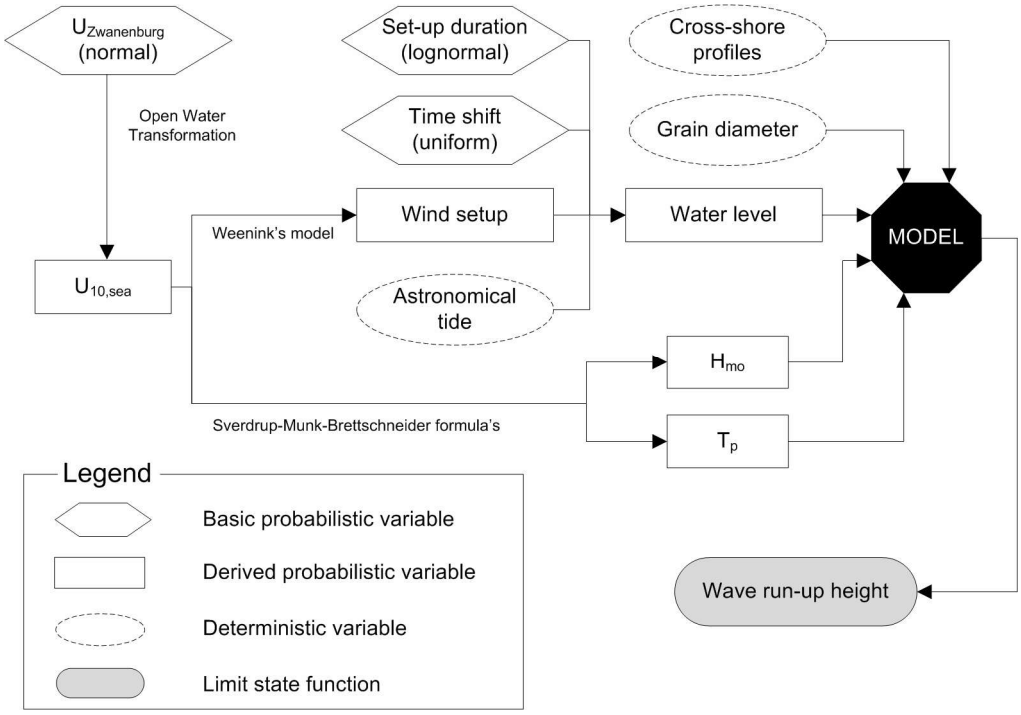

Figure 3.1 Schematization of the various modelling steps for the XBeach 1D-runs.

The modelling steps are described below. In the next paragraphs, the various modelling steps are discussed in more detail.

- The wind speed at the North Sea ($U_{10,max}$) can be transformed from the wind speed in Zwanenburg ($U_{Zwanenburg,max}$) using a so called 'open water transformation': transform the estimated wind speed to a meso wind speed and use this meso wind speed at sea together with the Charnock relation for the roughness length at sea to calculate the potential wind speed at sea (see paragraph 3.2)
- From $U_{10,max}$, wave characteristics ($H_{m0,max}$, $T_{p,max}$) can be determined using the Sverdrup-Munk-Brettschneider method (Holthuijsen, 2007). For $H_{m0}(t)$ and $T_p(t)$, a symmetrical block function is assumed (see paragraph 3.3).
- The maximum wind induced setup (S_{max}) can be estimated by assuming a certain distribution of wind speeds over the North Sea and using Weenink's model (Weenink, 1957): this gives the wind-induced water level setup along the Dutch coast given different wind speeds over different areas of the North Sea and the Channel (see paragraph 3.4).
- The water level (storm surge water level) in time can be determined as a function of the astronomical tide (paragraph 3.5), the water level setup in time (S_{max} determined above, assuming a certain shape in time), storm surge duration and phase shift between tide and setup (paragraph 3.6). The maximum water level should be around the same value as $h_{Petten,max}$, which has been observed during the storm surge.
- To limit the water level to the measured maximum value, all possible, realistic combinations of wind setup, astronomical tide, storm duration and a random time shift will be tested with the Monte Carlo simulation (see paragraph 3.9).
- Six characteristic cross-shore profiles will be selected from the bathymetry; for each profile the Monte Carlo simulation will be done with the same samples (see paragraph 3.8).
- With the wave characteristics, water level, grain diameter (paragraph 3.7) and bathymetry, the XBeach runs can be done.

- As a primary model outcome, the maximum wave run-up height in the cross-shore profile will be used to calculate the probability that the shells have been deposited at NAP + 6.5 m.

The following input variables will be treated as probabilistic variables; the other input variables are taken deterministic:

$U_{zwanenburg,max}$	the (maximum) observed wind speed at Huize Swanenburgh;
D	storm surge duration;
φ	time shift, the difference between the time of the maximum tidal elevation and the maximum wind setup.

3.2 From observed wind to potential wind over sea

3.2.1 Method

The wind speed over sea needs to be calculated from the observed wind data at Zwanenburg station (see paragraph 2.3.1), as this is the only available wind data series that has been recorded during the 1775 storm surge. The following procedure ('Open water transformation') has been followed:

1 Compute the (meso) wind at blending height ($z_b \approx 60$ m) using a visual estimation of roughness at Zwanenburg for the terrain classification (Wieringa, 1996).
5 Move the regional meso wind $U(z_b)$ over land to sea, because at this height no effect of local roughness is present.
6 Determine the friction velocity u_* at sea using the (empirical) Charnock relation (Charnock, 1955) for the roughness length over water.
7 Use the Charnock relation with u_* to calculate the potential wind U_{10} (at z = 10 m) over sea.

The various above steps are explained in the paragraphs 3.2.3 – 3.2.4 below. Steps 2-4 have been taken from Van Ledden *et al.* (2005). Wind directions are not transformed from land to sea, but simply moved.

3.2.2 Potential wind

As local effects, such as bushes, trees, buildings and other obstacles, largely influence wind speeds, a reference wind speed, free of local effects, is defined. This is called potential wind. The potential wind is compliant with requirements of the World Meteorological Organization, which state that the wind measurements should refer to a height of 10 m in an unobstructed area (typical roughness length of 3 cm).

3.2.3 From observed wind to meso wind

A locally observed wind is mostly not representative for large scale phenomena such as storm surges, because wind near the earth surface is largely influenced by local obstructions. Local wind is driven by the large-scale air motion U_b at height z_b, where local obstructions are not of any influence. The height z_b is called the *blending height*, which is around 60 m above the surface (Figure 3.2).

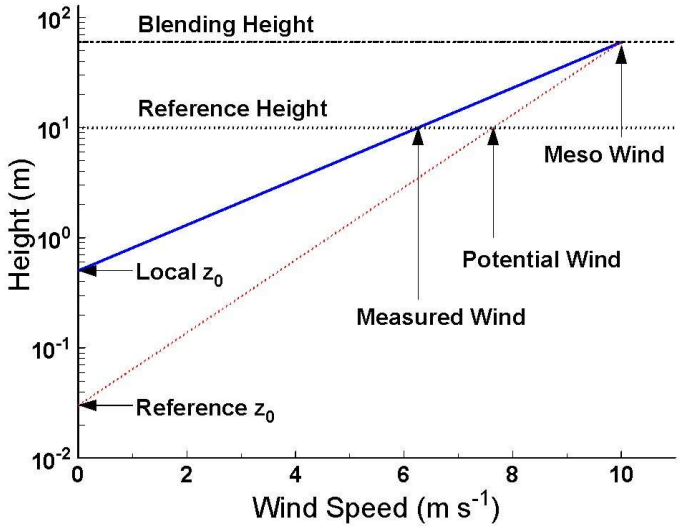

Figure 3.2 *Logarithmic wind speed transformation model. A measured wind speed at reference height with a local z_0 has a certain corresponding meso wind speed; the accompanying potential wind speed can be calculated from the meso wind with the Reference z_0. For step 1 of our transformation method, the blue line is used to calculate the wind speed at blending height; for step 4, the dotted red line is used to calculate the potential wind over sea from the meso wind (from KNMI Hydra Project).*

The wind profile below the blending height is assumed logarithmic (Wieringa (1996), eq. 2):

$$\frac{U_1}{U_2} = \frac{\ln\left(\frac{z_1}{z_0}\right)}{\ln\left(\frac{z_2}{z_0}\right)} \tag{3.1}$$

in which:

z_0 roughness length [m]
z_1 height 1 (e.g. observation height) [m]
z_2 height 2 (e.g. blending height) [m]
U_1 wind speed at height 1 (e.g. observed wind speed) [m/s]
U_2 wind speed at height 2 (e.g. meso wind speed) [m/s]

The roughness length can be determined in several ways (Wieringa, 1996), but only one method is practical for the historic measurements at Zwanenburg. This is the use of a terrain classification for visual estimation of roughness. The best choice for ordinary terrain is the updated Davenport classification (Table 3.3).

Table 3.3 *Revised Davenport terrain roughness classification (taken from Wieringa (1996))*

Class		Roughness	Landscape description
Number	**Name**	**length (m)**	
1	Sea	0.0002	Open water. tidal flat, snow, with free fetch > 3 km
2	Smooth	0.005	Featureless land with negligible cover, or ice
3	Open	0.03	Flat terrain with grass or very low vegetation, and widely separated low obstacles: airport runway
4	Roughly	0.10	Cultivated area. low crops. occasional obstacles

	open		separated by more than 20 obstacle heights *H*
5	Rough	0.25	Open landscape, crops of varying height, scattered shelterbelts etcetera. separation distance ≈ 15 *H*
6	Very rough	0.5	Heavily used landscape with open spaces ≈ 10 H; bushes. low orchards, young dense forest
7	Closed	1.0	Full obstacle coverage with open spaces ≈ H, e.g. mature forests. low-rise built-up areas
8	Chaotic	22	Irregular distribution of very large elements: city centre, big forest with large clearings

Geurts and Van Engelen (1992) state that wind speeds at Zwanenburg were always estimated based on the wind mill scale probably set up by Noppen. From the description at the KNMI website about the Zwanenburg measurements (KNMI, 2008) and paintings of the Zwanenburg station (Figure 3.3 and Figure 3.4), it can be assumed that the local roughness length is probably higher than the standard 3 cm, but how that effected the wind speed estimations, cannot be easily indicated (email correspondence KNMI Klimaatdesk). It is therefore difficult to give accurate values for the observation height and the roughness length (z_0). The values below (Table 3.4) are estimated and have been used in the simulations for the 1775 storm.

Table 3.4 Parameter values transformation observed wind to meso wind

Parameter	Symbol	Value	Remark
Observation height	z_1	10 m	In a later stage adjusted (from the (arbitrary) value of 12 m) to get a better prediction for the mean max. storm surge level in the Monte Carlo analysis.
Roughness length	z_0	0.5 m	In a later stage adjusted to 0.5 m (from the value of 0.25 m) to get a better prediction for the mean max. storm surge level in the Monte Carlo analysis (see also note in the above paragraph.

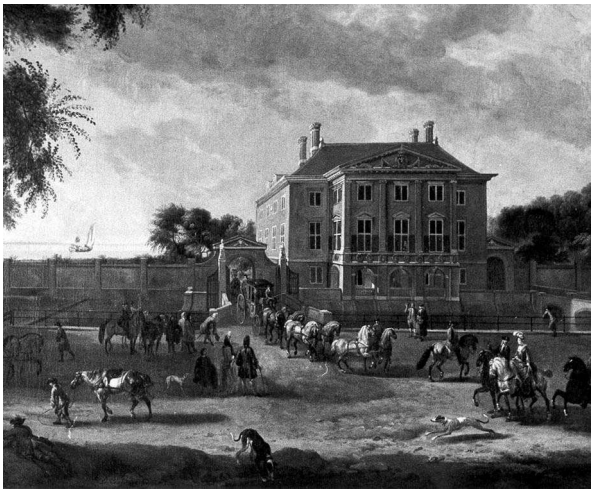

Figure 3.3 Huize Swanenburgh in 1702; painting by Dick Maas (from KNMI website)

Figure 3.4 Location of Huize Swanenburgh in 1702 on the small strip of land between the two lakes (from KNMI website)

3.2.4 From meso wind to potential wind over sea

The potential wind over sea can be computed from the meso wind using a log-normal velocity profile and the Charnock relation for the roughness length (Charnock, 1955). The Charnock relation accounts for increased roughness as wave height grows due to increasing surface stress. This computation can be described in two steps:

a First compute the friction velocity u_* belonging to the logarithmic wind profile with the meso wind $U(z_b)$ as input;

b Use the friction velocity u_* to calculate (1) the corresponding potential wind U_{10} at z=10 m or to calculate (2) the corresponding surface drag τ .

The following equations are used:

$$U = \frac{u_*}{\kappa} \ln\left(\frac{z}{z_0}\right) \tag{3.2}$$

$$z_0 = \alpha_c \frac{u_*^2}{g} \tag{3.3}$$

in which:

z height corresponding with $U(z)$ [m]
  z = 60 m for meso wind/blending height
  z = 10 m for potential wind

u_* friction velocity [m/s]

κ Von Karman constant = 0.41 [-]

α_c Charnock coefficient = 0.032 [-]

Charnock (1955) originally suggested a value of 7×10^{-3} for α_c, but later the range of values has been extended in literature between 8×10^{-3} and 6×10^{-2} (Peña and Gryning, 2008). Lower values correspond with the open ocean, while in coastal areas higher values are used. Here the same value as Van Ledden *et al*. (2005) is used: α_c = 0.032, which is the optimal value for the North Sea as suggested by Gerritsen *et al.* (1995).

The equations combined with the z-height filled in lead to the following two equations.

For step a:

$$U_{60} = \frac{u_*}{\kappa} \ln\left(\frac{60}{\alpha_c \, u_*^2 / g}\right) \tag{3.4}$$

The friction velocity u_* needs to be calculated iteratively in this step with U_{60} as input in the equation.

For step b1:

$$U_{10} = \frac{u_*}{\kappa} \ln\left(\frac{10}{\alpha_c \, u_*^2 / g}\right) \tag{3.5}$$

in which u_* is the input (calculated in step a) and U_{10} is the output. With U_{10}, the wave characteristics can be computed (see paragraph 3.3).

For step b2:

$$\tau \equiv \rho_{air} u_*^2 \tag{3.6}$$

With the friction velocity u_* and the air density ρ_{air}, the surface drag τ can be calculated. The surface drag τ is used in Weenink's model to compute wind induced water level setup (see paragraph 3.4).

3.3 From potential wind over sea to wave characteristics

With the maximum potential wind over sea, $U_{10,max}$ (see paragraph 3.2), the significant wave height H_{m0} and wave peak period T_p can be calculated using the so-called SMB (Sverdrup-Munk-Brettschneider) growth curves for finite-depth water (Holthuijsen, 2007). These parameterizations use dimensionless parameters that make them applicable to a large range of situations (from storms at sea to small-scale flume experiments). The finite-depth equations account for both depth-limitation and fetch-limitation. The coefficient set used is the one derived by Young and Verhagen (1996) and modified by Breugem and Holthuijsen (2007).

The growth curves for H_{mo} and T_p are given by the following dimensionless expressions, which are visualized in Figure 3.5:

$$\widetilde{H} = \widetilde{H}_\infty \left[\tanh(k_3 \tilde{d}^{m_3}) \tanh\left(\frac{k_1 \widetilde{F}^{m_1}}{\tanh(k_3 \tilde{d}^{m_3})} \right) \right]^p \tag{3.7}$$

$$\widetilde{T} = \widetilde{T}_\infty \left[\tanh(k_4 \tilde{d}^{m_4}) \tanh\left(\frac{k_2 \widetilde{F}^{m_2}}{\tanh(k_4 \tilde{d}^{m_4})} \right) \right]^q \tag{3.8}$$

in which:

$k_1 - k_4$, $m_1 - m_4$	coefficients (see Table 3.5)
$\widetilde{H}_\infty$ and $\widetilde{T}_\infty$	coefficients (see Table 3.5)
$\widetilde{H} = \frac{gH_{m_0}}{U_{10}^2}$	dimensionless significant wave height
$\widetilde{T} = \frac{gT_{peak}}{U_{10}}$	dimensionless peak wave period
$\tilde{d} = \frac{gd}{U_{10}^2}$	dimensionless water depth
$\widetilde{F} = \frac{gF}{U_{10}^2}$	dimensionless fetch
H_{m_0}	significant wave height [m]
U_{10}	potential wind speed over sea [m/s]
T_{peak}	peak wave period [s]
d	water depth [m]
F	fetch length [m]

Table 3.5 Coefficients representing wind-wave growth in the idealised situation (from Holthuijsen (2007))

Deep water and finite-deep water coefficients			
Young and Verhagen (1996) modified by Breugem and Holthuijsen (2007)			
$\widetilde{H}_\infty$	0.24	$\widetilde{T}_\infty$	7.69
k_1	4.14×10^{-4}	k_2	2.77×10^{-4}
m_1	0.79	m_2	1.45
p	0.572	q	0.187
k_3	0.343	k_4	0.10
m_3	1.14	m_4	2.01

For this research, the following values for the depth and the fetch length in the Southern North Sea have been used:

Fetch length F : 500 km (average width of the North Sea)
Water depth d : 29 m (estimated from ZuNo model, (Roelvink et al., 2001))

With a quick sensitivity analysis, it has been concluded that in storm surge conditions in the southern North Sea, wave characteristics are depth-limited rather than fetch-limited. Therefore, the exact fetch length is not important for wind (waves) from north-west, as this is not the limiting factor as long as it is not much shorter than 500 km.

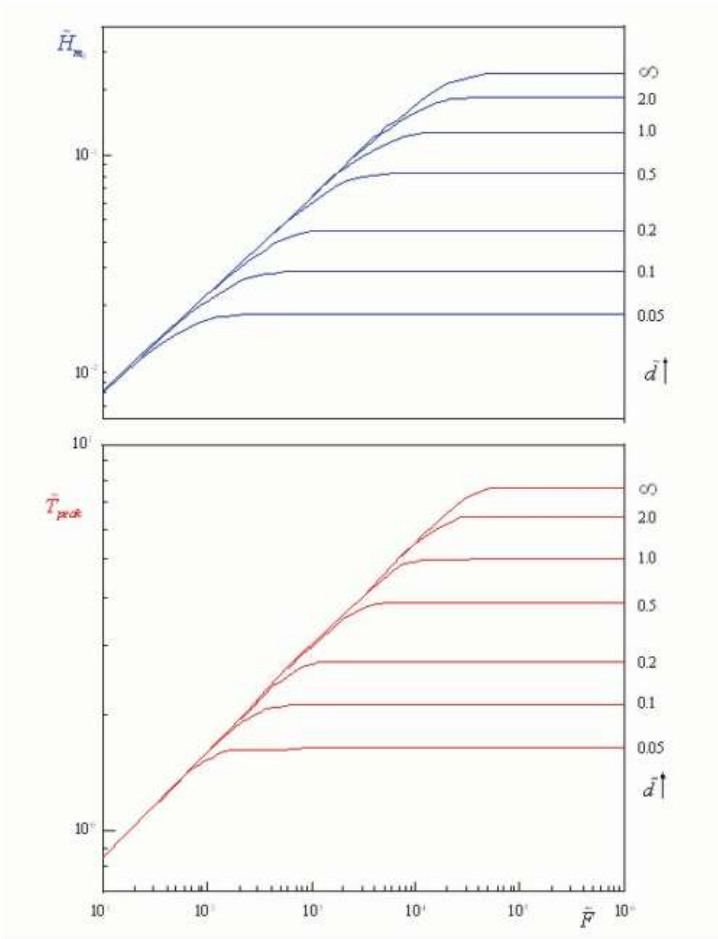

Figure 3.5 The dimensionless significant wave height and period (left hand vertical axes) as a function of dimensionless fetch (horizontal axes) and depth (right-hand vertical axes) (from Holthuijsen (2007)).

3.4 From potential wind over sea to maximum wind setup

With the maximum potential wind speed over sea, as calculated in paragraph 3.2, it is possible to calculate a maximum wind-induced water level setup in Heemskerk using Weenink's method (Weenink, 1957).

Weenink developed a mathematical method of computing the effect of the wind on the sea levels along the Netherlands coast from the wind field over the North Sea and the Channel. The method is an equilibrium method, since its basic idea is that the main part of the wind effect is what is the equilibrium effect (i.e. the effect that would be present at a certain moment if the wind field prevailing at that moment had been stationary all the time). The actual wind effect may be derived from the equilibrium effect by applying certain corrections, taking into account the dynamic effects when non-stationary (Delta committee, 1961).

In a shallow sea with sufficiently strong tidal currents, the slope of the sea surface in equilibrium state is determined by the wind stress on the water and by the volume transport of the current, which gives a Coriolis force and a bottom friction stress. The height at an arbitrary place can then be computed (using a water level boundary at the Northern edge of the North Sea) as a sum of two independent factors: the static effect (depending on the wind stress field) and the current effect (depending on the current field). The current effect may be regarded as composed of three components: a "wind shear effect", a "bottom slope effect" and a "leak effect".

For practical computational purposes, the wind field acting upon the North Sea and the Channel has been schematized into a pattern of five subfields, each of which has a uniform wind field (Figure 3.6). Since the equations involved are linear, the wind effect at a particular place may be considered as being built up from the separate contributions of the subfields.
After a quantitative relation between the winds of the subfields and the wind effect at one particular place has been determined empirically, the remaining empirical parameters have been computed and the relation between the wind field and the equilibrium wind effect at any other place of the coast can be computed. Weenink (1957) did this for various places; for the Dutch coast these are Vlissingen, Hoek van Holland, Den Helder and the Eierlandse Gat.

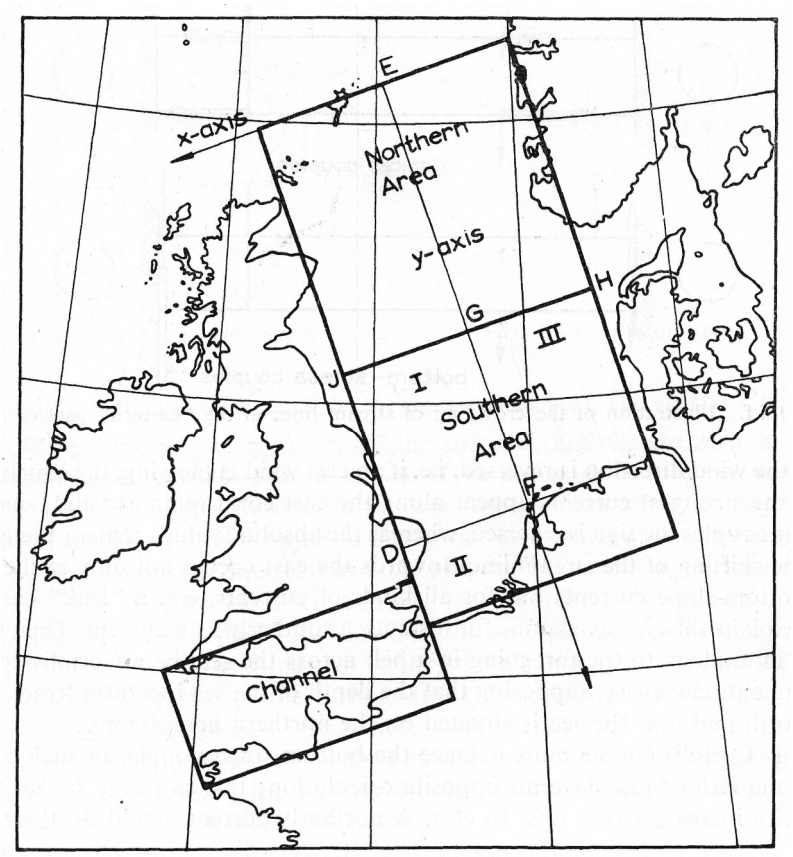

Figure 3.6 *The five subfields used in Weenink's method: the Northern Area, Area I, II and III in the Southern North Sea and the Channel. Each area has a uniform wind field (from Weenink, 1957).*

As he did not calculate parameters for Heemskerk, the values for Den Helder have been used, as this location is closest to Heemskerk.

Almost all coefficients / parameters for Weenink's method are determined by Weenink himself. The only input parameters left are the wind speeds and wind directions (relative to the model's y-axis) for every subfield. The wind speed in Area II is the wind speed calculated with the 'open water transformation' (paragraph 3.2); the wind speeds in the other areas have a fixed ratio with the wind speed in Area II. This ratio and the wind direction have been taken identical to the February 1953 storm surge, as that was a large storm surge from northwestern direction as well. In Figure 3.7 the grid of Weenink's method is laid over a wind field of the 1953 storm and it has been estimated what the average wind speeds and directions in every subfield are. The same ratios and directions have been used for the 1775 simulations.

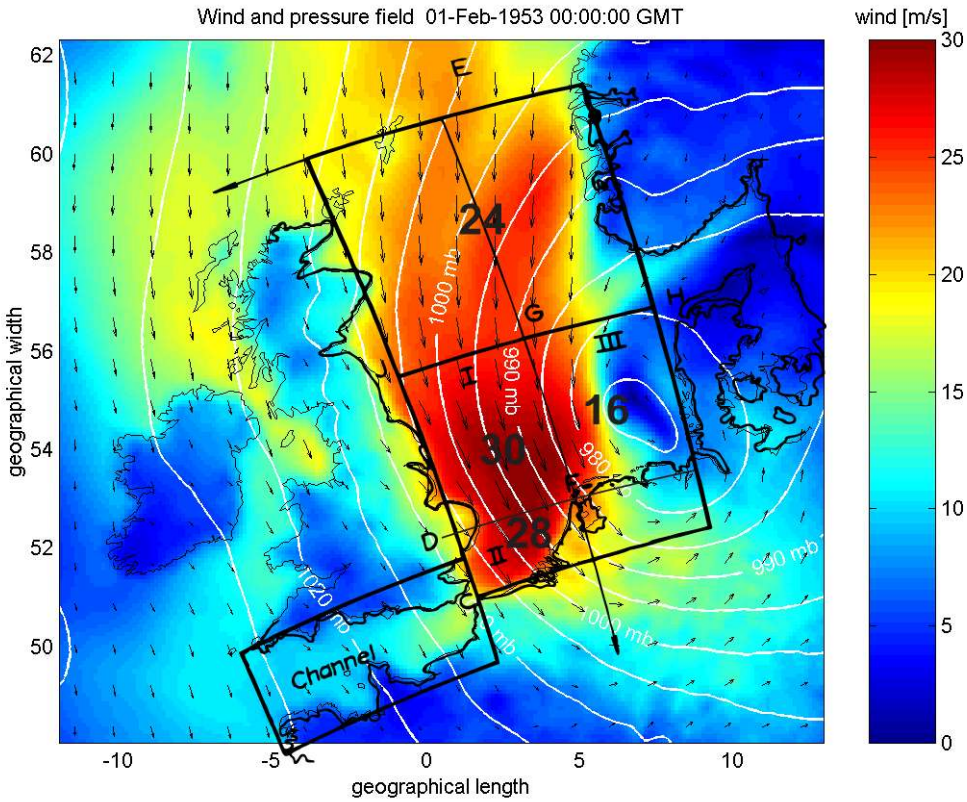

Figure 3.7 *The five subfields of Weenink's method over the wind and pressure field of February 1st, 1953 (0:00 GMT). The black numbers give the average wind speed in each subfield (adapted from Van Haaren (2005)).*

The values used for the wind speed ratios and wind directions in every subfield can be found in Table 3.6.

Table 3.6 *Values for wind speed ratio to area II and wind direction in all areas of Weenink's method.*

Subfield	Wind speed ratio to area II	Wind direction (in degrees w.r.t. y-axis)
Northern Area	24/28	20
Area I	30/28	335
Area II	1	325
Area III	16/28	10
Channel	*	350

* The equation for the Channel area does not use wind speed (or surface drag) as input, but V_S, 0.75 times the gradient wind speed. As the contribution of the Channel area to the wind setup is not significant, this value has been fixed at 12 m/s.

3.5 Astronomical tide

The tide in Heemskerk in 1775 has been determined with tidal analysis, using data for the entire southern North Sea for 1998 and (hourly) observations in Katwijk from 1737-1739, made for the design of a new outlet sluice (Buisman, 2006). First, tidal time series for Katwijk and Heemskerk for the entire year 1998 have been computed using the ZuNo model in Delft3D (Roelvink *et al.*, 2001). These time series have been analysed with T_Tide, a Matlab toolbox for tidal / harmonic analysis, using 59 tidal components (Pawlowicz *et al.*, 2002).

The observations from Katwijk (1737-1739) are available from the DONAR database of Rijkswaterstaat (www.waterbase.nl). These observations have also been analysed, this time with the R_T_Tide toolbox (Leffler and Jay, 2009), a robust fitting implementation of T_Tide, because it handles non-zero mean sea levels and limited datasets better. With the historical tidal components for Katwijk, based on the 1737-1739 data, a prediction for the tide in Katwijk in 1775 has been made.

Finally, the tidal components for Heemskerk in 1775 have been calculated, assuming identical ratios for the tidal components (amplitude and starting phase) in Katwijk/Heemskerk in 1775/1998:

$$\frac{a_{i,Heemskerk,1998}}{a_{i,Heemskerk,1775}} = \frac{a_{i,Katwijk,1998}}{a_{i,Katwijk,1775}} \tag{3.9}$$

The resulting tidal time series for Heemskerk is shown in Figure 3.8. It can be seen that the mean sea level is around NAP - 18 cm. This is in agreement with other sources/research (personal communication A. Bijlsma; Jensen et al., 1993; Hollebrandse, 2005), stating that the relative sea level rise was very small or absent before around 1900. Data processed by Rijkswaterstaat with their tidal analysis software, give a MSL of NAP – 16 cm, being comparable with the data found with R_T_Tide.

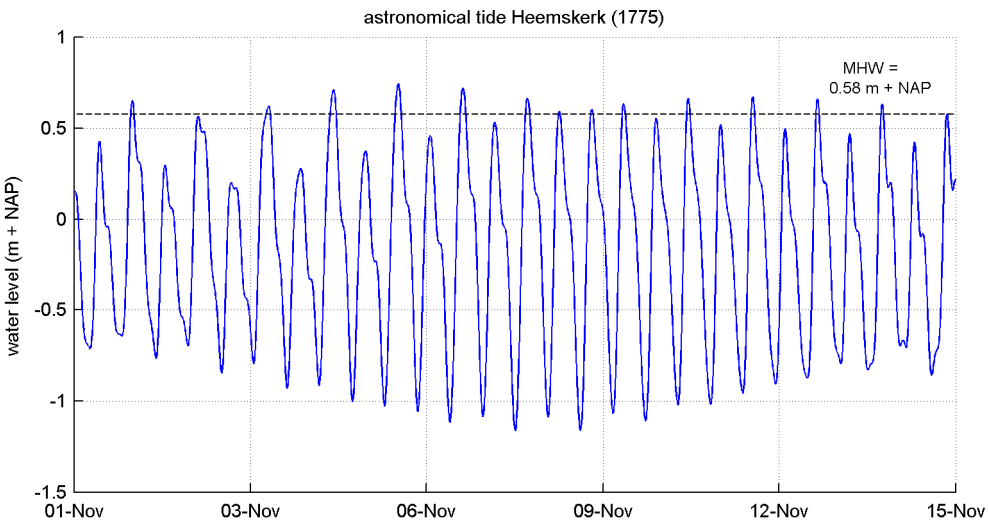

Figure 3.8 Astronomical tide Heemskerk for the period November 1, 1775 to November 15, 1775.

3.6 Storm surge duration and shape

Research into storm surge duration on the North Sea has been done by Vrijling and Bruinsma (1980) and later by Van Weerden *et al.* (1987). The latter concludes that the setup shape in time is distinctive and independent from the course of the wind field above the North Sea. Vrijling and Bruinsma (1980) found virtually no correlation between the maximum wind setup and the duration of the setup. Van Weerden *et al.* (1987) evaluated three shapes for the water level setup in time using 125 storm surge events in the North Sea for the period 1898-1986. The shapes under investigation were:

- a trapezoidal shape
- a cosine^2 shape
- a triangular shape

They conclude that the cosine^2 shape gives a close approximation of the rising part of the setup shape, while it also gives the best approximation of the entire setup shape. Therefore, the cosine^2 shape will be used to describe the shape of the setup in time (Figure 3.9):

$$s(t) = S_{\max} \cos^2\left(\frac{\pi t}{D}\right) \tag{3.10}$$

Where:

S_{max} Maximum wind setup during the storm

D Duration of the wind setup

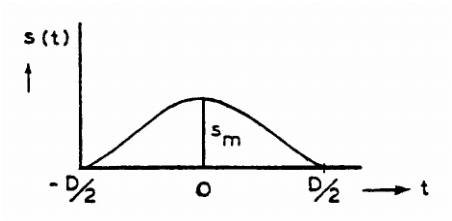

Figure 3.9 The wind setup as a function of time (cos^2 shape) (from Vrijling and Bruinsma, 1980).

The duration of the wind setup (storm surge duration) was found to be log-normally distributed. See Table 3.7 for the statistical values (Van Weerden *et al.*, 1987). These values have also been used in this research.

Table 3.7 Statistical values of chosen distribution for the storm surge duration.

Schematization	Distribution	μ	σ
cosine^2 shape	log-normal	ln(38.2)	ln(1.43)

A storm surge can now be represented as a linear superposition of the astronomical tide (paragraph 3.5) and a certain (random) wind setup (paragraph 3.6), whose maximum occurs at a random time shift (phase difference) φ with respect to the maximum tidal elevation closest to the maximum wind setup (S_{max}). As the astronomical tide and the wind setup are assumed to be independent, the time shift φ has a uniform probability density function. For symmetry reasons (the astronomical tide is almost symmetrical due to the influence of the M_2 component), time shifts of more than one tidal period T_0 are irrelevant and the probability density function of φ becomes:

$$P(\phi) = 0 \qquad for\ |\phi| > \tfrac{1}{2}T_0$$

$$P(\phi) = \frac{1}{T_0} \qquad for\ |\phi| \le \tfrac{1}{2}T_0$$

For this research, it is more convenient to apply the time shift relative to a fixed moment in time than to exactly high water, because the moment of the maximum storm surge was, according to the reports, somewhere in the night between 14 and 15 November 1775. Therefore, the time shift has been applied to 15 November 1775, 0:00.

3.7 Grain diameter

The grain diameters of the sediment (d_{50} and d_{90}) have been determined by a sieve analysis of one of the samples from the storm surge layer (taken from TV site; HK7). Before the sieve analysis, shells and shell fragments have been removed from the sample. Figure 3.10 shows the result of the sieve analysis, while Table 3.8 gives the values needed for the XBeach model runs.

Table 3.8 Values of the sediment parameters used in XBeach.

Sediment parameters	
d_{50}	210 µm
d_{90}	280 µm

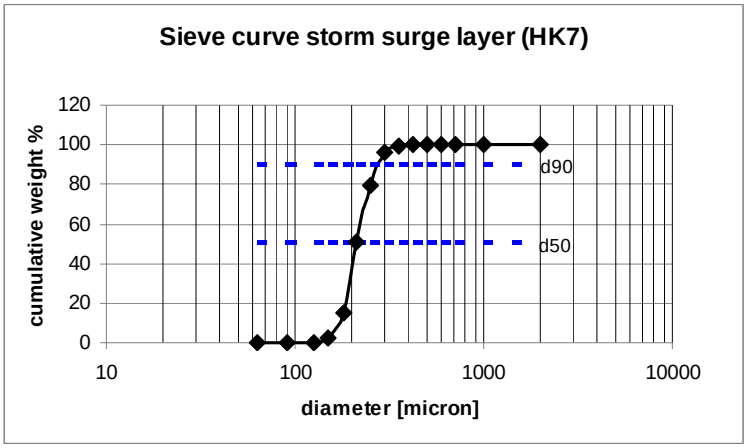

Figure 3.10 Sieve curve of a sand sample from the storm surge layer (TV site; HK7).

3.8 Bathymetry & cross-shore profiles

It is assumed that the bathymetry below the nearshore zone did not change much over the last centuries (Haartsen *et al.*, 1997; see also paragraph 2.4.1). The bathymetry of the nearshore and the beach may have changed, but it is not clear how much that will influence the storm surge simulations. Therefore, the same bathymetry up to the beach has been used for the 1775 simulations as for the 2007 calibration runs (paragraph 4.2.1).This means that two data sources have been used to construct the bathymetry: Vaklodingen data obtained in 2005 for the deeper part of the bathymetry (lower than NAP -6 m) and JARKUS data obtained in 2007 for the nearshore and beach part of the bathymetry.

Because no accurate data of the dune topography in the 18th century is available, the situation is approximated using today's available high density altitude data (Dutch: Actueel Hoogtebestand Nederland (AHN); Actual Elevation Model of the Netherlands). It is assumed that the dunes behind the first, partially artificial, dune row ('zeereep') still have their natural shape (Figure 3.11). Thus, if the first artificial dune row is removed and the remaining dune area moved towards the beach, it will resemble a more or less natural situation.

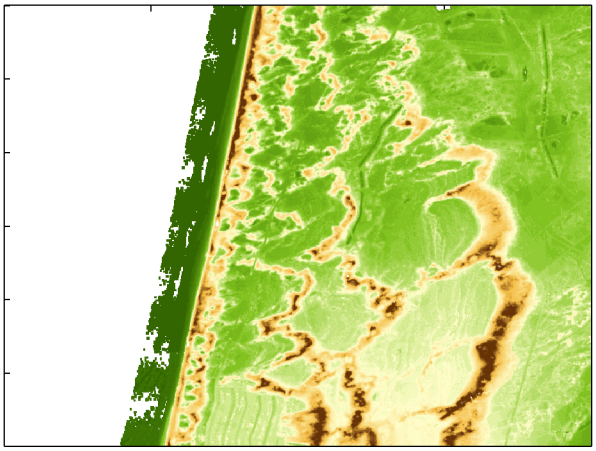

Figure 3.11 *Detailed AHN data for the Heemskerk dune area (data from 2007; source: AHN, Rijkswaterstaat).*

Construction topography 1775

The topography used for the 1775 simulations, has been constructed in the following way:

- Beach data and 'zeereep' data were removed from the AHN data, following the height contours of the 'zeereep'.
- The remaining AHN data was moved 60 m in westerly direction (towards the beach/sea) to re-establish the position of the coastline.
- With all the remaining data (Vaklodingen, Jarkus and AHN), an XBeach bottom with varying grid sizes in x- and y-direction was interpolated.
- Three locations along the beach were selected to create low-lying areas (gaps) for allowing overwash; one area has been created with a sill at NAP + 5 m, one area was created with an average height of NAP + 5 m and finally the last area has been created with an average height of NAP + 3 m. The low areas are about 150-200 m wide, to prevent quick filling-in of gaps that are too narrow (Steijn *et al.*, 2008).
- Finally, six profiles have been selected for the 1D-runs. Three profiles were selected from the low-lying areas created in the step before and three profiles were selected from the remaining areas (with high dunes directly after the beach).

The profiles were selected to be distinctive / characteristic:

(1) A profile with a relative high-lying, but small beach with a (moderate) steep dune behind it;
(2) A profile with a relative high-lying and wide beach with a steep dune directly behind it;
(3) A profile with a relative low-lying beach with a steep dune behind it;
(4) A profile with a low area with a sill at NAP + 5 m (average height low area NAP + 3 m);
(5) A profile with a low area with a height of approximately NAP + 3 m;
(6) A profile with a low area with a height of approximately NAP + 5 m.

A plan view of the 2D bathymetry with the locations of the created low areas and the 'TV site' is shown in Figure 3.12. The six cross-shore profiles with a close-up of the beach and dune areas can be found in Figure 3.13 - Figure 3.18.

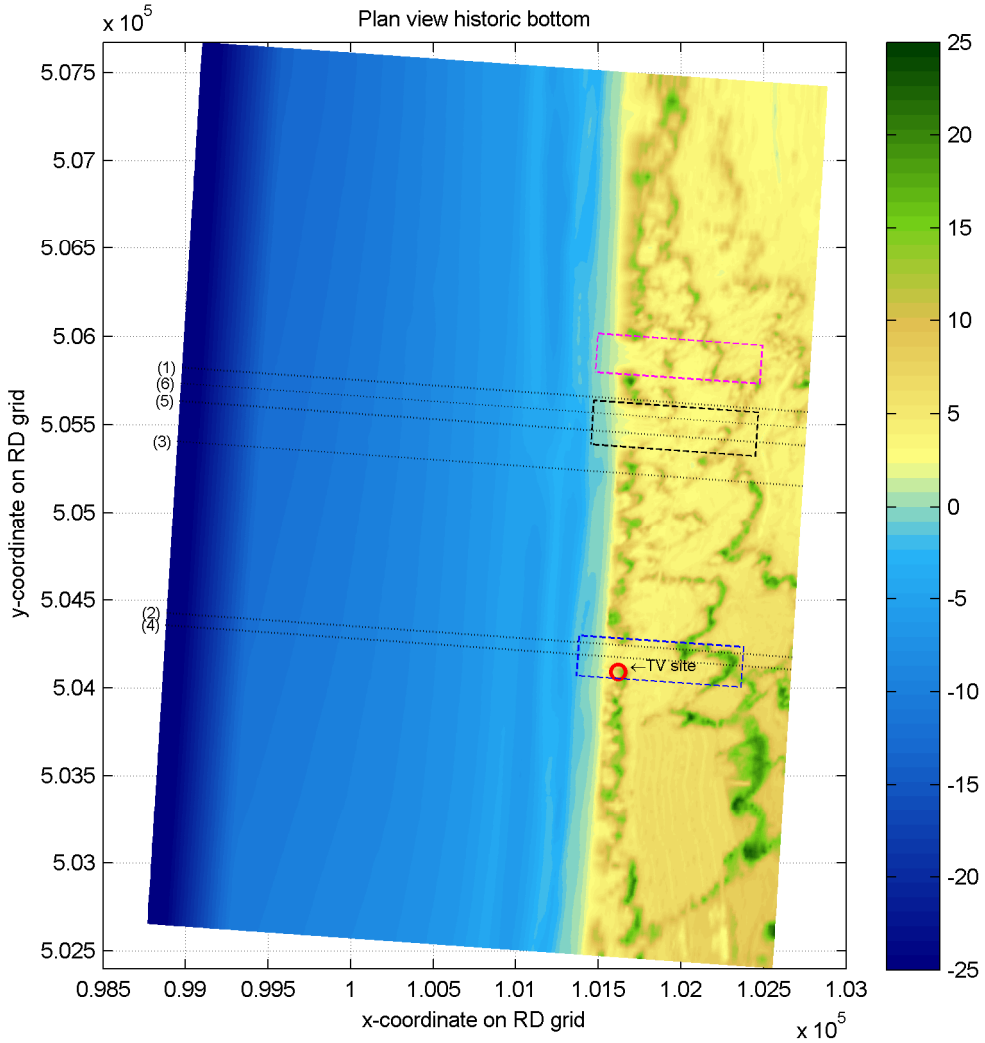

Figure 3.12 *Plan view of the historic bottom with the low areas indicated by the rectangles. The six profiles are indicated by the dotted lines.*

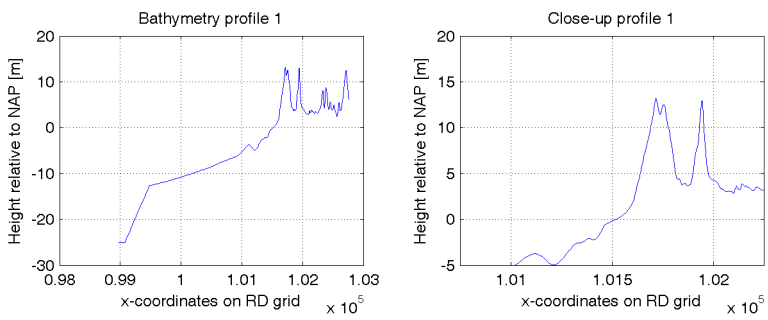

Figure 3.13 *Bathymetry profile 1 (left panel) and detail beach and dune area profile 2 (right panel).*

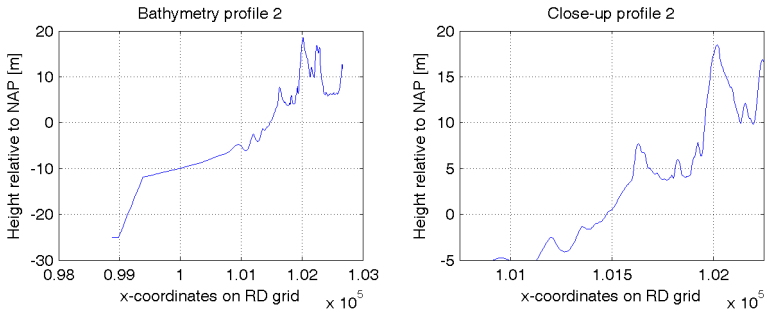

Figure 3.14 *Bathymetry profile 2 (left panel) and detail beach and dune area profile 2 (right panel).*

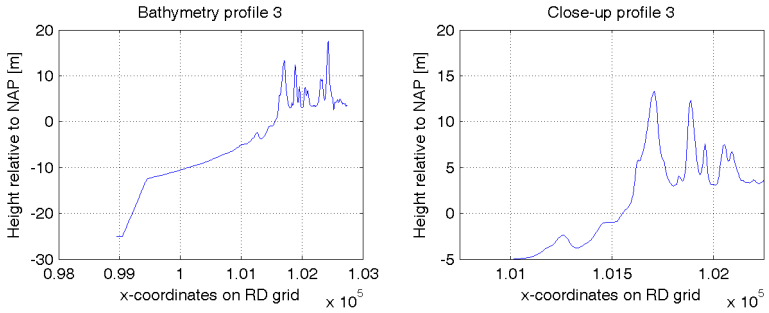

Figure 3.15 *Bathymetry profile 3 (left panel) and detail beach and dune area profile 3 (right panel).*

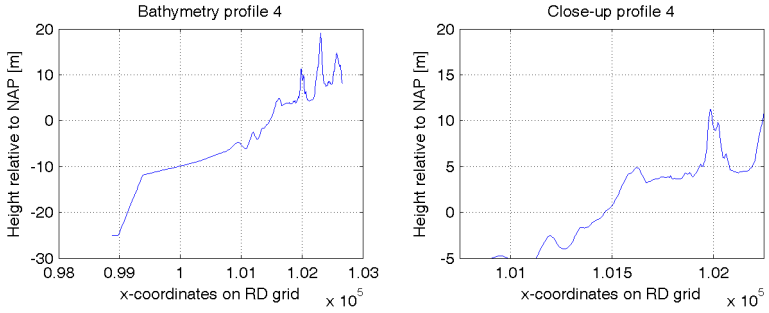

Figure 3.16 *Bathymetry profile 4 (left panel) and detail beach and dune area profile 4 (right panel).*

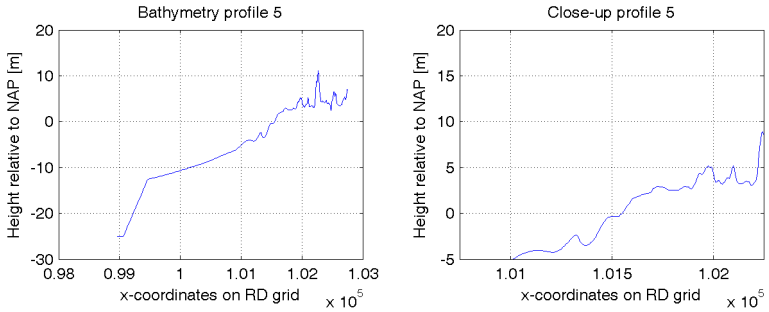

Figure 3.17 *Bathymetry profile 5 (left panel) and detail beach and dune area profile 5 (right panel).*

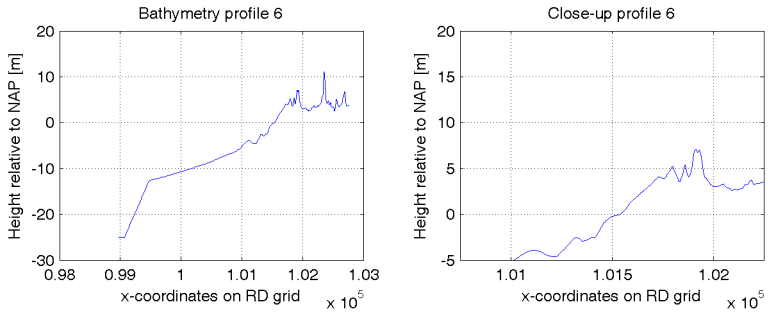

Figure 3.18 *Bathymetry profile 6 (left panel) and detail beach and dune area profile 6 (right panel).*

3.9 Monte Carlo simulation

Because there is limited data available from the November 1775 storm, there are many uncertainties in boundary conditions, effects, etc when modelling this storm. A probabilistic approach can be used to deal with these uncertainties. In a probabilistic approach, each input variable to the probability function (reliability function) is or can be a random variable with a certain distribution (e.g. normal, exponential, Weibull, uniform distribution, etc.). There are different calculation methods, classified on the level of probabilistics and linearization involved (CUR, 1997).

For this research, a Monte Carlo simulation has been applied. It is a level III method, which means that the probability density functions of all variables are considered and no linearization of the reliability function has taken place. The Monte Carlo simulation method uses the possibility of drawing random samples from the distributions of the input parameters. If a large number of samples are drawn, a good estimation of the realization space can be made. For this research, a large number of simulations with slightly different boundary conditions result in a large number of post-storm situations. The boundary conditions that have been varied (the probabilistic variables) are the maximum wind speed in Zwanenburg $U_{Zwanenburg,max}$, the storm surge duration D and the time shift φ (see paragraph 3.1). The output value of interest is the (maximum) wave run-up relative to NAP $Z_{2\%}$, because this will give an idea if the level at which the storm surge layers have been found, is reaches during the simulation.

Based on the central limit theorem, the relative error ε of a Monte Carlo simulation is normally distributed, provided the number of simulations n is sufficiently large (CUR, 1997). The probability that the relative error is smaller than the given value E is then:

$$P(\varepsilon < E) = \Phi\left(\frac{E}{\sigma_\varepsilon}\right) \tag{3.11}$$

in which:

ε Relative error in the Monte Carlo simulation
E Wanted/required limit value for the relative error
σ_ε Standard deviation of the relative error
Φ Standard normal distribution

Thus, for a reliability of $\Phi(k)$, the relative error is smaller than E = k σ_ε. For a wanted k (level of reliability) and E, the required minimum number of simulations to run in a Monte Carlo simulation can be determined using the following equation (CUR, 1997):

$$n > \frac{k^2}{E^2}\left(\frac{1}{P_f} - 1\right) \tag{3.12}$$

in which:

n number of simulations

k level of reliability in Φ(*k*)

E relative error

P_f probability of failure

For a wanted reliability of 95% (Φ(*k*) = 0.95 → *k* = 2 for the standard normal distribution) and a relative error *E* = 0.1, the required number of simulations is:

$$n > 400\left(\frac{1}{P_f} - 1\right) \tag{3.13}$$

In this case, we are interested in the mean value of the run-up, so P_f = 0.5. This leads to a minimum number of required simulations of *n* = 400.

As that requires still a large simulation time, a lower value for *n* is chosen (*n* = 200). For *n* = 200, P_f = 0.5 and *k* = 2, the maximum relative error *E* will be 0.14 (instead of 0.1); the reliability of a maximum relative error *E* = 0.1, is 84% (*k* = 1.41).

3.10 Samples Monte Carlo simulation

For the Monte Carlo simulation, 200 samples from the above random variables ($U_{Zwanenburg,max}$ *D* and *φ*) have been drawn. Below are the results of the realizations of $U_{Zwanenburg,max}$ in Figure 3.19 and *D* in Figure 3.20. As *φ* is uniformly distributed, the sampled values are not displayed.

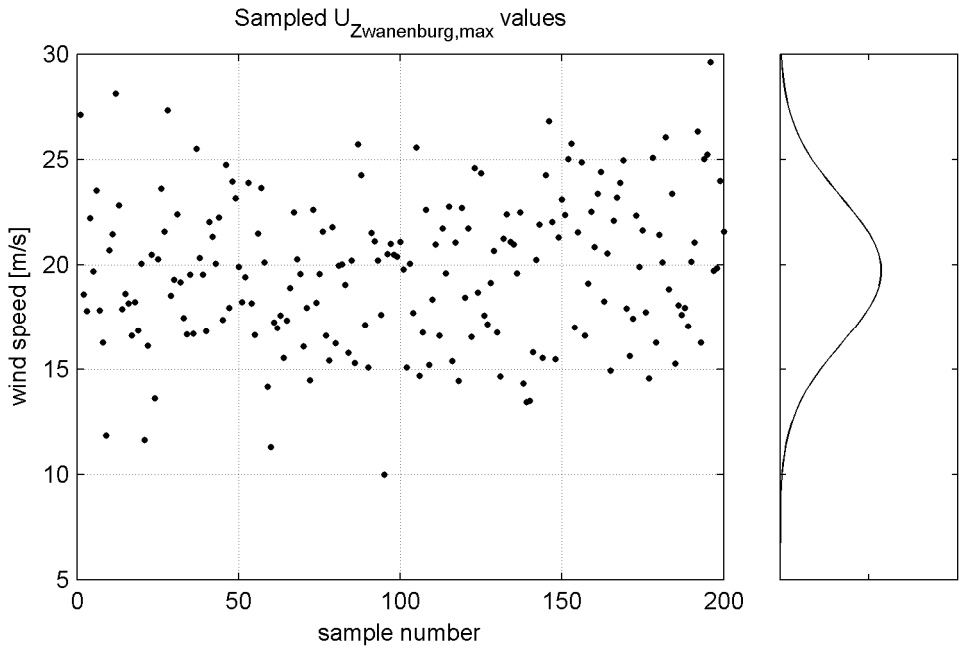

Figure 3.19 Sampled values for $U_{Zwanenburg,max}$ (left panel) and its normal distribution (right panel).

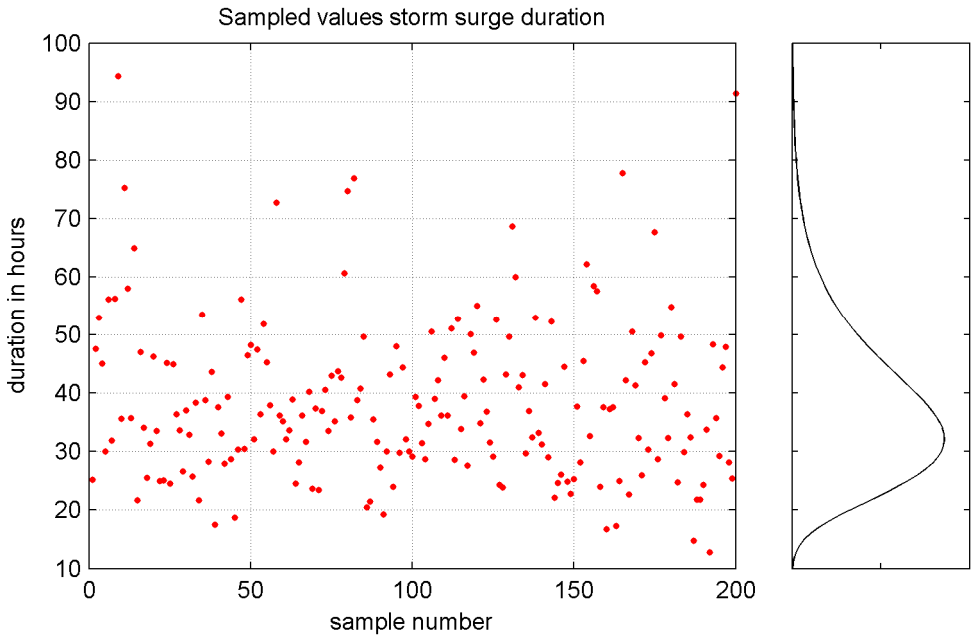

Figure 3.20 *Sampled values for the storm surge duration D (left panel) and its lognormal distribution (right panel).*

With the sampled values for $U_{Zwanenburg,max}$, D and φ and with the 'Open water transformation' and Weenink's model (see Figure 3.21), the following water levels at the coast near Heemskerk are computed (Figure 3.22).

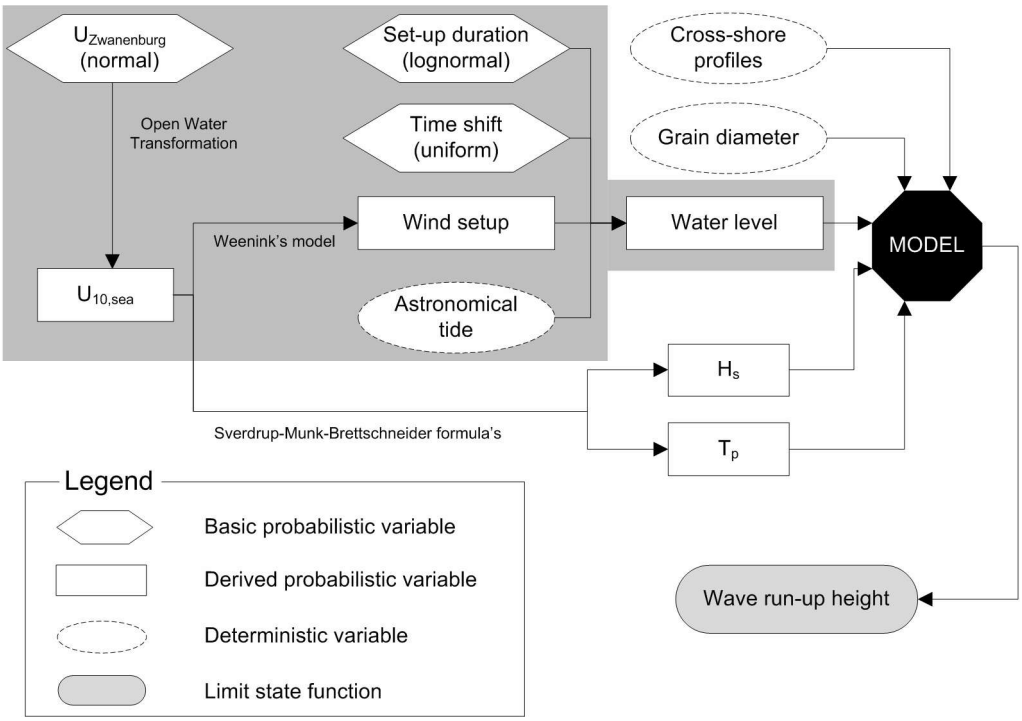

Figure 3.21 *The variables and transformations in the grey box are used to compute the water level.*

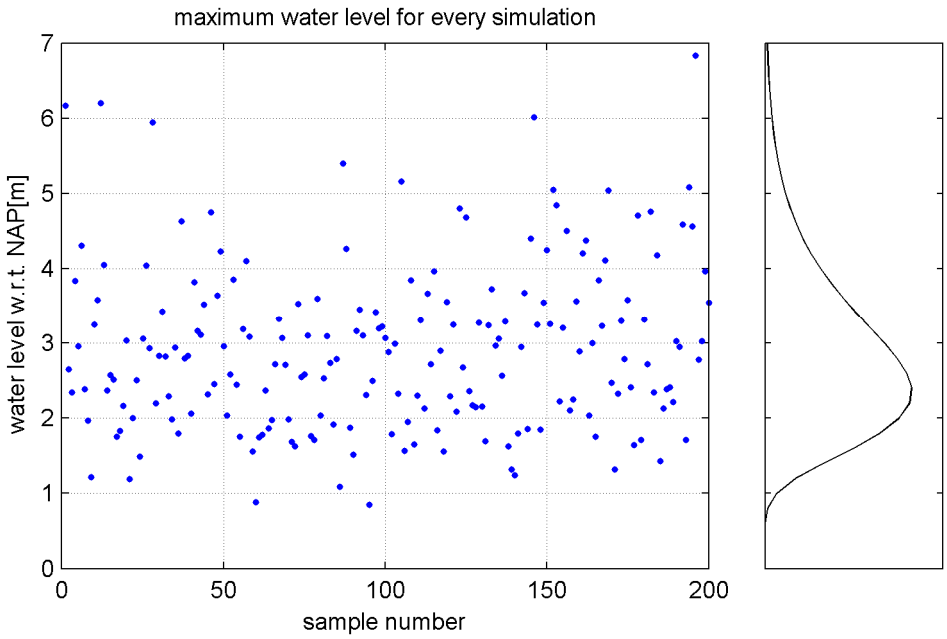

Figure 3.22 *Maximum storm surge level for all 200 MC samples (left panel) and its (fitted) lognormal distribution (right panel).*

Figure 3.23 shows the maximum values for H_{m0} (significant wave height at deep water) and T_p (peak wave period) based on the sampled $U_{Zwanenburg,max}$ values and the SMB growth curves.

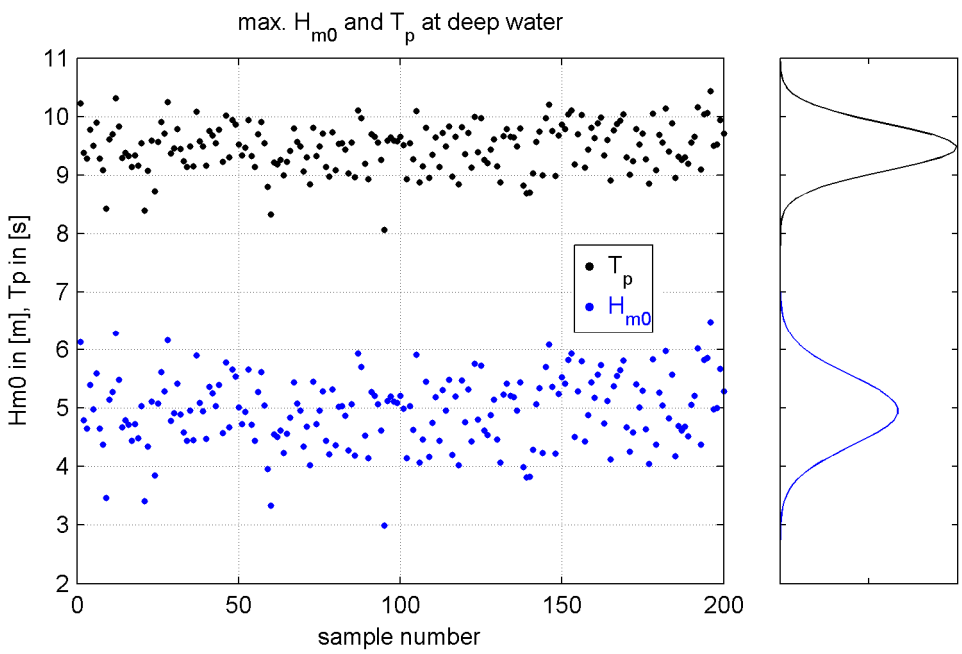

Figure 3.23 *Maximum H_{m0} and T_p for all 200 MC samples (left panel) and their (fitted) normal distributions (right panel).*

3.11 Summary

The following is a summary of the results of this chapter:

- A modelling framework has been set up to transform all available historical data to boundary and initial conditions for the XBeach model.
- It is easy to change parts of the modelling framework as other data comes available, such as air pressure fields over the North Sea.
- Although historical observed/estimated wind speed data from Huize Swanenburgh was available, it is difficult to translate this data to useable form.
- The tidal time series computed for Katwijk, on which the time series for Heemskerk is based, is comparable to the time series calculated by Rijkswaterstaat.
- The mean calculated maximum storm surge water level for Heemskerk (based on 200 samples and calculated with the transformations in the framework) is comparable to the recorded (observed) maximum storm surge level in Petten.

4 XBeach

This chapter introduces the numerical model XBeach, developed by the joint forces of the UNESCO|IHE, Deltares and Delft University of Technology. XBeach is a nearshore numerical 2DH (depth averaged) model that is capable of modelling the natural coastal response during time-varying storm and hurricane conditions, including dune erosion, overwash and breaching (Roelvink *et al.*, accepted). The program contains a number of routines for short wave propagation, non-linear shallow water equations, sediment transport and coupled morphology that are designed to cope with extreme storm and hurricane conditions. This makes XBeach the preferred model to simulate the conditions during the 1775 storm surge. In paragraph 4.1, the XBeach model is presented. Its functionality, the numerical schemes that are used, the applied coordinate system and computational grid and the required boundary conditions are described. In paragraph 4.2, the application of XBeach for the Heemskerk region is tested, using data from the November 2007 storm surge. For detailed information about the XBeach model, the reader is referred to McCall (2008) and Roelvink *et al.* (accepted).

4.1 XBeach model description

4.1.1 Model functionality and numerical implementation

The XBeach code has the following functionalities:

- Depth-averaged shallow water equations including time-varying wave forcing terms; combination of sub- and supercritical flows;
- Time-varying wave action balance including refraction, shoaling, current refraction and wave breaking;
- Roller model, including breaker delay
- Wave amplitude effects on wave celerity;
- Depth-averaged advection-diffusion equation to solve suspended transport;
- Bed updating algorithm including possibility of avalanching;
- Numerical scheme in line with Stelling and Duinmeijer method, to improve long-wave runup and backwash on the beach. The momentum-conserving form is applied, while retaining the simple first-order approach. The resulting scheme has been tested against the well-known Carrier and Greenspan test.
- Generalised Lagrangean Mean (GLM) approach to represent the depth-averaged undertow and its effect on bed shear stresses and sediment transport.
- Roelvink (1993) wave dissipation model for use in the nonstationary wave energy balance (in other words, when the wave energy varies on the wave group timescale)
- Soulsby – Van Rijn transport formulations.
- Multiple sediment fractions and bed layer bookkeeping.
- Automatic time step based on Courant criterion, with output at fixed or user-defined time intervals.
- Avalanching mechanism with separate criteria for critical slope at wet or dry points.
- MPI (Message Passing Interface) implementation with automatic domain decomposition for parallel (multi-processor) computing.

The propagation of short wave action and roller energy can be computed with two numerical schemes, including an explicit upwind scheme and an explicit (central) Lax-Wendroff scheme. Hydrodynamics are computed explicitly and the momentum advection terms are computed

with a first-order momentum conservative scheme (according to Stelling and Duinmeijer). The pressure gradient, horizontal viscosity, the advection-diffusion equation for sediment and the bed update are explicitly solved for with an upwind scheme.

4.1.2 Coordinate system and grid

XBeach uses a coordinate system with the computational x-axis always oriented towards the coast, approximately perpendicular to the coastline, and the y-axis oriented alongshore. This coordinate system is defined relative to world coordinates (x_w,y_w) through the origin (x_{ori},y_{ori}) and the orientation alfa (defined counter-clockwise with respect to the x_w-axis.

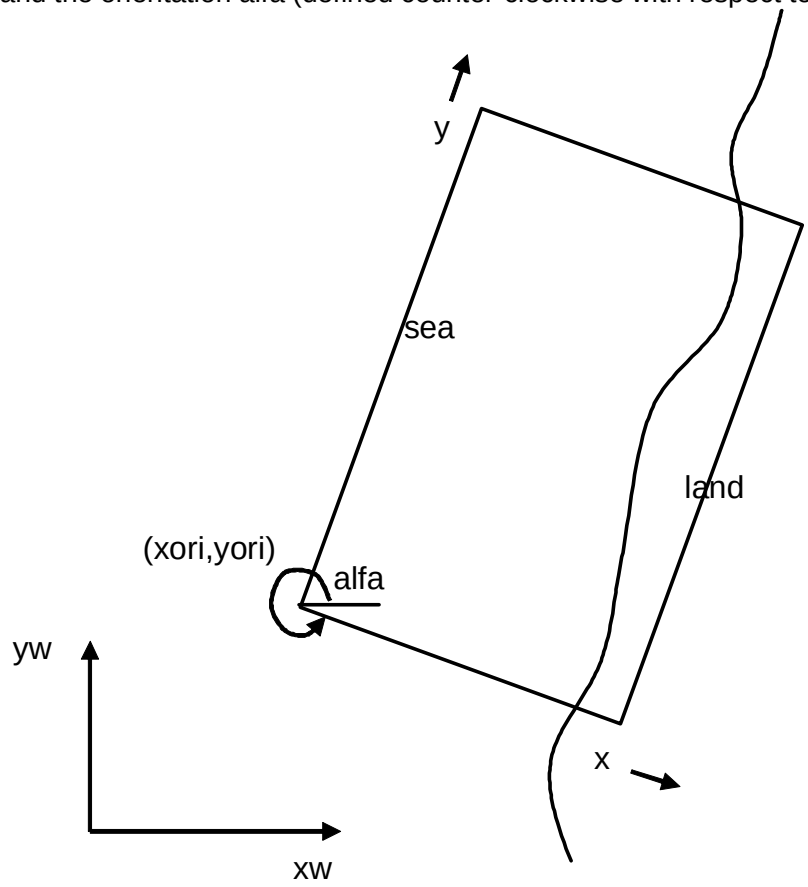

Figure 4.1 XBeach coordinate system

The applied grid is a rectilinear, non-equidistant, staggered grid, where bed levels, water levels, water depths and concentrations are defined in cell centres, and velocities and sediment transports are defined at the cell interfaces ('u- and v-points'). In the wave energy balance, the energy, roller energy and radiation stress are defined in the cell centres, whereas the radiation stress gradients are defined at the u- and v-points. Velocities u and v at the cell centres (see Figure 4.2) are obtained by interpolation and are for output purpose only.

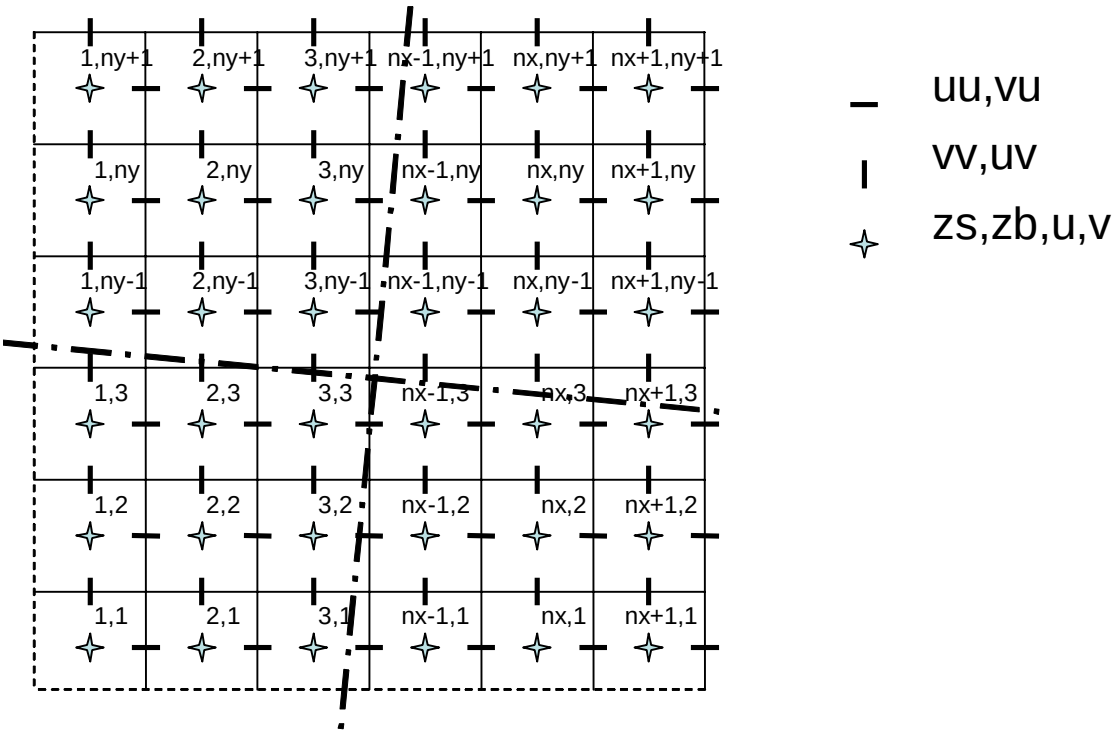

Figure 4.2 Staggered grid in XBeach

4.1.3 Boundary conditions

XBeach requires boundary conditions for the water level and offshore wave conditions. Water level time series can be applied to all four corners of the model domain or only on the offshore boundary. Wave forcing is only applied on the offshore boundary. XBeach allows the generation of spatially, directionally and temporally varying irregular wave groups and associated bound infragravity waves, based on an input short wave spectrum. An absorbing-generating boundary condition allows infragravity waves to propagate freely out of the model on the offshore or back barrier bay boundary with minimal reflection. Neumann boundary conditions are applied for the flow, short wave energy and sediment transport on the lateral (shore normal) boundaries.

4.2 Test case: November 2007 storm surge

The first step in using the model, is calibrating it to obtain a certain level of accuracy. In this study, the XBeach model is calibrated on the storm of November 2007, because numerous input data is available (wave parameters, water level, wind data, etc.) and to a certain degree also the effect of the storm is known. Next to the available observations, post-storm photo's and statements from coastal managers that the dune retreat was up to 7 meter, also post-storm data is available through the JARKUS profiles from spring 2008. These can be found in Figure 4.3.

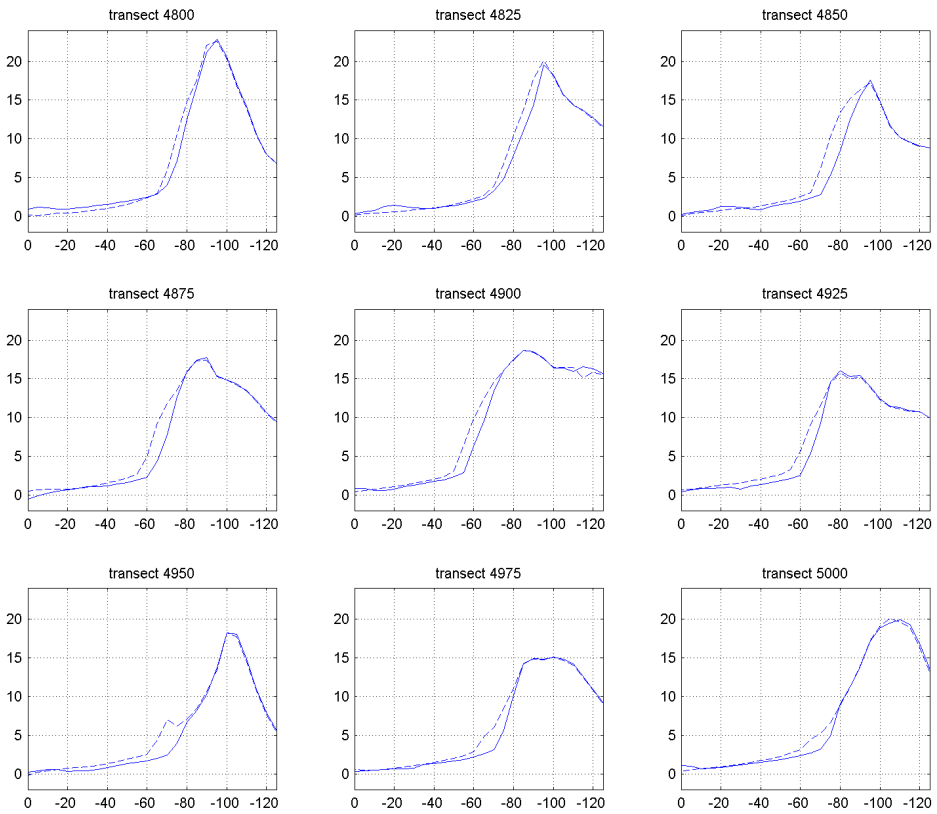

Figure 4.3 *Nine JARKUS transects in the study area; dotted lines are measured data from spring 2007 (pre-storm), solid lines are measured data from spring 2008 (post-storm).*

4.2.1 Bathymetry and topography

Elevation data for Heemskerk in November 2007 is available from different sources:

- Topography (dune) data from the AHN database; data has been obtained in 2007 (see also Figure 3.11). The accuracy on the beach looks limited, because observations seems obfuscated by high water levels and/or waves. Therefore, only AHN data landward from the dunefoot (NAP + 3 m) is taken into account.
- Beach and nearshore data from the JARKUS database; data has been obtained in spring 2007. The JARKUS data are originally transect data, but they also have been transformed into grid data. In this translation some accuracy loss may have occurred, but the data seems reasonably reliable. JARKUS data is used for the bathymetry between NAP -6 m and NAP + 3 m.
- Foreshore data from the Vaklodingen database; data has been obtained in 2005. The measurement rate of these data is lower (once per several years), but because the morphological changes are also smaller at this depth, this is not a problem. Also, the influence of variations in the deeper part of the shore is limited during storm surges. The Vaklodingen data is used for the bathymetry lower than NAP -6 m.

A limitation of XBeach is that it does not take wave transformation into account when waves propagate through the model domain (frequency shift an frequency dispersion). Also, the calculation time increases linear with the number of grid cells used. These are reasons to limit

the length (x-direction) of the computational domain. Therefore an artificial deep water boundary with a steep slope leading up to the 'normal' bathymetry is introduced at the seaward side of the domain to have deep water wave conditions where the wave forcing boundary is. The resulting bathymetry used in the November 2007 runs can be seen in Figure 4.4.

Besides the 2DH simulations, also 1D simulations have been carried out. For the 1D runs, transects from the original 2D bathymetry are taken. In total, three different cross-shore profiles (transects) have been used. They differ in the steepness and the height of the dune.

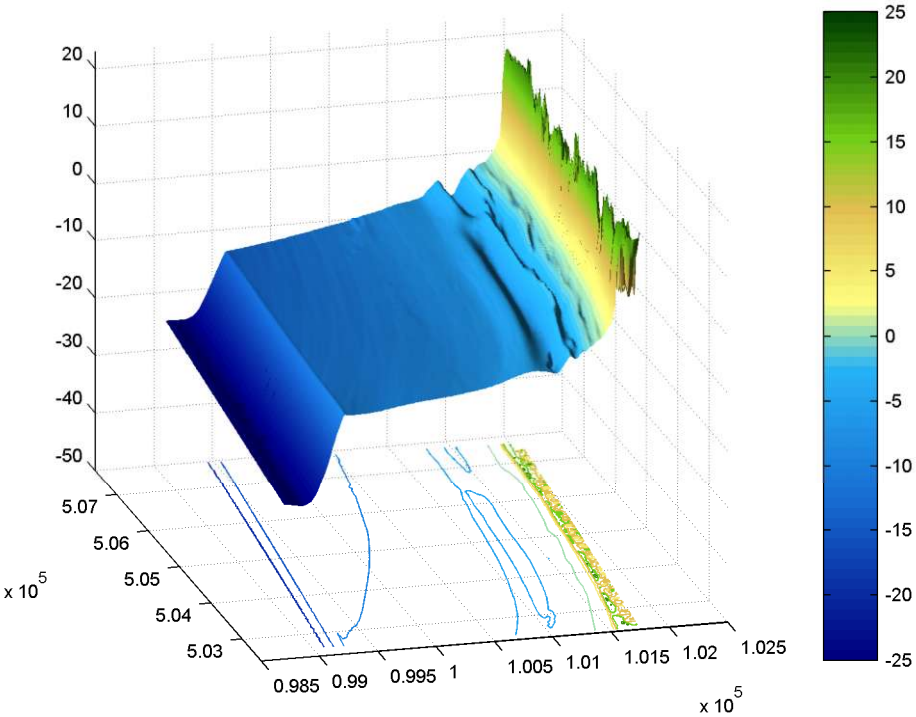

Figure 4.4 *Bathymetry and topography in m relative to NAP used in the XBeach November 2007 storm surge model runs. Contour lines every 5 m, starting at -20 m.*

4.2.2 Water level

Water level data is obtained from Rijkswaterstaat's Waterbase database (www.waterbase.nl). Water level is recorded at a 10 minute interval, which is good enough for these runs. The measurements from station 'IJmuiden Buitenhaven' have been taken, because it is the closest station to the area of interest (distance around 7 km). For the water level during the storm, see Figure 4.5.

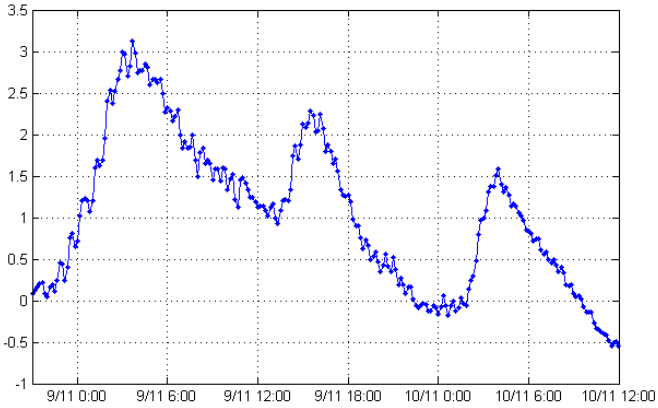

Figure 4.5 Water level at IJmuiden Buitenhaven between November 8th 21:00 and November 10th 12:00.

4.2.3 Wave conditions

The closest wave measurements are from the wave buoy 'IJmuiden munitiestortplaats', where wave conditions are averaged over a 10 minutes interval (see Figure 4.6). It is located around 25 km from the area of interest. These wave conditions (wave height, wave period and wave direction) have been used directly at the offshore (deep water) boundary of the model. They have been used in two ways:

- Using the (raw) 10-minutes interval data. With a morphological calculation factor (see below) of 5 (morfac = 5) in XBeach, this results in a wave condition that is imposed only 2 minutes (10 / 5 = 2). This is relatively short for the generation of bound long (infragravity) waves; in 2 minutes, only 3 long waves can be generated (based on a T_p of 10 seconds, $f_{long} = f_p/4$). This alternative is used in the 1D simulations.
- Averaging the 10-minutes interval data over a period of 1 hour. This leaves less wave conditions, which means less calculation time; a higher morphological factor can be used (morfac = 10), which also means a decrease in calculation time and there is more time for the generation of long waves (60/10 = 6 minutes). This alternative is used for the (computational intensive) 2DH simulations.

The morphological acceleration factor (morfac in XBeach) is a concept first stated in Lesser *et al.* (2004). It is used to deal with the difference in time scale between hydrodynamics and morphological developments. It works by multiplying the changes in bed sediments by a constant factor:

$$\Delta t_{morphology} = f_{MOR} \Delta t_{hydronamic} \tag{4.1}$$

In XBeach, this concept is used to reduce the (hydronamic) simulation time by f_{MOR} and get the morphological change of the original time scale. The order of this factor is O(1-10). All times and time steps in XBeach are entered as real world / morphological times; XBeach automatically computes the hydronamic time based on f_{MOR}.

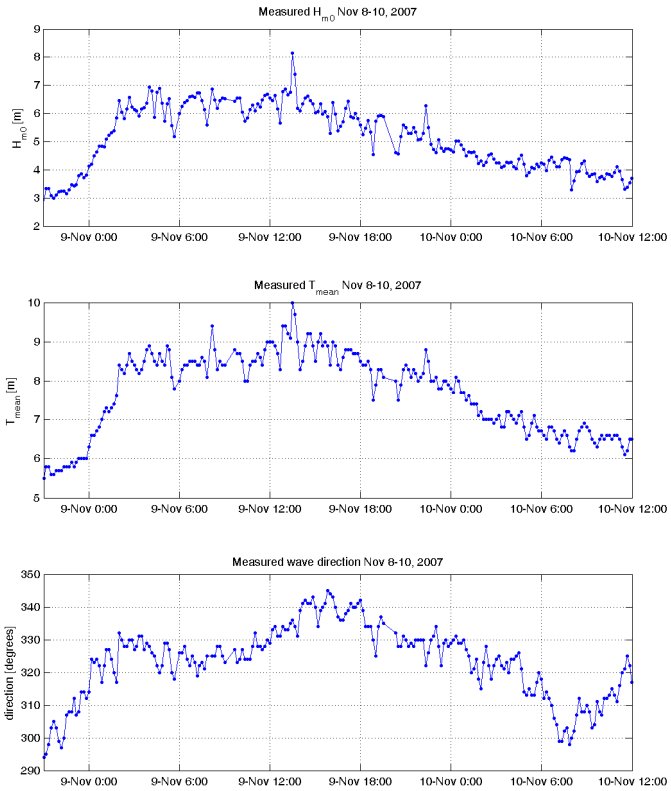

Figure 4.6 *Significant wave height (upper panel), mean wave period (middle panel) and wave direction (lower panel), measured by the wave buoy 'IJmuiden munitiestortplaats' between November 8th 21:00 and November 10th 12:00.*

4.2.4 Numerical parameters

Because accurate boundary conditions are available for this calibration case, the influence of the numerical parameters in XBeach is tested and adjusted where necessary. This is done with both 2DH and 1D simulations, as the latter are quicker to run and produce results. The limitation of the 1D model however is that it can handle only normally incident waves (at this stage of development). The primary reason to adjust the numerical parameters was because the first model runs did not predict as much erosion as expected: around 2 m instead of 7 m. The following numerical parameters have been varied:

- Numerical calculation scheme. Default an Upwind scheme (scheme=1) is used, but the implemented Lax-Wendroff scheme (scheme=2) should give less numerical dispersion.
- Gammax, the maximum ratio between H_{rms} and hh (the local water depth). This limits the wave height in very shallow water. The default value is 2, while values up to 5 can be used, depending on the situation.
- Threshold depth for drying and flooding (eps). Default this is 0.1 m (at the time of the calibration runs, later the default eps-value is lowered to 0.01), a lower value allows for more cells to be considered wet and is expected to give more erosion.

The 'base case' is a simulation with the following numerical parameters: scheme=2, gammax=2 and eps=0.1.

4.2.5 Results

The first comparison that is made, is between the numerical calculation scheme. This has been done with a 1D simulation for the middle transect (transect 147). In the rest of this paragraph this transect is taken as the 'base transect'. The result of the simulation with both numerical schemes is found in Figure 4.7. As can be seen, there is hardly any difference between the two schemes, although the Lax-Wendroff scheme gives a little more erosion, because this scheme gives less numerical dispersion.

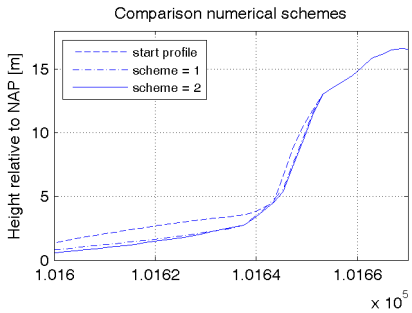

Figure 4.7 *Comparison between the Upwind scheme (default) and the Lax-Wendroff scheme (transect 147).*

The next comparisons are for different values of gammax and eps. These comparisons have again been made with 1D simulations. The results are found in Figure 4.8 (gammax comparison) and Figure 4.9 (eps comparison).

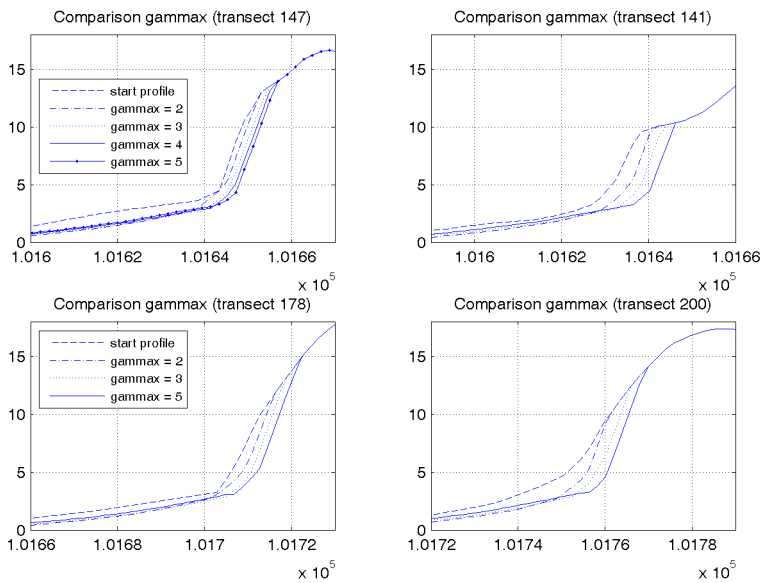

Figure 4.8 *Comparison between different values of gammax, ranging from 2 to 5. Upper left panel: transect 147; upper right panel: transect 141; lower left panel: transect 178; lower right panel: transect 200). The legend for the right panels is equal to the legend of the lower left panel.*

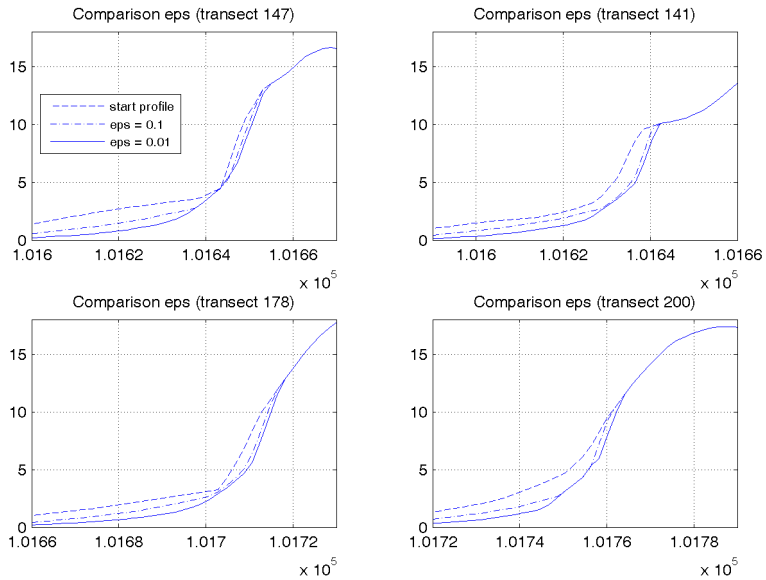

Figure 4.9 *Comparison between two different values of eps, 0.1 and 0.01. Upper left panel: transect 147; upper right panel: transect 141; lower left panel: transect 178; lower right panel: transect 200). The legend for all panels is equal.*

An analysis of these results show:

- A raise in the gammax value is almost linearly translated in a higher dune retreat for all transects. However, the dune erosion rate for transect 141 (the most retreat) is much higher than for transect 147 (the least retreat). The difference is almost 5 m for gammax=5 (10 m versus 5 m).
- A lowering of the eps value shows deeper erosion at the dunefoot / beach. The extra dune retreat comparable to the base case is almost negligible.
- Transect 141 and 200 seem to be out of equilibrium, as the dune erosion is large and no 'rotation point' can be seen (transect 147 and 178 both show a rotation point).
- Based on the 1D simulations, using the Lax-Wendroff scheme (scheme=2) and a gammax of 5 gives erosion rates which are in the same order as observed (around 5 meter or more at several places) for all transects.

Next, a number of 2D simulations is carried out. The gammax and eps values has been adjusted (2, 3 and 5 and 0.1 and 0.01 respectively) in the same way as the 1D simulations. In addition, a 2D simulation with gammax=5 and eps=0.01 has been run. For the 2D simulations, a number of changes have been made to the computational grid and de boundary conditions to speed up computations. The computational grid has been made coarser (280x290 grid cells instead of 400x290) resulting in a coarser schematization of the bathymetry and small differences in interpolation of the bottom compared to the 1D simulations. At the offshore boundary, wave conditions have been averaged over a longer period and the directional wave bins have been made coarser. The results can be found in Figure 4.10 –Figure 4.12.

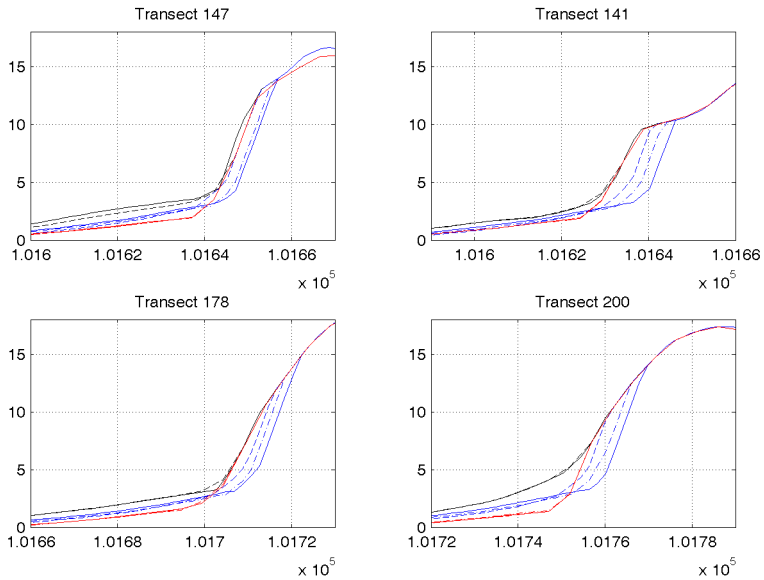

Figure 4.10 *Comparison of gammax with 1D and 2D simulations for the four transects; legend: start profile 1D (solid black line), start profile 2D (dashed black line), 1D end situations (blue lines), gammax=2 (dashed blue line), gammax=3 (dashed-dotted blue line), gammax=5 (solid blue line), 2D end situations (red lines), gammax=2 (dashed red line), gammax=3 (dashed-dotted red line) and gammax=5 (solid red line).*

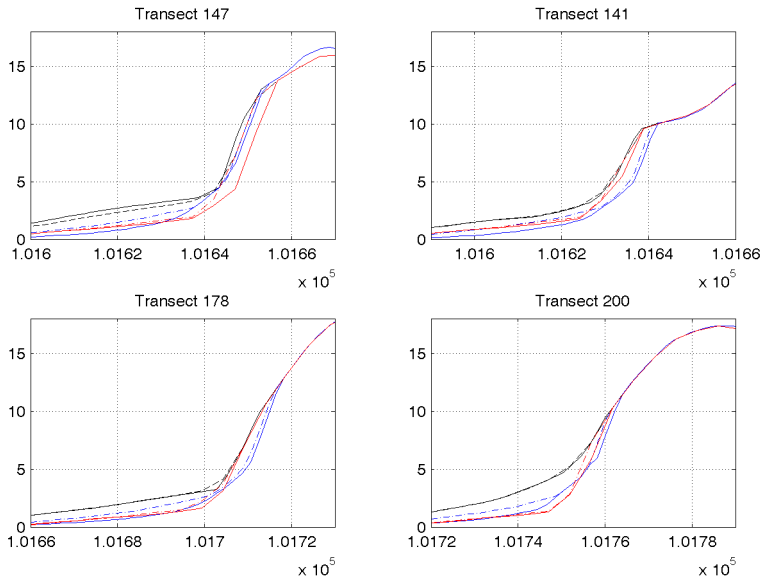

Figure 4.11 *Comparison of eps with 1D and 2D simulations for the four transects; legend: start profile 1D (solid black line), start profile 2D (dashed black line), 1D end situations (blue lines), eps=0.1 (dashed-dotted blue line), eps=0.01 (solid blue line), 2D end situations (red lines), eps=0.1 (dashed-dotted red line) and eps=0.01 (solid red line).*

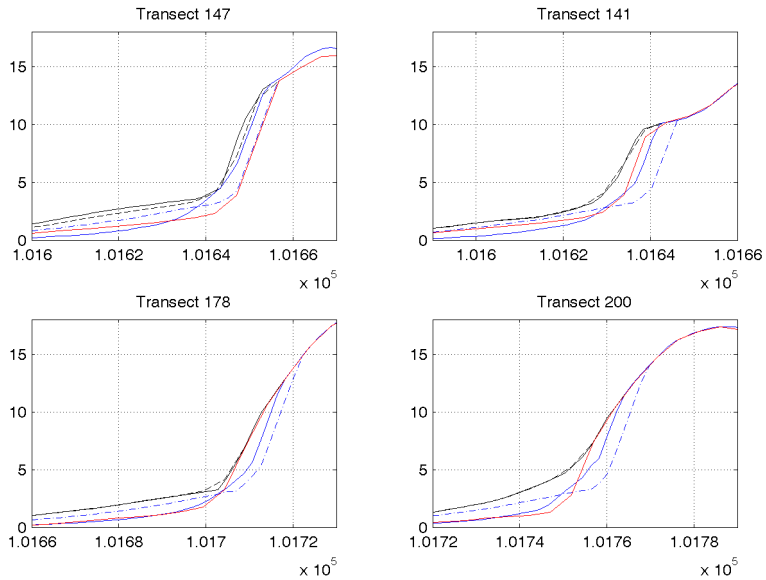

Figure 4.12 *Comparison of gammax/eps with 1D and 2D simulations for the four transects; legend: start profile 1D (solid black line), start profile 2D (dashed black line), 1D end situations (blue lines), gammax=5 (dashed-dotted blue line), eps=0.01 (solid blue line), gammax=5 and eps=0.01 for 2D simulation (solid red line).*

An analysis of the above figures shows the following:

- In general, the dune retreat is far less for the 2D simulations than for the 1D simulations. Most likely this is cause by the oblique incident waves, which generate smaller low-frequency waves and deliver less power to the dune slope.
- For 2D simulations, the gammax value is not important. All gammax values give roughly the same profile change. The difference with the 1D simulations depends on the profile: for transect 147, the 2D profile lines follow the line of gammax=5 (1D) for dune erosion, but the line of eps=0.01 for beach erosion, at the other profiles the 2D erosion lines follow the line for eps=0.01 more closely.
- The beach erosion on the other hand is stronger for the 2D simulations than for the 1D cases. It is possible that longshore surf zone processes (which are absent in the 1D simulations) increase the beach/surf zone erosion.
- The 2D simulations for transects 141 and 147 and with eps=0.01 produce results that are closest to the observed dune erosion values (Figure 4.11 and Figure 4.12). It is not known why hardly any dune erosion occurs for the 2D simulations at transects 178 and 200 (Figure 4.10 – Figure 4.12).

For the simulations of the 1775 storm surge in the next chapter, the values of 2 for gammax and 0.01 for eps are used. They are partially based on the results of this chapter and partially on the most recent insights in the optimal (default) values for XBeach simulations.

5 Results simulations 1775 storm

In this chapter, the results from the simulations of the November 1775 storm surge are presented. The input for these simulations has been discussed in chapter 3. First, the results of a Monte Carlo simulation with 200 simulations and six different profiles is discussed. After that, a number of sensitivity analyses based on the 1D simulations is shown. Next, nine relevant samples from the set of 1D simulations have been chosen to do 2DH simulations with. The results of the 2DH runs are presented in paragraph 5.2. The input parameters for the XBeach simulation can be found in Appendix A.

5.1 1D simulations

The main parameter of interest in the 1D simulations, is the maximum water level elevation at the shoreline, as this gives a measure of the height the water has reaches and thus the height at which the shell layer could have been deposited. The maximum water level elevation is usually reached by wave run-up (swash motion). Therefore, the shoreline water level has been registered by a runupgauge (output method) in XBeach. To prevent an outlier (a single large wave) influencing the outcomes, the statistical parameter $Z_{2\%}$ is introduced. $Z_{2\%}$ is the water level at the shoreline with respect to a reference level (NAP) that is exceeded by 2% of the largest run-up peaks. It is calculated as the 98th percentile of all 'measured' water level peaks.

5.1.1 Histograms and distributions

The hypothesis that is tested, is if the average $Z_{2\%}$ water level elevation has reached the observed value of NAP + 6.5 m. For every one of the six profiles, 200 $Z_{2\%}$ values are computed, a histogram is drawn and the data is fitted to the best matching distribution with the software package 'BestFit', using the three goodness-of-fit measures available: the χ^2–test, the Kolmogorov-Smirov test and the Anderson-Darling test. The total output of the distribution fitting is found in Appendix B.

The results for all six profiles, both the histogram and the best fitting distribution, are shown below in Figure 5.1 –Figure 5.6.

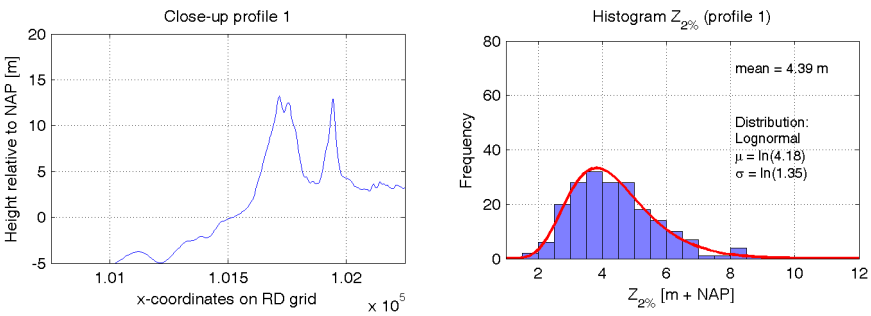

Figure 5.1 *Left panel: close-up bathymetry profile 1. Right panel: histogram $Z_{2\%}$ and best-fit distribution for profile 1.*

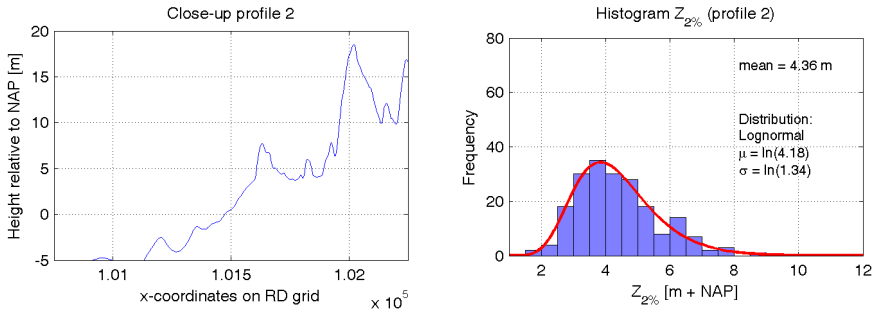

Figure 5.2 *Left panel: close-up bathymetry profile 2. Right panel: histogram $Z_{2\%}$ and best-fit distribution for profile 2.*

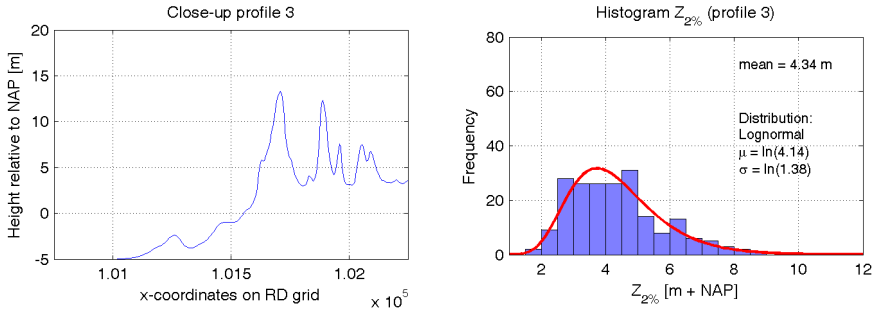

Figure 5.3 *Left panel: close-up bathymetry profile 3. Right panel: histogram $Z_{2\%}$ and best-fit distribution for profile 3.*

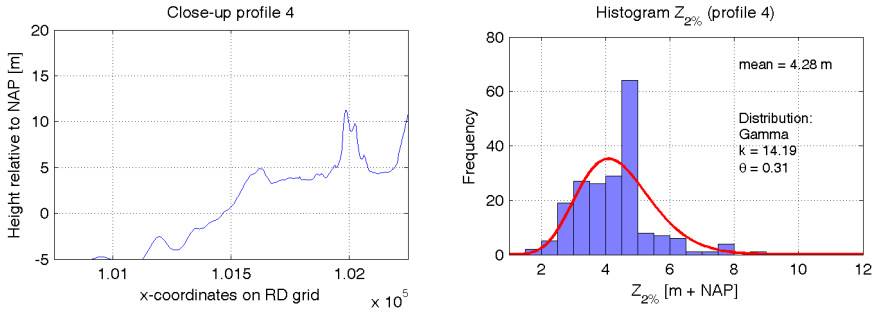

Figure 5.4 *Left panel: close-up bathymetry profile 4. Right panel: histogram $Z_{2\%}$ and best-fit distribution for profile 4.*

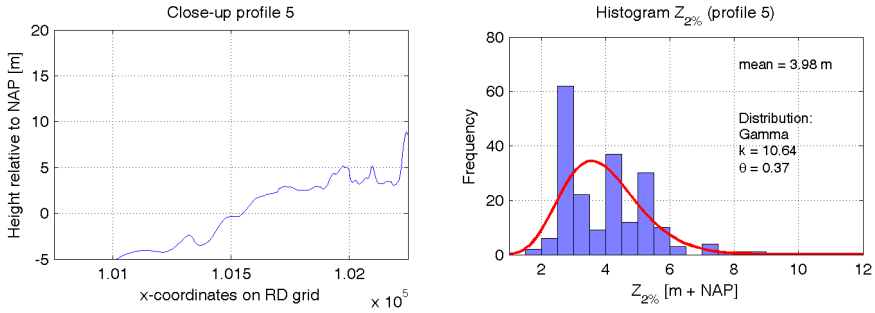

Figure 5.5 *Left panel: close-up bathymetry profile 5. Right panel: histogram $Z_{2\%}$ and best-fit distribution for profile 5.*

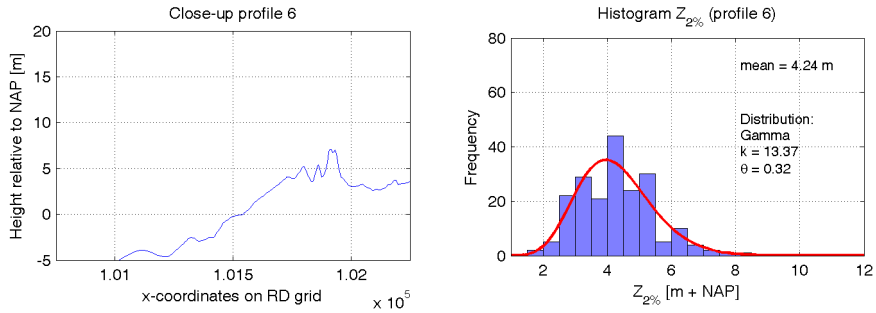

Figure 5.6 *Left panel: close-up bathymetry profile 6. Right panel: histogram $Z_{2\%}$ and best-fit distribution for profile 6.*

Analysis of the profile's histograms and associated distributions shows the following:

- For profiles 1-3 (with a high dune directly behind the beach) $Z_{2\%}$ values are all lognormal distributed and have histograms that follow the distribution well; for profiles 1 and 2 they have almost a perfect match, while profile 3 shows deviations from the perfect fit at the top of the distribution. For profiles 1-3 the type of distribution of $Z_{2\%}$ (lognormal) is the same as the maximum storm surge water level, which suggests that the run-up to a (natural) dune is strongly dependent on the storm surge level.
- Profiles 4-6 (the low-lying areas) all have results that fit best to a Gamma-distribution, although the histograms deviate a lot from the distribution.
- For profile 4, there is a large peak in the histogram for the bin 4.5-5 m + NAP. This indicates that for a large number (more than 60) of simulations, the water is / waves are able to reach to the top of the sill or to overtop it, but not to breach it or to run-up to the next dune.
- Profile 5 shows three peaks: at 2.5-3 m, at 4-4.5 m and at 5-5.5 m. They correspond to certain heights in the bathymetry: an elevation in the slope at NAP + 3 m and the first small dune, with a change in slope at NAP + 4.5 m and the top around NAP + 5.5 m. It is remarkable that in a large number of simulations, the $Z_{2\%}$ level is at the first elevation. Probably due to the long and gentle sloping terrain (400 m), all large waves are already broken and all energy is dissipated before they can reach the first dunes.
- Profile 6 shows a peak at NAP + 4-4.5 m and at NAP + 5-5.5 m, corresponding to the change in slope and the first dune top respectively.

To test the hypothesis that the $Z_{2\%}$ level is close to the observed value of NAP + 6.5 m, for every profile is calculated for which part of the simulations the $Z_{2\%}$ level reached the observed value (of NAP + 6.5 m). To take uncertainties into account, a margin of 0.5 m is used, so the probability that is calculated, is if $Z_{2\%}$ is in the domain [6.0, 7.0]. The computed probabilities are displayed in Table 5.1.

Table 5.1 *$P(Z_{2\%} \in [6.0, 7.0])$ and distribution parameters for all profiles.*

Profile	$P(Z_{2\%} \in [6.0, 7.0])$	Distribution Name	a	b
1	0.09	Lognormal	ln(4.18)	ln(1.35)
2	0.11	Lognormal	ln(4.18)	ln(1.34)
3	0.10	Lognormal	ln(4.14)	ln(1.38)
4	0.04	Gamma	14.19	0.31
5	0.02	Gamma	10.64	0.37
6	0.07	Gamma	13.37	0.32

The second objective of this study is to find out if the modelled water level (including set-up and run-up) is within the range of the discovered storm surge layers. It can be concluded that the probability that the run-up water level has reached NAP + 6.5 m is not 50% for every one of the profiles, which was the hypothesis. However, it is not needed to reject the hypothesis based on these results. It is common to reject a hypothesis only when the probability is lower than 0.05, which is clearly not the case for these 1D simulations.

5.1.2 Probability of exceedance

For the calculation of the probability of exceedance, the third objective of this study, two available 'exceedance lines' of locations close to Heemskerk have been used: those of IJmuiden and Petten-Zuid (Philippart *et al.*, 1995). These exceedance lines are used as-is and no research into the accuracy or reliability of them is done. The exceedance lines are based on the highest water level that is measured during a storm surge event and are based on recorded data: 1884-1985 for IJmuiden and 1933-1985 for Petten-Zuid.

From all available simulation results, those that lead to a $Z_{2\%}$ level of [6.0, 7.0] have been selected together with the maximum offshore storm surge level (zs0 in XBeach) of that simulation. All these selected maximum levels are then used to compute a mean storm surge level for the 1775 storm.

The inversed calculated mean value of the selected range of water levels is NAP + 4.70 m. This level is plotted on both exceedance lines. The results are shown in Figure 5.7 and Figure 5.8. The recorded maximum surge level at Petten-Zuid (NAP + 2.9 m) is also plotted on the exceedance line for Petten-Zuid.

The exceedance line for Petten-Zuid gives a probability of exceedance of $8*10^{-5}$, compared to a probability of exceedance of $3*10^{-4}$ according to the exceedance line for IJmuiden. Petten-Zuid gives a probability of $6*10^{-2}$ for the observed level of 2.9 m + NAP.

The Heemskerk dunes are closer to IJmuiden (distance 7 km) than to Petten-Zuid (distance 25 km). It therefore seems reasonable to prefer the exceedance line of IJmuiden over the exceedance line of Petten-Zuid. That surge and tidal levels are generally lower in Petten-Zuid than IJmuiden, can also be observed from the November 2007 records (Figure 1.1).

The values for Petten-Zuid seems either unrealistically high (computed level) or low (observed level), but this exceedance line is based on only 50 years of data. On the other hand, the probability of exceedance of $8*10^{-3}$ is also quite unusual and is close to the present design criterion (10^{-4}). This is not in line with the reports of the 1775 storm. It was an unusual event, but there have been more storm surges in recent history which seem to have had more impact, according to reports and known data (e.g. 1825, see also Table 2.1).

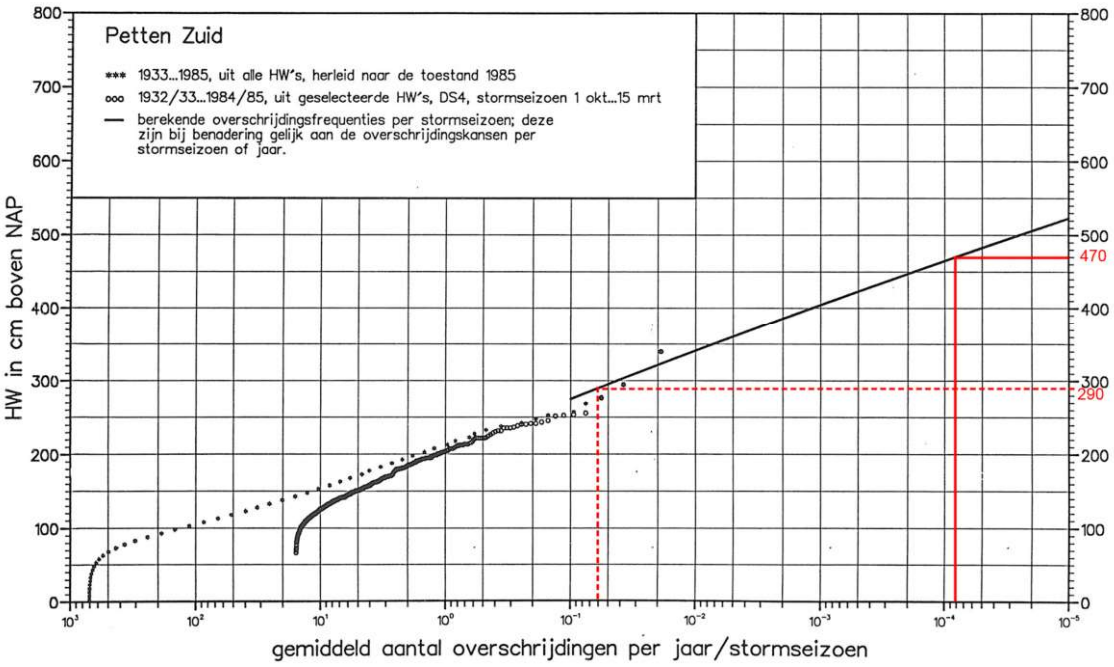

Figure 5.7 *Exceedance line for Petten-Zuid, based on observations between 1933 and 1985 (Philippaert et al., 1995). The red solid line indicates the computed level; the dashed red line indicates the observed maximum level in Petten-Zuid in 1775.*

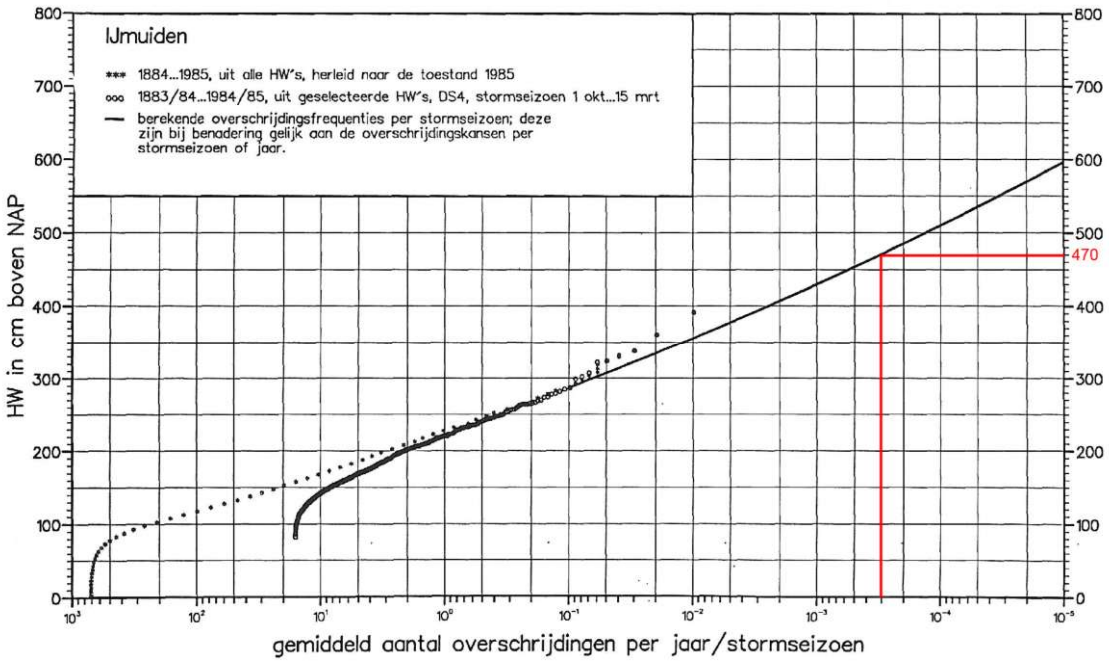

Figure 5.8 *Exceedance line for IJmuiden, based on observations between 1884 and 1985 (Philippaert et al., 1995). The red solid line indicates the computed maximum storm surge level.*

5.1.3 Regression analysis

In this section, different statistical techniques are applied to find (mathematical) relations between $Z_{2\%}$ and one or more of the input values. If such a relation is found, it is possible to give an estimation of $Z_{2\%}$ based on these input variables, without using the numerical model.

The first analysis that has been done is simple linear regression. One assumes a linear relation between the dependent variable *y* and one independent variable *x*. The accompanying linear regression equation is of the form y = a + bx + e. Linear regression analysis is performed for $Z_{2\%}$ vs. the maximum storm surge level and $Z_{2\%}$ vs. the maximum H_{m0} (at deep water). For each relation the R^2 value has also been calculated. This value gives the part of the variance in *y* that can be explained from the variance in *x*. A value of 1 indicates a perfect linear relation; a value of 0 no relation at all. Note that a high value of R^2 can arise though the relationship between the two variables is non-linear. The fit of a model should therefore never simply be judged from the R^2 value alone. The resulting figures are found below (Figure 5.9 – Figure 5.14); numerical data is shown in Table 5.2.

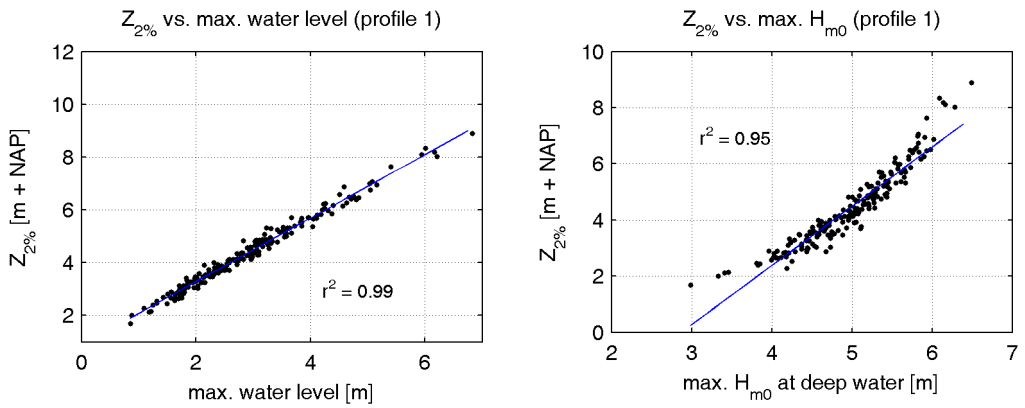

Figure 5.9 *Left panel: scatter plot of $Z_{2\%}$ vs. water level. Right panel: scatter plot of $Z_{2\%}$ vs. deep water H_{m0} (profile 1).*

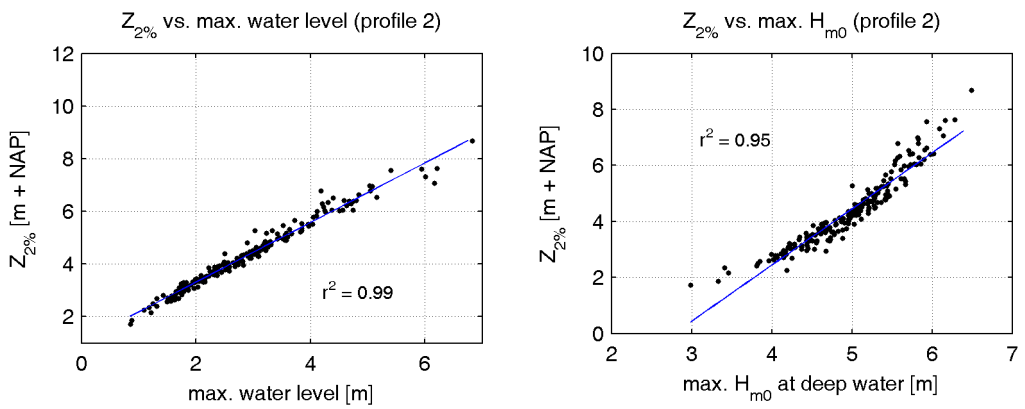

Figure 5.10 *Left panel: scatter plot of $Z_{2\%}$ vs. water level. Right panel: scatter plot of $Z_{2\%}$ vs. deep water H_{m0} (profile 2).*

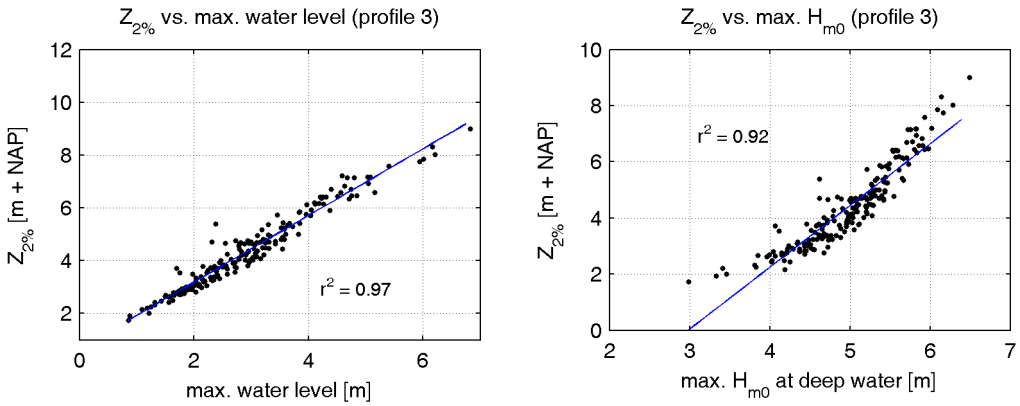

Figure 5.11 *Left panel: scatter plot of $Z_{2\%}$ vs. water level. Right panel: scatter plot of $Z_{2\%}$ vs. deep water H_{m0} (profile 3).*

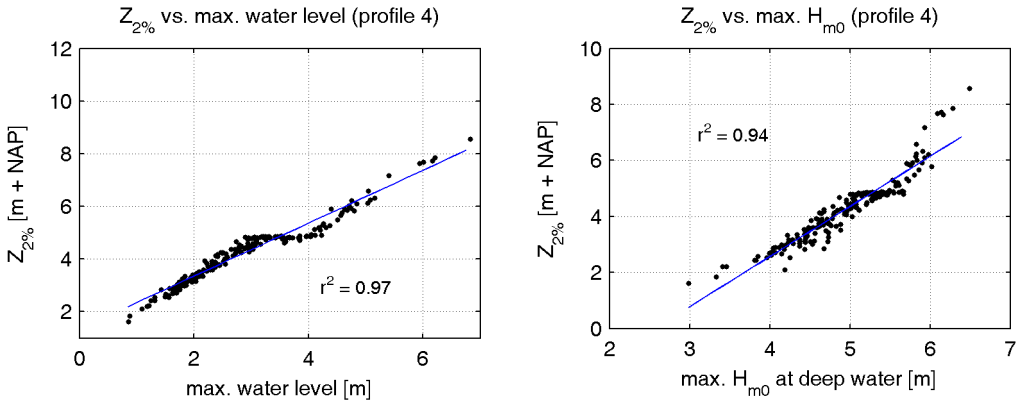

Figure 5.12 *Left panel: scatter plot of $Z_{2\%}$ vs. water level. Right panel: scatter plot of $Z_{2\%}$ vs. deep water H_{m0} (profile 4).*

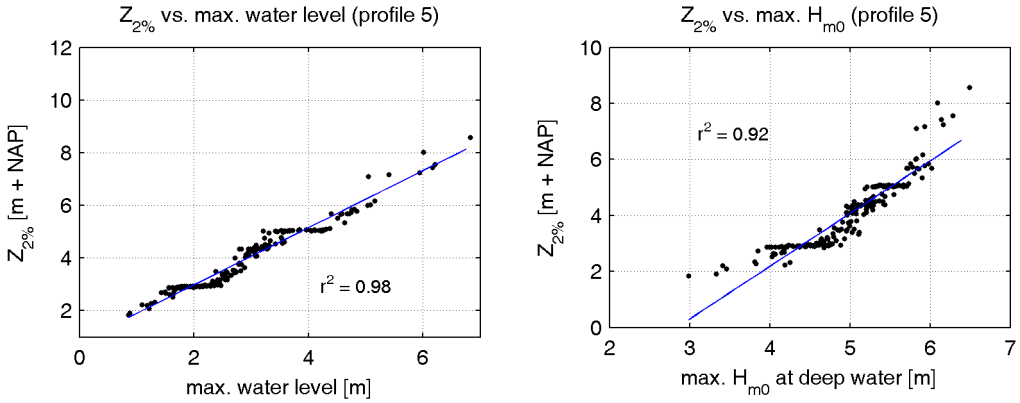

Figure 5.13 *Left panel: scatter plot of $Z_{2\%}$ vs. water level. Right panel: scatter plot of $Z_{2\%}$ vs. deep water H_{m0} (profile 5).*

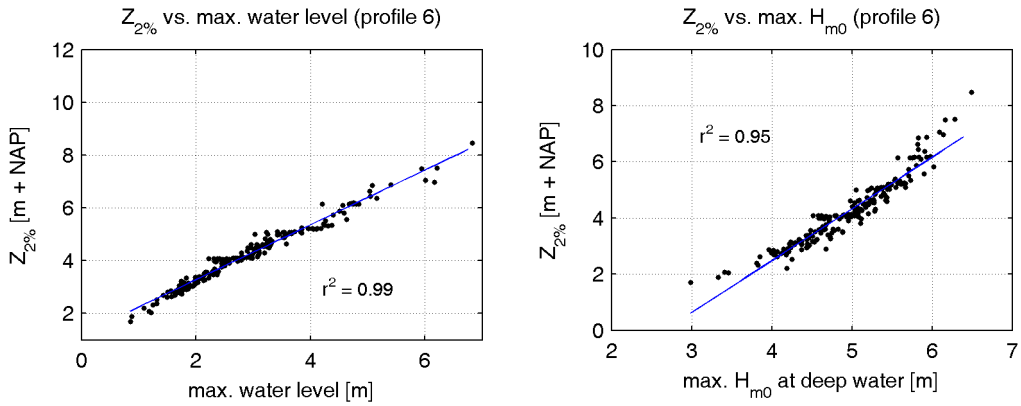

Figure 5.14 *Left panel: scatter plot of $Z_{2\%}$ vs. water level. Right panel: scatter plot of $Z_{2\%}$ vs. deep water H_{m0} (profile 6).*

Table 5.2 *Results simple linear regression analysis.*

	***$Z_{2\%}$* versus storm surge water level**				***$Z_{2\%}$* versus deep water wave height**			
Profile	***R^2***	***a***	***b***	**visual assess.**	***R^2***	***a***	***B***	***visual assess.***
1	0.99	0.8855	1.2015	++	0.95	-6.0574	2.1078	o
2	0.99	1.0540	1.1320	++	0.95	-5.5848	2.0056	o
3	0.97	0.6611	1.2625	+	0.92	-6.5619	2.2003	o
4	0.97	1.3443	1.0049	+	0.94	-4.5966	1.7900	o
5	0.98	0.8196	1.0836	o	0.92	-5.3515	1.8828	o
6	0.99	1.2100	1.0380	++	0.95	-4.8948	1.8425	o

The simple linear regression analysis shows the following phenomena:

- All scatter plots of $Z_{2\%}$ versus water level show a almost perfect linear relation. This is expressed in the R^2 values, which are 0.97 or higher for all profiles.
- The linear relation between $Z_{2\%}$ and the deep water significant wave height is less clear. The R^2 values are high, 0.92 or above, but all profiles show deviations from the linear relation in the lowest and highest regions. Based on a visual estimation, it seems that the relation between $Z_{2\%}$ and H_{m0} is not linear, but quadratic. However, fitting a line of the form $y = ax^2 + bx + c$ did not give much better results, both visually assessed as measured by the R^2 value.
- The scatter plots of profiles 4 – 6 show a number of dots on the same horizontal line (same $Z_{2\%}$ value). These correspond with the peaks found in the histograms and the explained features in the profile's bathymetry.
- Profile 3 shows a number of outliers in the scatter plot of $Z_{2\%}$ versus H_{m0} around (H_{m0}=4.5, $Z_{2\%}$=5). Furthermore, profile 3 has the lowest R^2 values overall.
- For profile 4, there are some outliers with $Z_{2\%}$ values of NAP + 8 m which don't correlate with the maximum H_{m0} values.

After the simple linear regression, a multiple linear regression on the $Z_{2\%}$ data has been performed, using both the storm surge level and H_{m0} as input variables. The multiple linear regression gives an equation of the form: $y = a + bx_1 + cx_2$. The results are visualized in Figure 5.15 –Figure 5.19 below, where also the underlying equation and the R^2 value of each profile are displayed. In Table 5.3 the R^2 values of the multiple linear regression are compared to the R^2 values of the simple linear regressions with water level and H_{m0}.

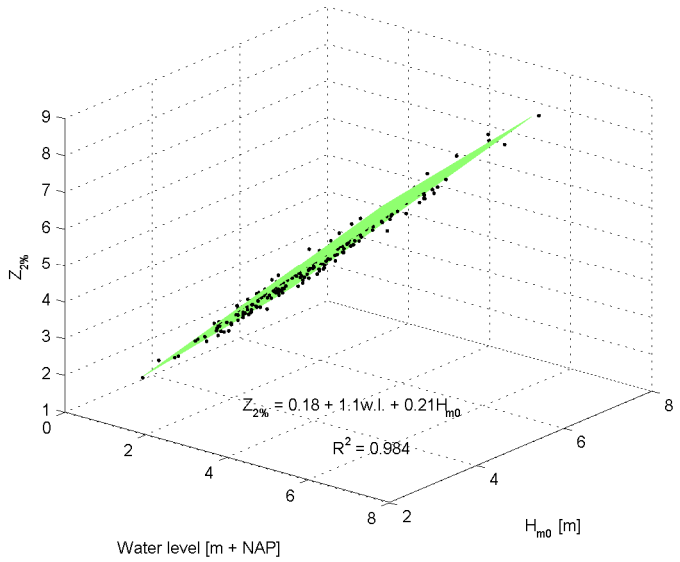

Figure 5.15 *$Z_{2\%}$ versus water level and deep water H_{m0} (profile 1).*

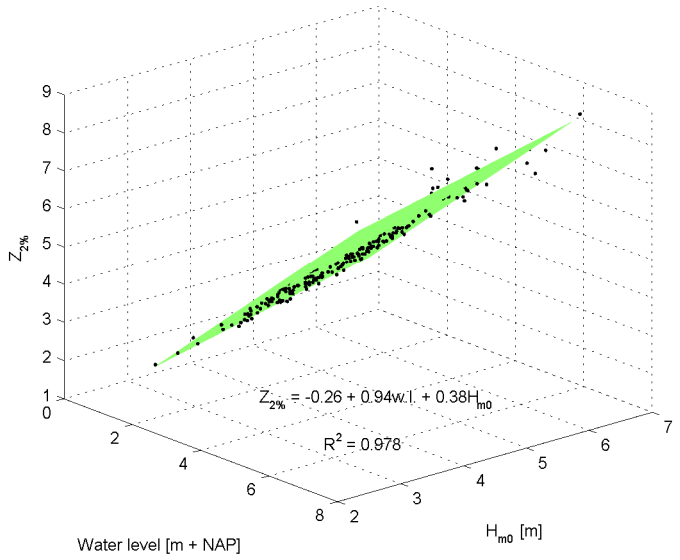

Figure 5.16 *$Z_{2\%}$ versus water level and deep water H_{m0} (profile 2).*

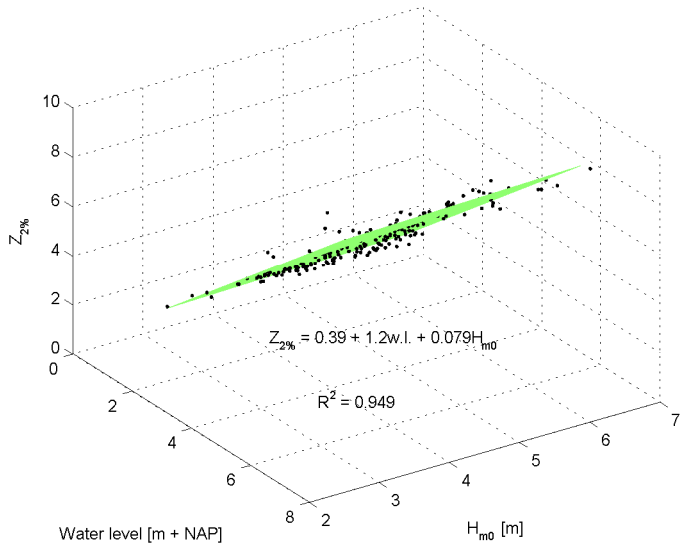

Figure 5.17 *$Z_{2\%}$ versus water level and deep water H_{m0} (profile 3).*

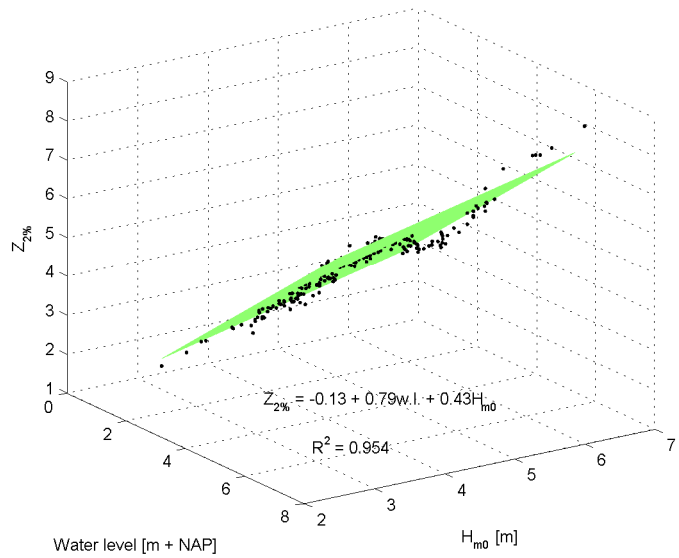

Figure 5.18 *$Z_{2\%}$ versus water level and deep water H_{m0} (profile 4).*

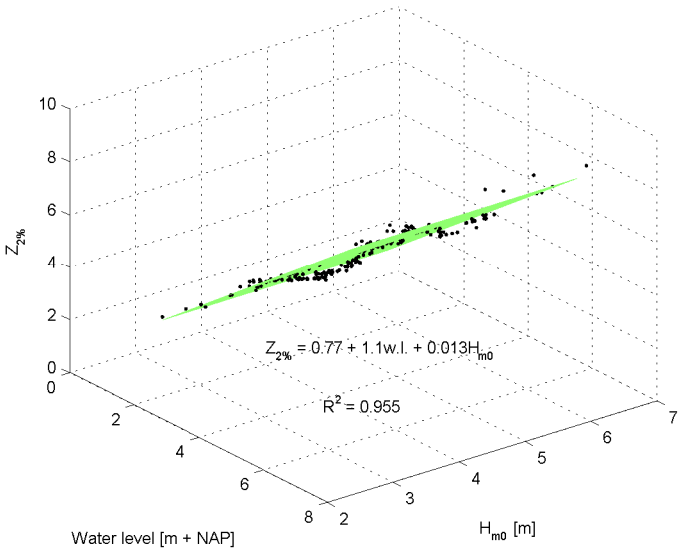

Figure 5.19 $Z_{2\%}$ *versus water level and deep water* H_{m0} *(profile 5).*

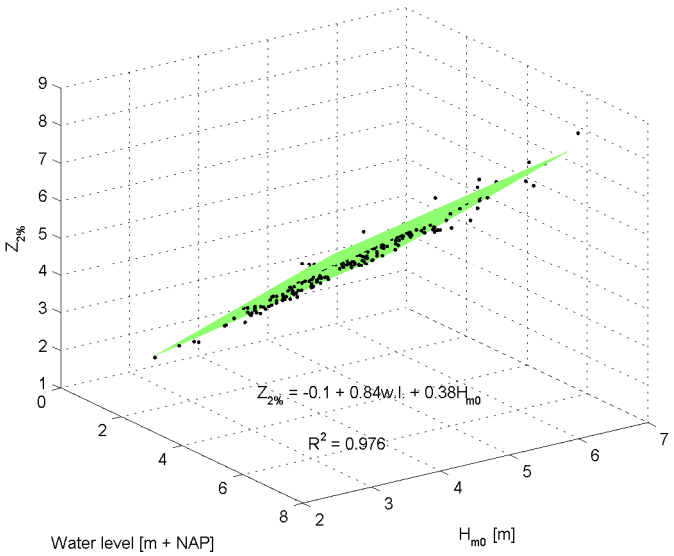

Figure 5.20 $Z_{2\%}$ *versus water level and deep water* H_{m0} *(profile 6).*

Table 5.3 R^2 *values multiple linear regression compared to simple linear regressions.*

	Multiple linear regression	***Simple linear regression***	
Profile	***R^2***	***R^2 ($Z_{2\%}$ vs. water level)***	***R^2 ($Z_{2\%}$ vs. H_{m0})***
1	0.984	0.99	0.95
2	0.978	0.99	0.95
3	0.949	0.97	0.92
4	0.954	0.97	0.94
5	0.955	0.98	0.92
6	0.976	0.99	0.95

As can be seen from the figures, the calculated regression lines are a good fit to the data in case of all profiles. It is notable that in case of profile 3 and profile 5 the addition of H_{m0} to the total regression is very small or almost absent. Furthermore, it seems possible to estimate the storm run-up level $Z_{2\%}$ as a function of the maximum storm surge water level and the maximum H_{m0} for the given profiles. As the relations for the six profiles differ too much from each other, a general equation for an arbitrary profile cannot be given at this moment.

From Table 5.3 it can be seen that the highest R^2 values are found for $Z_{2\%}$ versus the maximum water level. The R^2 values of the multiple linear regression are between those of the simple linear regressions for each profile. It can be concluded that $Z_{2\%}$ as a function of only the maximum water level gives the best results.

5.1.4 Relation with the Irribarren number

The Irribarren number (Battjes, 1974) is a dimensionless surf similarity parameter, which is a measure of the ratio between the steepness of a slope and the steepness of the incoming (significant) wave. For this study a deep water Irribarren parameter is used, based on the deep water significant wave height, as the nearshore H_s was not available.

$$\xi_0 = \frac{\tan\alpha}{\sqrt{H_{m_0}/L_0}} \tag{5.1}$$

in which:

ξ_0 deep water Irribarren number

α dune slope near water line (see below)

H_{m_0} deep water significant spectral wave height

L_0 deep water wave length based on peak spectral wave period: $L_0 = gT_p^2/2\pi$

The H_{m_0} that has been taken is the maximum H_{m_0} value from each of the 200 runs (occurring at the maximum of the storm). L_0 is based on the corresponding peak wave period.

The Irribarren number is often used as an input parameter for parametric relations for the wave run-up (Holman, 1986; Stockdon *et al.*, 2006). In these studies, the wave run-up is defined as $R_{2\%}$, the 2% exceedance height associated with individual run-up peaks <u>relative to the time-varying still water level</u> without local set-up(zs0 in XBeach). In this way it is not possible to find the maximum height the water has reached (relative to a reference level such as NAP), but the peaks are made relative to the water level, thereby eliminating the influence of water level changes and thus better comparable.

As the Irribarren number is used as a measure to compare the $R_{2\%}$ values with, it is not directly clear which slope to take. The dune slope, other than a Dutch dike slope, changes under influence of the varying water levels and the wave attack (avalanching, collapsing). Also the dune slope varies between the beach (level) and the dune top. It has been decided to take the slope at the level of the wave attack of the highest wave in the record (maximum zs value of the run-up gauge record in XBeach). The slope is calculated using the x and z coordinates of the dune slope at the levels zs (the highest recorded water level including wave run-up) and zs0 (the momentaneous still water level at the same moment).

As the momentaneous bed level (zb in XBeach) is only recorded at a certain discrete interval (tintg in XBeach, 900 seconds in case of the 1D runs), it is unlikely that the bed level has been recorded at the same time as the highest wave run-up. In that case, the last bed level recorded before the highest run-up has been taken.

It is questionable if the slope at the moment of the highest run-up is representative for Irribarren number to compare $R_{2\%}$ with. Therefore, also the slope at the start of the simulation and at the end of the simulation have been used to calculate the Irribarren number (at the same z level as described above), so they can be compared with each other. The scatter plots of R2% versus ξ_0 for the six profiles are shown in Figure 5.21 – Figure 5.23.

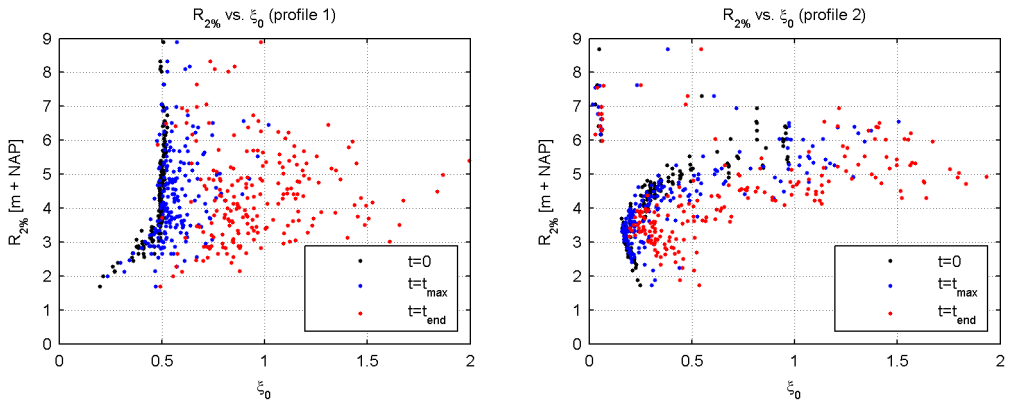

Figure 5.21 *$R_{2\%}$ wave run-up height as a function of the deep water Irribarren number, calculated with the dune slope at the start of the simulation (black dots), at the moment of the maximum wave attack (blue dots) and at the end of the simulation (red dots).Left panel: profile 1; right panel: profile 2.*

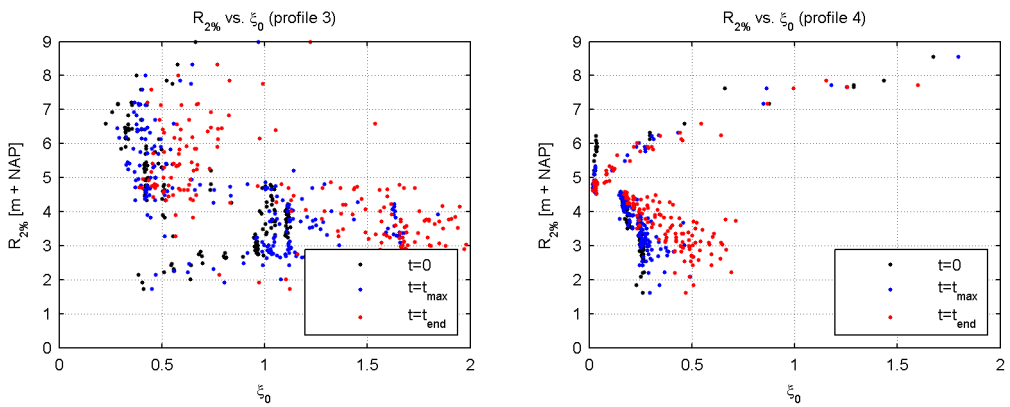

Figure 5.22 *$R_{2\%}$ wave run-up height as a function of the deep water Irribarren number. Data as in Figure 5.21. Left panel: profile 3; right panel: profile 4.*

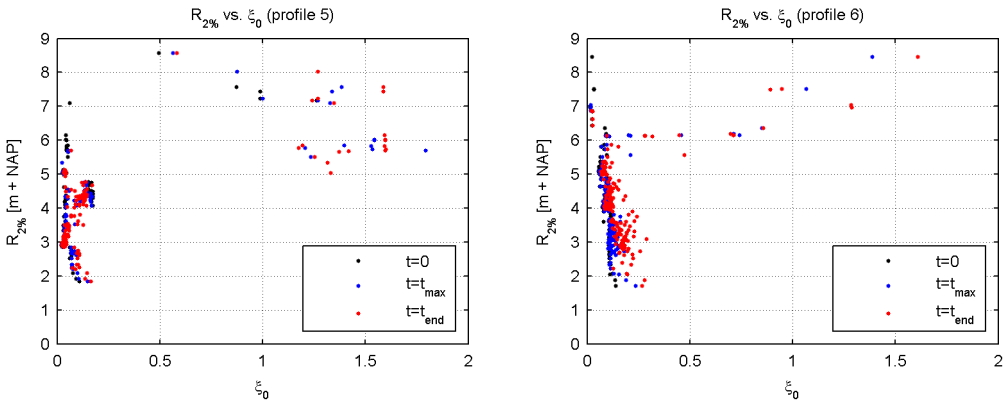

Figure 5.23 *$R_{2\%}$ wave run-up height as a function of the deep water Irribarren number. Data as in Figure 5.21. Left panel: profile 5; right panel: profile 6.*

As the figures above show, there is lots of scatter ('noise') in the data. Therefore, it is hardly possible to find a relation between $R_{2\%}$ and ξ_0 using the available data, regardless of which data set is taken (the slope at the start of the simulation, at the highest wave or at the end of the simulation).

A number of possible methods is suggested to improve the estimation of a relation between $R_{2\%}$ and ξ_0, which has been shown in literature to exist (Holman, 1986; Stockdon *et al.*, 2006). Because of the highly varying conditions during a storm, it is hardly sensible to calculate a single Irribarren number for an entire storm. If data is split up in small (time) series of about 30 minutes to a few hours, conditions are more uniform (quasi-stationary): significant wave height, significant wave period and mean water level. Also within a short time frame the slope of the shoreline / dune does not change much. This is the method Holman (1986) used. If on the other hand the dune profile is recorded more frequently, better estimations of the slope can be made.

It could also be possible that there is no or little relation between the $R_{2\%}$ wave run-up height and the dune slope. Holman and Stockdon et al. derived relations for natural beaches, which are under more or less constant influence of wave action. The main influence on (Dutch) dune slopes is aeolian action, not waves. The relation between $R_{2\%}$ and the dune slope might be absent at the start of the storm and gradually develop during the storm, which can be suggested from Figure 5.21 –Figure 5.23.

5.2 2DH simulations

Based on the maximum recorded water level of all 200 XBeach 1D simulations for the 6 profiles, 9 samples have been selected for 2DH simulations (s026, s053, s081, s105, s108, s129, s173, s184 and s196). The characteristics of these samples during the 1D simulation:

- Five simulations have a maximum run-up level of around NAP + 6.0 – 6.5 m for one or more of the profiles;
- Two simulations have relatively high run-up levels, with a maximum of NAP + 9 – 10 m for one profile and NAP + 6 – 7 m for the other profiles;
- One simulation is the most extreme simulation of all 200 with run-up levels higher than NAP + 9 m for all six profiles.

Each of those 9 samples have been run with the same boundary conditions as during the corresponding 1D simulation. After that, the 9 samples have been run with the topography of 2007. The topography of both 1775 and 2007 is shown in Figure 5.24.

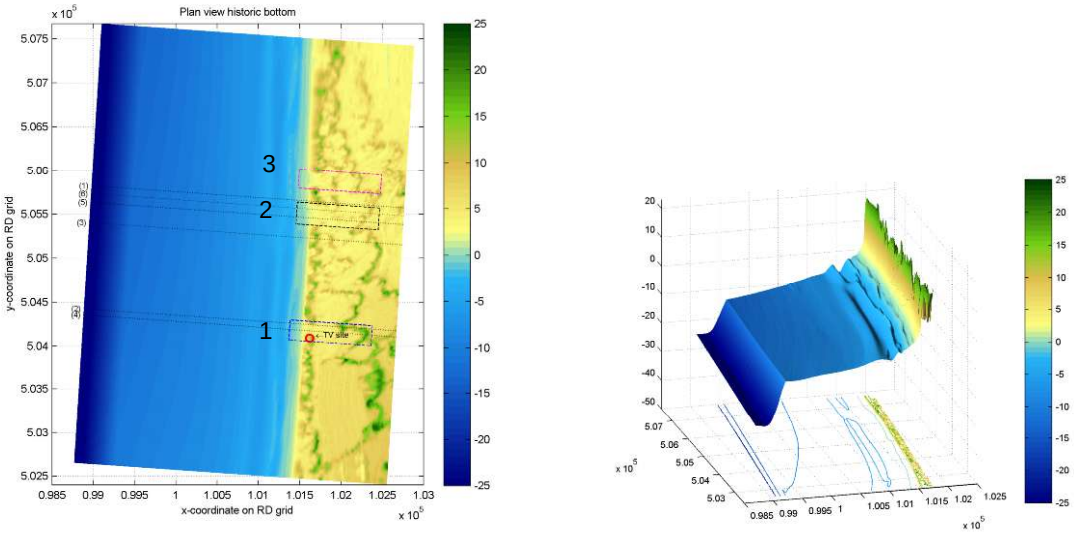

Figure 5.24 *Left panel: plan view constructed topography 1775 with the three low-lying areas indicated with dashed rectangles, numbered from bottom to top 1 to 3. Right panel: topography 2007.*

5.2.1 1775 topography

After analyzing the nine simulations with the topography of 1775, it can be concluded that the biggest differences between the simulations is if the sill in front of low-lying area 1 is breached or not. All simulations show overwash of the low-lying areas without a sill, some more than others, but only a few (4) show breaching of the sill. Visualizations of the bathymetry (zb in XBeach) and the water level (zs in XBeach) both at the moment of the largest inundated area and at the end of the simulation for four characteristic simulations can be found in the following figures (Figure 5.25 –Figure 5.28). The characteristics of these 4 simulations are as follows:

- Sample 53 is moderately flooded at low-lying areas 2 and 3, but no breach has occurred at low-lying area 1.
- Sample 129 shows only little flooding at areas 2 and 3 and also no breaching at area 1.
- Sample 184 shows the same amount of flooding for areas 2 and 3, but also breaching of the sill at area 1.
- Sample 196 shows total flooding of the entire dune area.

Besides the visualizations, also sedimentation/erosion plots are produced for the four simulations (Figure 5.29 – Figure 5.32). Table 5.4 contains an overview of the relevant overwash and breaching moments of all nine simulations.

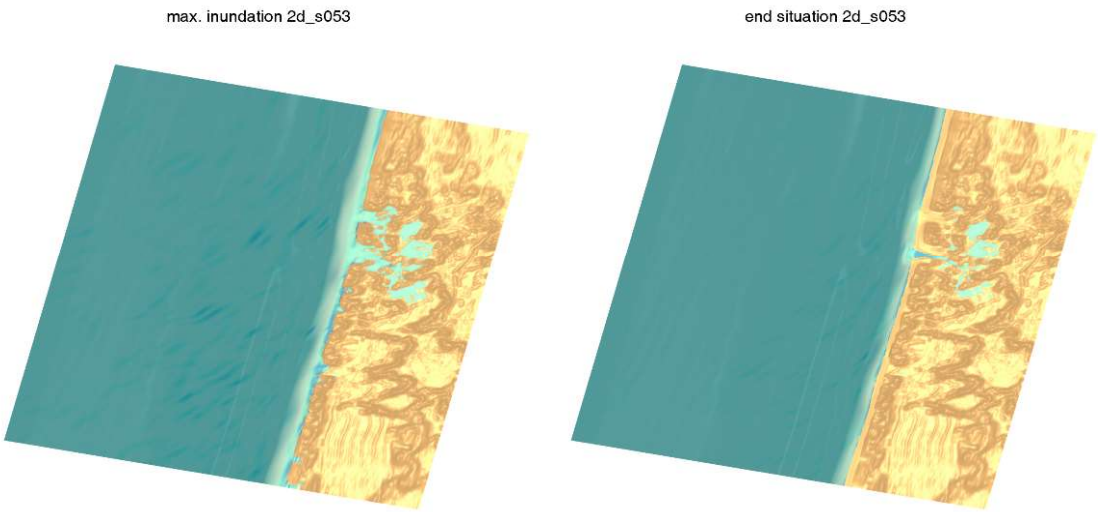

Figure 5.25 *Snapshot of water level and bed elevation for sample 053; after 23.50 hours (left panel) and after 36.25 hours (right panel).*

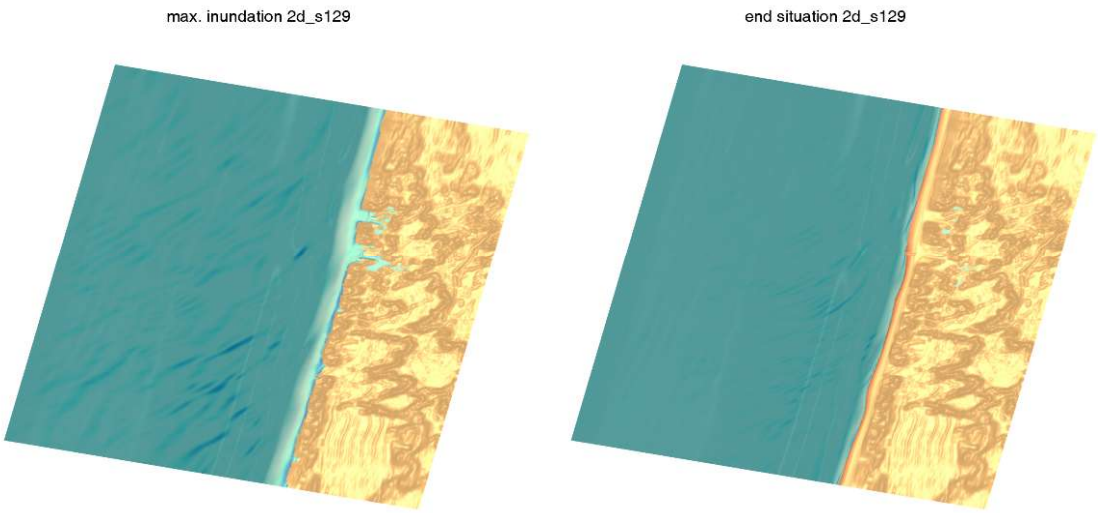

Figure 5.26 *Snapshot of water level and bed elevation for sample 129; after 21.50 hours (left panel) and after 43.00 hours (right panel).*

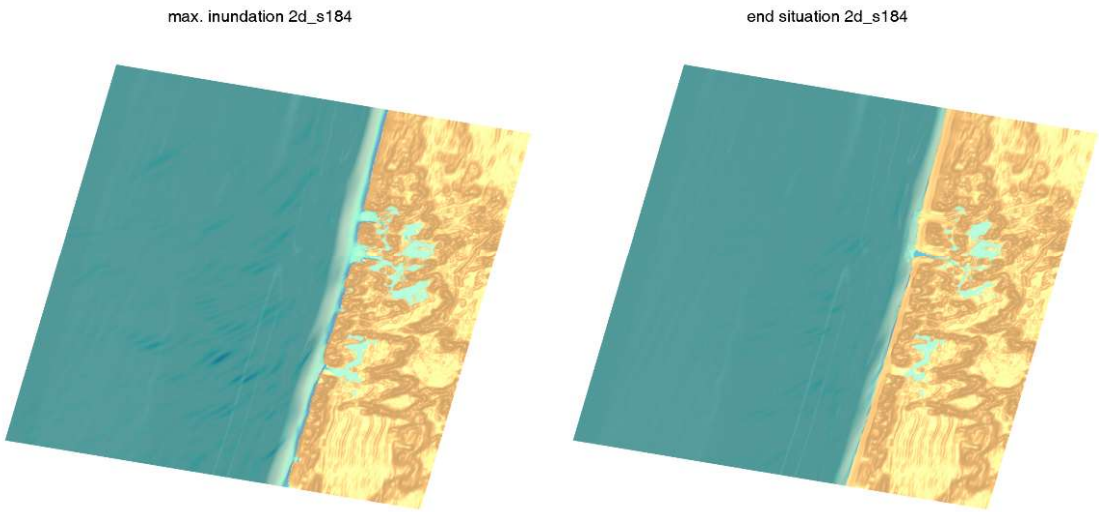

Figure 5.27 *Snapshot of water level and bed elevation for sample 184; after 20.50 hours (left panel) and after 29.75 hours (right panel).*

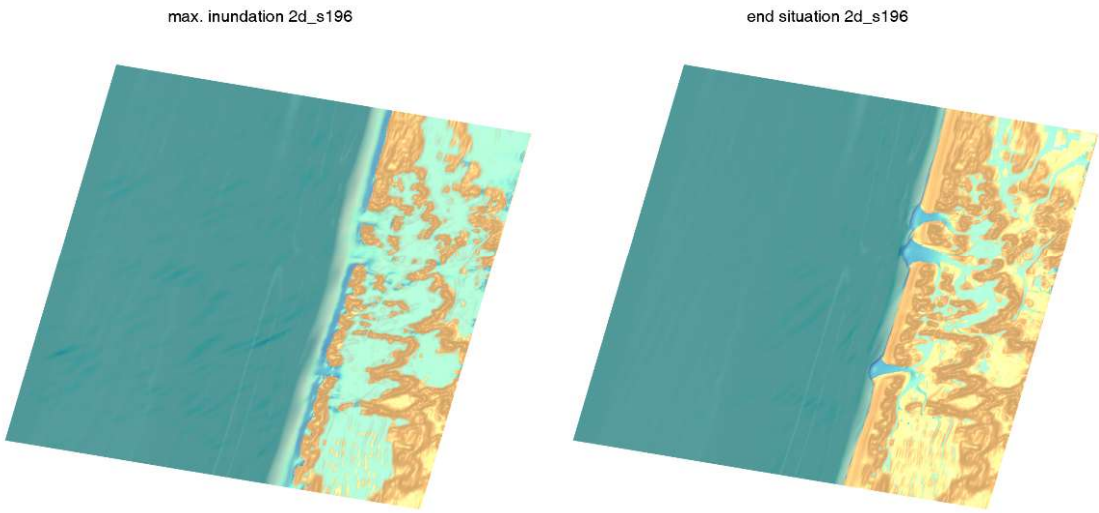

Figure 5.28 *Snapshot of water level and bed elevation for sample 196; after 30.25 hours (left panel) and after 44.25 hours (right panel).*

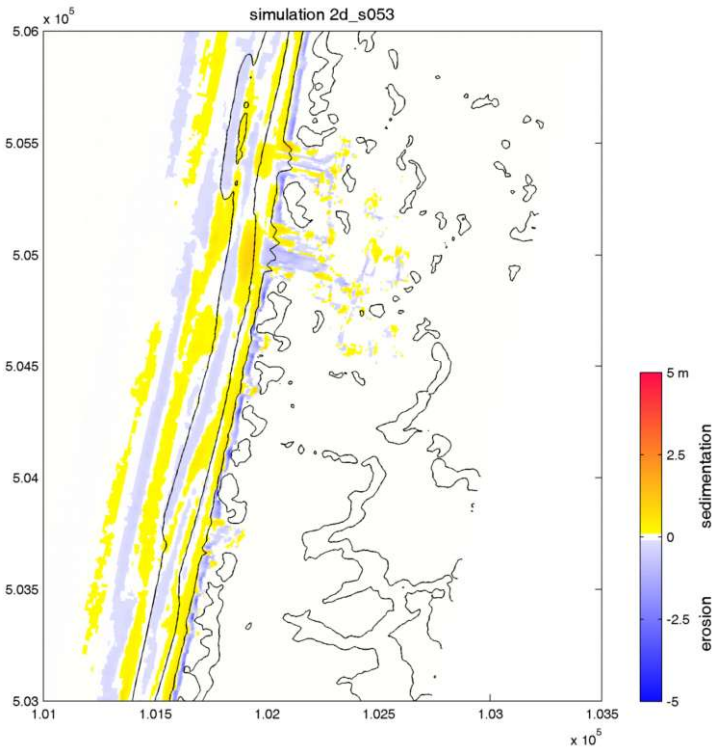

Figure 5.29 *Simulated sedimentation and erosion at the end of the simulation for sample 053.*

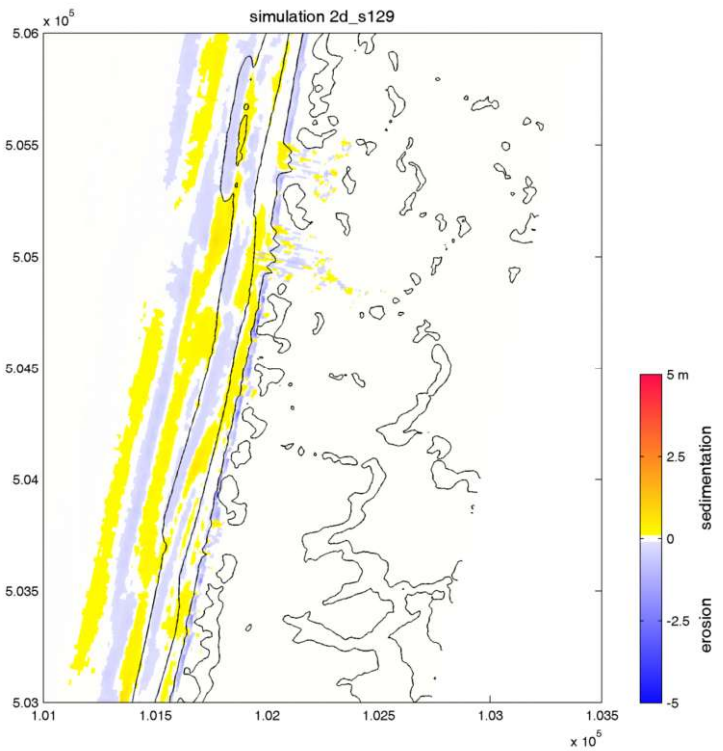

Figure 5.30 *Simulated sedimentation and erosion at the end of the simulation for sample 129.*

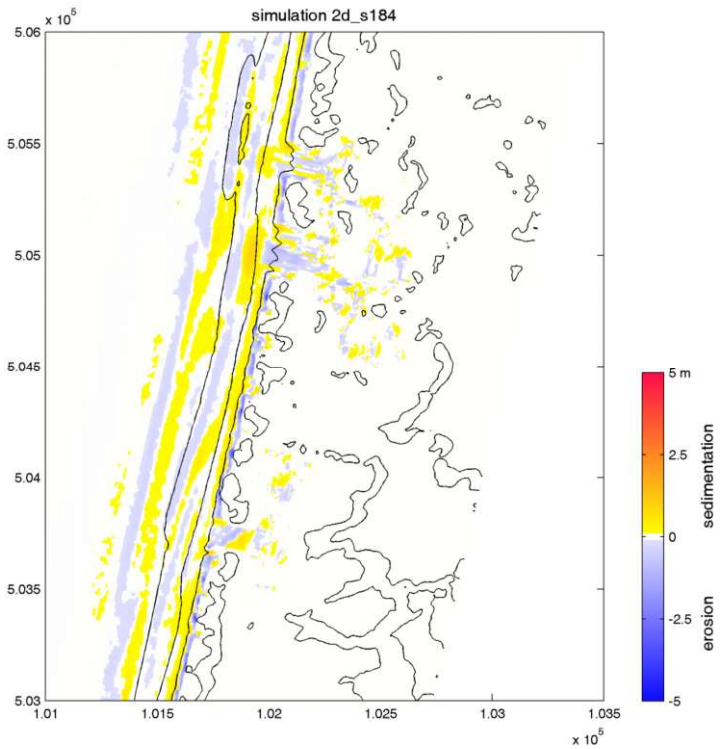

Figure 5.31 *Simulated sedimentation and erosion at the end of the simulation for sample 184.*

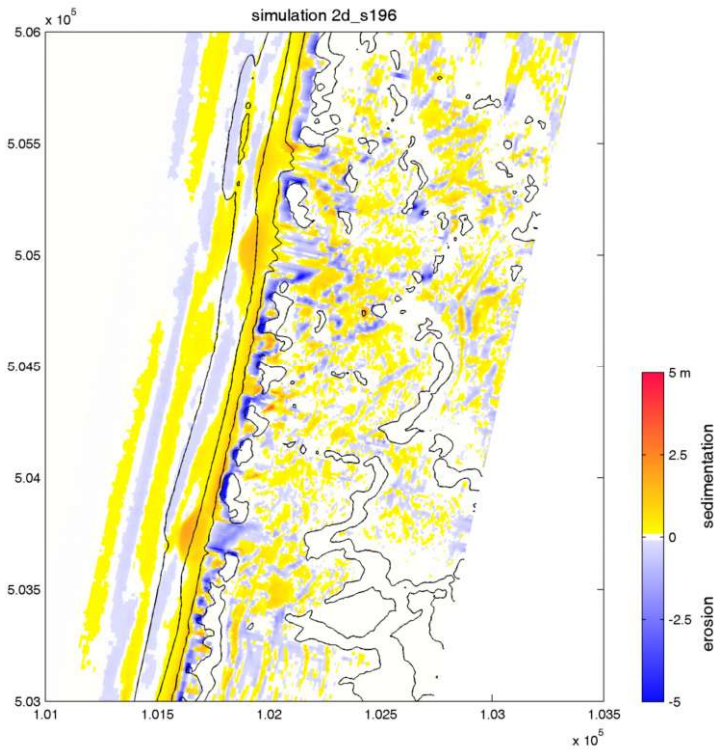

Figure 5.32 *Simulated sedimentation and erosion at the end of the simulation for sample 196.*

Table 5.4 Overview of relevant moments for nine selected samples: simulation time, start of overwash, moment of breaching of the sill and moment of maximum inundation (all times in hours).

Sample	Simulation time	Start overwash	Breaching sill	Maximum inundation
026	44.75	12.50	26.25	28.75
053	36.25	10.50	-	23.50
081	35.75	15.75	-	16.00
105	34.50	10.00	16.75	21.75
108	42.00	16.00	-	26.75
129	43.00	18.75	-	21.50
173	30.25	8.75	-	15.75
184	29.75	12.00	17.50	20.50
196	44.25	11.00	13.50	30.25

An analysis of the visualizations and the sedimentation/erosion plots shows the following:

- The sill, present at the entrance of low-lying area 1, is washed over and breached in four of the nine simulations. Although in de 1D simulations higher run-up values than the height of the sill were recorded, the wave action / energy is apparently not enough to continuously overwash the sill at the peak of the storm surge.
- Almost always an erosion channel forms at the second low-lying area (with an entrance height of NAP + 3 m).
- Water is able to penetrate into the dunes and flow around and behind dunes. This is confirmed by GPR mapping of the landward extent of the storm surge deposits (Bakker et al, in prep.). This 2D behaviour cannot be modelled with 1D profiles.
- Except for simulation 196, the inflow of water seems to be under control and stopped by the second row of dunes. Therefore, as long as there are no large gaps between those dunes, there seems no direct problem with the safety of the dunes.
- In simulation 196, water flows into the entire dune area once it reached the back side of the model. This is most likely due to a model limitation (boundary type). In ‘reality’, the inundated area would be smaller.
- Both sedimentation and erosion take place in the dune area. Erosion is dominant at the entrance of the low-lying areas; this eroded sediment is deposited at the beach. Further up the dune area, sedimentation and erosion are both present in small (net) quantities.

5.2.2 2007 topography

The boundary conditions of the same nine samples as in the section before have also been applied to the topography of 2007 (see paragraph 4.2.1). Only the deposition/erosion plots are shown for the selected four samples, because no dune breaches took place and so no notable events happened in the dune area (other occurring processes are not easily visualized). The erosion/deposition plots can be found in Figure 5.33 – Figure 5.36.

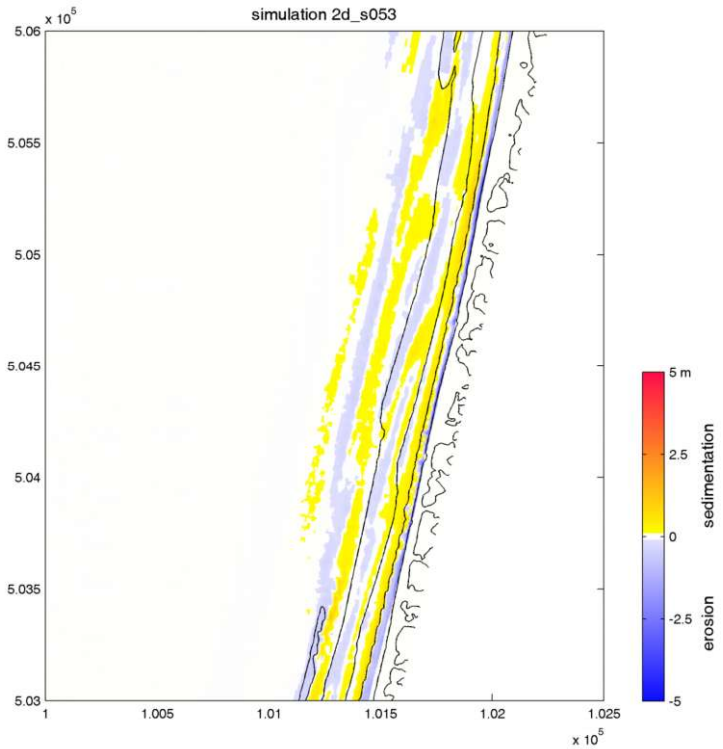

Figure 5.33 *Simulated sedimentation and erosion at the end of the simulation for sample 053 with the topography of 2007.*

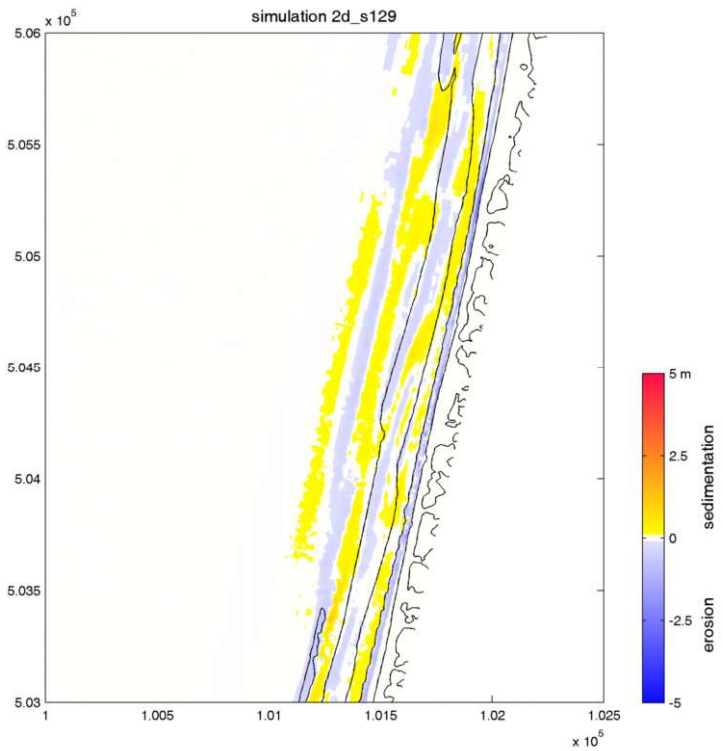

Figure 5.34 *Simulated sedimentation and erosion at the end of the simulation for sample 129 with the topography of 2007.*

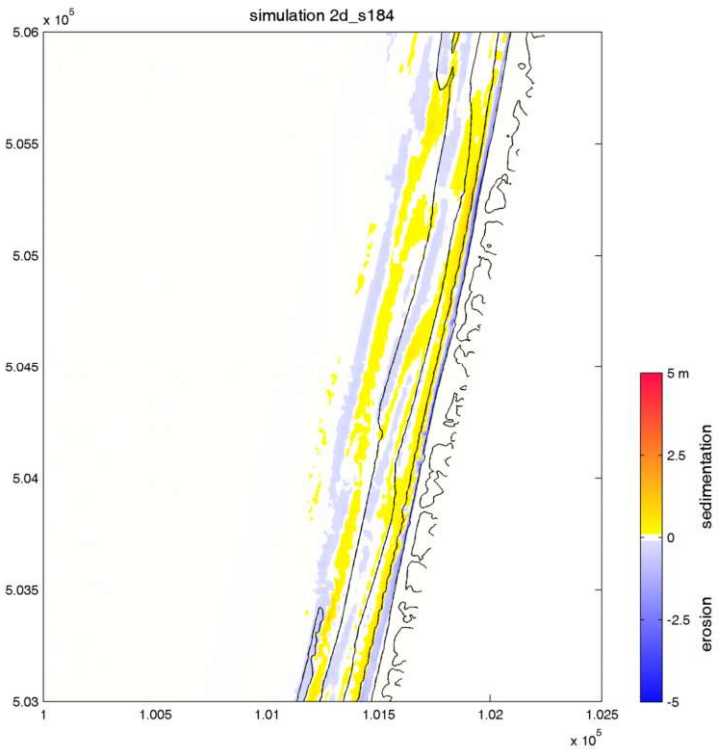

Figure 5.35 *Simulated sedimentation and erosion at the end of the simulation for sample 184 with the topography of 2007.*

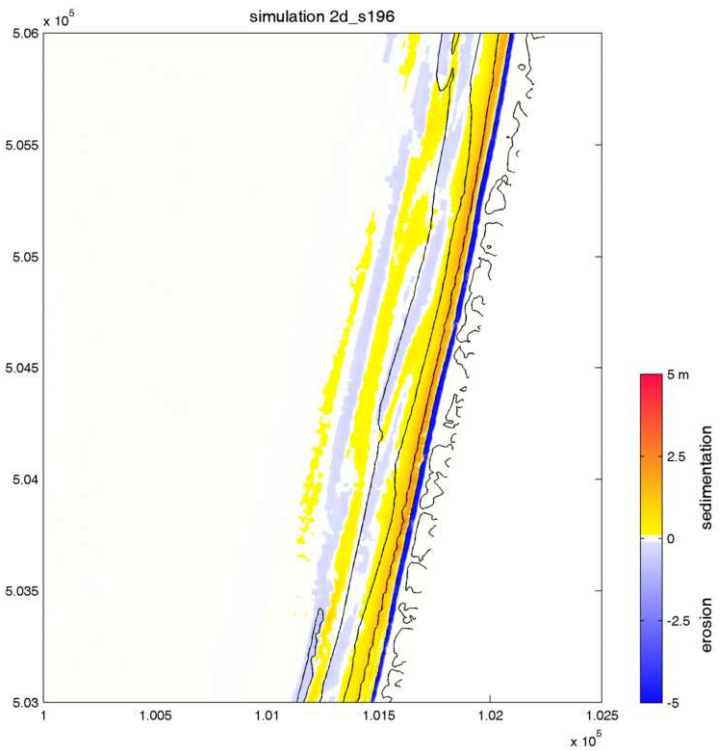

Figure 5.36 *Simulated sedimentation and erosion at the end of the simulation for sample 196 with the topography of 2007.*

A comparison of the erosion/deposition plots of both the 1775 and the 2007 topographies, shows the following phenomena:

- Both erosion and sedimentation levels are higher for the 2007 topography than for the 1775 topography when the same samples are compared. The wave action on the sand dike ('zeereep') causes high erosion rates along the entire dune system; the eroded sediment is deposited at the beach / in the nearshore zone.
- Erosion and deposition takes place along the entire dune system for the 2007 topography, while for the 1775 topography erosion and sedimentation shows more variation, with high peaks before and in the entrance to the low-lying areas.
- Bar erosion and trough infilling show comparable results for both topographies, indicating that the processes are not influenced nor disturbed by the avalanching and overwash processes.

5.3 Conclusions

Based on the results of this chapter, the following conclusions are drawn:

- The Monte Carlo analysis with 200 1D simulations lead to a distribution and a probability of reaching [6.0, 7.0] for all six profiles. The probabilities range from 2% to 11%. These values are high enough to accept the hypothesis that the 1775 storm surge reached the observed value of NAP + 6.5 m at at least one location, given the historical input data. It is common to reject an hypothesis when the probability is lower dan 5% and accept it when the probability is higher than 5%.
- The existing exceedance line for IJmuiden is the closest to the Heemskerk area. Using this exceedance line, the probability of exceedance of the 1775 storm surge is $3*10^{-4}$. This is close to the Dutch design criterion for primary flood defences.
- A regression analysis with $Z_{2\%}$ as dependent variable and the maximum water level and maximum significant wave height as independent variables show that a simple linear relation between the maximum water level and $Z_{2\%}$ gives very good results for all profiles. Therefore, this relation can certainly be used as a first estimation for the *Z2%* value without the need for running simulations.
- No good relation between the Irribarren parameter and $R_{2\%}$ could be found, although relations are known from literature. This could be due to either a lack of quasi-stationarity or the absence of such a relation for (mostly aeolian shaped) dune slopes.
- 2DH simulations with the 1775 topography show that the storm surge can easily enter the dune area through the low-lying entrances. However, the water is always stopped by the second dune row (except for a single simulation with very extreme conditions). A sill in front of one of the entrances was not as frequently breached as was expected on beforehand.
- A comparison between the 1775 topography and the 2007 topography shows that erosion of the first dune row is generally larger for the 2007 topography. The 1775 topography shows more variation and lower mean erosion values of the first dune row. The 1775 topography shows mostly deposition in the dune valleys and erosion of the low-lying entrances to the dune valleys. The depositions confirms the discovery of the storm surge deposits.

5.4 Discussion

- Modelling the transport and deposition of shells is not included in the XBeach model. Therefore the deposition (locations and heights) of shells could not be reconstructed. However, it is doubtful that it shell transport will ever be included, because modelling of shells is very difficult. Laboratory experiments and observations show that the shells doe not follow any pattern and go their own way (Pers. comm. Roelvink).
- The influence of vegetation (extra roughness and resistance to erosion) and the infiltration of water in dry sand are not included in the XBeach simulations for this study. The infiltration and ground water flow have been implemented in XBeach and could therefore be incorporated in further study. The influence of vegetation should be implemented in XBeach.
- Regarding the probabilistic 1D approach, it is not necessary that the $Z_{2\%}$ value is NAP + 6.5 m for all profiles, because the observed shell layers were only found up to NAP + 6.5 m at certain places. Generally in a open, natural dune environment, depositions take place at all locations that are not under heavy erosion. The locations that are subject to erosion are the first (steep) dune slopes which are under full wave attack and the centre of the gaps to the dune valleys, where erosion channels form. But, the highest run-up levels, close to NAP + 6.5 m, in the simulations are found at the first dune slopes (profiles 1-3) and not at the low-lying areas (profiles 4-6). This suggests that even higher water levels are necessary or a different dune topography was in place in 1775.
- The probability of exceedance estimated from the exceedance lines, both from Petten-Zuid and IJmuiden, is very small and close to the Dutch design criterion for primary flood defences in highly populated areas. But if one looks at Table 2.1, the 1775 storm surge is not regarded a very large storm surge, based on historical records. It could be possible that locally in the Heemskerk dune area higher surge levels took place than at other places along the coast, but that they were not observed, because there is no village along the coast and most likely nobody was present in the Heemskerk dune area during the storm surge.

6 Conclusions and recommendations

This study investigates the influences of an historical storm on a natural dune environment. As a case study the storm of November 1775 is modelled with the aid of probabilistic methods and a process-based numerical model, because identified storm surge layers are thought to be deposited by this storm surge. The four main objectives of this study are:

1 Set up a model to run Monte Carlo simulations for the 1775 storm surge and collect as much historical data as possible to use in the model.
8 Find out if the modelled maximum water level, including set-up and wave run-up, is within the range of the discovered storm surge layers.
9 Find the most probable combination of boundary conditions and geometry that predicts the storm surge layer height at Heemskerk for the 1775 storm surge. Make an estimate for the probability of exceedance for the 1775 storm surge, in terms of water level and wave height.
10 Compare the effects of a storm on natural dunes (historical situation) with effects of a storm surge on an artificial dune row (present situation).

The conclusions of this study are found in the next paragraph. Paragraph XX gives a number of recommendations to improve this research.

6.1 Conclusions

The first objective was to set up a model, using as much historical data as possible as input, to run Monte Carlo simulations for the 1775 storm surge. A flexible modelling framework has been set up to transform all available historical data to boundary and initial conditions for the XBeach model. It is easy to change parts of this framework as other data comes available, such as air pressure fields over the North Sea or other tidal time series. The main input of the model were observed wind speeds at Huize Swanenburgh. These wind speeds seemed reliable, but it was difficult to translate this data into useable form for calculations on wind set-up and wave heights. On the other hand, tidal time series computed for Katwijk, on which the time series for Heemskerk is based, are comparable to the time series calculated by Rijkswaterstaat, which suggest a good estimation of the tidal constituents.

With the modelling framework, the mean calculated maximum storm surge water level for Heemskerk (based on 200 samples) is comparable to the recorded (observed) maximum storm surge level at Petten.

The second objective has been reached by performing a Monte Carlo analysis on 200 samples and using the generated boundary conditions for 1D XBeach models of six characteristic profiles. For each profile the probability is calculated that $Z_{2\%}$ is in the range [6.0, 7.0] (m + NAP). For all profiles, the probability was between 2% and 11%. This does not seem large, but the values are large enough not to reject the hypothesis.

Using simple and multiple linear regression techniques, linear relations between $Z_{2\%}$ and the maximum storm surge level / H_{m0} have been established. With these relations, quick estimations of the peak run-up level can be made.

The third objective was to make an estimation for the probability of exceedance. Using the exceedance line of IJmuiden, this probability is calculated at $3*10^{-4}$. This is rather close to the Dutch design criterion for the primary flood defences.

The fourth objective is to compare the results of a storm on a natural dune system and on an artificial system with a sand dike ('zeereep'). The most obvious difference is of course the possibility with a natural dune system that the surge can enter the dune area behind the first dunes through low-lying areas/gaps. However, the fact that the surge can enter the dunes easily does not make it an unsafe situation. Energy is quickly dissipated and the water is almost always stopped by the second dune row (only in one extreme situation a larger area got flooded).

It is observed that the natural dune system experiences less erosion than the system with the human-maintained sand dike. Possible causes are gentler slopes of the natural dunes, such that less avalanching takes place and the possibility for the surge to enter the area between the dunes and bringing sediment into the dune system instead of removing sediment from it. A second effect of the low-lying areas is that the wave energy is dissipated over a larger area instead of only at the beach and the first dune row.

6.2 Recommendations

To improve the reliability and accuracy of the modelling framework, it is recommended to use air pressure data from various locations around the North Sea (see paragraph 2.3.1) to reconstruct the air pressure field of the 1775 storm instead of the wind force estimated at Huize Swanenburgh. These estimated wind forces turned out to be not of much use for the purpose of this study. With an air pressure field in space and time, more detailed wind speeds and surface drags can be computed. These can serve as improved input for the Weenink model used in this study or as input for other numerical models (WaveWatch III, SWAN and/or Delft3D) which then can generated boundary conditions for the XBeach model.

An other area where the results of the modelling framework could be improved, is the use of 2DH models in the probabilistic Monte Carlo analysis. Longshore effects, oblique incident waves and water penetration around dunes are not taken into account in the 1D Monte Carlo simulations, but in the 2DH models they can be taken into account.

To improve the understanding of the processes in a dune valley that is flooded, it is recommended to study a number of idealized dune valleys of different widths, e.g. 20 – 200 m wide and different shapes. In this way, the difference in wave run-up, wave penetration, water infiltration, etc. can be studied in more detail. As forcing boundary conditions, different water levels and significant wave heights should be used. With this study, it is also possible to study the effect of the removal of the artificial sand dike ('zeereep') and the creation of natural dunes in more detail.

To describe the physical processes involved in dune overwash and infiltration better, more processes should be taken into account or improved in XBeach or the model. It is recommended to improve or add the following features:

- The possibility to force oblique incident waves in 1D models. This will give lower, more realistic values of e.g. wave run-up in 1D cases.
- The influence of water infiltration in the dune sand and the ground water level in the dunes. Dune sand is very porous, which makes it easy for the sea water to infiltrate the

sand in a flooded valley and flow back to the sea (it would not flow down a lot because of high ground water levels in the dunes). As a result, water levels in the valley decrease quickly after a storm surge. At this stage, a ground water module has been implemented in XBeach, but it has not been used for this study.

- The influence of vegetation. Vegetation such as marram grass, sand sedge, etc will cause more flow resistance and resistance against erosion. This last effect will also cause dunes slopes to steepen beyond their angle of repose and slump in large packets when oversaturated.

This study only considered the 1775 storm surge. From records and literature, it is known that in 1776 also a storm surge with the same order of magnitude hit the Netherlands. Most dune areas probably were still not fully recovered from the damage of the 1775 storm surge, so the 1776 surge entered a weakened dune area. It is recommended to run simulations of the 1776 storm surge with the end situations of the 1775 simulations of this study to investigate the effect of two surges after each other in a small time span.

A final recommendation would be to conduct a case study to validate the numerical model. A suitable example location is ‘De Kerf’ an area in Noord-Holland where water enters during very high floods and storm surges. The topography of the area could be measured (with LIDAR for example) just before and after the storm. Boundary condition data is available from the KNMI and Rijkswaterstaat, so it would be relatively easy to model the storm surge accurately and to try to reproduce the results of the storm surge with XBeach.

6.3 Closure

This study shows the possibilities of a multidisciplinary approach in modelling and understanding historical events. It combines field observations with historical data – observations, literature, painting – and numerical modelling. Hopefully this report could be a starting point in the discussion about the future of our dunes and their management. This study shows that it is possible to allow for a more dynamical dune management, where surges can enter the dune area, for dune areas that are wide enough, without sacrificing the safety of the primary sea defences.

7 Literature

Bakker, M.; van Heteren, S.; van der Valk, L.; van der Spek, A. & Oost, A. (in prep.), 'GPR Imaging of historical storm-surge deposits in the coastal dunes of the Netherlands'.

Battjes, J. (1974), Surf similarity, *in* 'Proceedings of the 14th Conference on Coastal Engineering', pp. 466–480.

Bergström, H. & Moberg, A. (2002), 'Daily Air Temperature and Pressure Series for Uppsala (1722–1998)', *Climatic Change* **53**(1), 213–252.

Boer, P. de (1979), 'Convolute lamination in modern sands of the estuary of the Oosterschelde, the Netherlands, formed as the result of entrapped air', *Sedimentology* **26**(2), 283–294.

Breugem, W. A. & Holthuijsen, L. H. (2007), 'Generalized Shallow Water Wave Growth from Lake George', *Journal of Waterway, Port, Coastal, and Ocean Engineering* **133**(3), 173–182.

Buisman, J. (1984), *Bar en boos: Zeven eeuwen winterweer in de Lage Landen*, Bosch & Keuning, Baarn, the Netherlands, chapter 1, pp. 166–171. (Dutch)

Buisman, J. (2006), *Duizend jaar weer wind en water in de Lage Landen, deel 5*, Vol. 5, Uitgeverij Van Wijnen, Franeker. (Dutch)

Buisman, J. (in prep.), *Duizend jaar weer wind en water in de Lage Landen, deel 6*, Vol. 6, Uitgeverij Van Wijnen, Franeker. (Dutch)

Charnock, H. (1955), 'Wind stress on a water surface', *Quarterly Journal of the Royal Meteorological Society* **81**(350), 639–640.

Cunningham, A.; Wallinga, J.; van Heteren, S.; Bakker, M.; van der Valk, B.; Oost, A. & van der Spek, A. (2009), Optically stimulated luminescence dating of storm surge sediments: a test case from the Netherlands, *in* J. Wallinga & J. Storms, eds., NCL Symposium Series, Volume 6, Netherlands Centre for Luminescence dating, Delft, pp. 1–2.

CUR. (1997), *Probabilities in Civil Engineering, Part 1: Probabilistic Design in Theory*, Stichting CUR, Gouda.

Deltacommissie & Koninklijk Nederlands Meteorologisch Instituut (1961), *Rapport Deltacommissie. Deel 2. Bijdragen 1: Meteorologische en oceanografische aspecten van stormvloeden op de Nederlandse kust*, Staatsdrukkerij en Uitgeverijbedrijf, ’s-Gravenhage. (Dutch)

Gelder, P. H. A. J. M. van (1996), 'A new statistical model for extreme water levels along the Dutch coast', *in* Kevin S. Tickle & Ian C. Goulter, eds.,'Stochastic Hydraulics '96', Taylor & Francis, Mackay, Queensland, Australia, 243–251.

Gerritsen, H.; De Vries, H. & Philippart, M. (1995), The Dutch Continental Shelf Model, *in* D.R. Lynch & A.M. Davies, eds., 'Quantitative Skill Assessment for Coastal Ocean Models', Vol. 47, American Geophysical Union, Washington, DC, pp. 425–467.

Geurts, H. A. M. & Van Engelen, A. F. V. (1992), 'Beschrijving antieke meetreeksen'(165-V), Technical report, KNMI. (Dutch)

Gottschalk, M. (1971-1977), *Storm surges and river floods in the Netherlands (3 parts)*, Van Gorcum, Amsterdam.

Haaren, H. van (2005), 'Validity of method de Haan for wind speed and set-up', Master's thesis, Delft University of Technology.

Haartsen, T.; Ligtendag, W. & Steenhuisen, F. (1997), 'Historische reconstructie dieptelijnen Nederlandse kust (Project KUST*2000)', Technical report, Arctisch Centrum, Rijksuniversiteit Groningen. (Dutch)

Heteren, S.van; Bakker, M.; Cunningham, A.; Wallinga, J.; Oost, A.; Van der Spek, A. & Van der Valk, B. (2008), 'Superstormvloedlagen in de zeereep bij Heemskerk', *Grondboor & Hamer* **Jaargang 62**(3/4), 82–85. (Dutch)

Hollebrandse, F. (2005), 'Temporal development of the tidal range in the southern North Sea', Master's thesis, Delft University of Technology.

Holman, R. A. (1986), 'Extreme value statistics for wave run-up on a natural beach', *Coastal Engineering* **9**(6), 527–544.

Holthuijsen, L. H. (2007), *Waves in oceanic and coastal waters*, Cambridge University Press, Cambridge.

Jelgersma, S.; Stive, M. J. F. & Van der Valk, L. (1995), 'Holocene storm surge signatures in the coastal dunes of the western Netherlands', *Marine Geology* **125**(1-2), 95–110.

Jensen, J.; Hofstede, L.; Kunz, H.; De Ronde, J.; Heinen, P. & Siefert, W. (1993), Long Term Water Level Observations and Variations, *in* R. Hillen & H.J. Verhagen, eds., 'Coastlines of the Southern North Sea', ASCE, New Orleans, Louisiana, pp. 110–130.

Jonkers, A. (1989), 'Over den schrikkelijken watervloed: Een onderzoek naar hoge waterstanden vóór 1825', Technical report, Ministry of Transport, Public Works and Water Management. (Dutch)

KNMI (2008), 'Antieke Reeksen' (online). (Accessed 18-02-2009), available from: http://www.knmi.nl/klimatologie/daggegevens/antieke_wrn/index.html. (Dutch)

KNMI (2007), 'Europa doeltreffend gewaarschuwd voor herfststorm' (online). (Accessed 2008-10-30), available from: http://www.knmi.nl/VinkCMS/news_detail.jsp?id=39475. (Dutch)

KNMI (2004), 'Drie eeuwen weer op internet' (online). (Accessed 18-02-2009), available from: http://www.knmi.nl/VinkCMS/news_detail.jsp?id=24219. (Dutch)

Ledden, M. van; Westra, M.; Groeneweg, J.; Wenneker, I. & Scholl, O. (2005), 'SWAN berekeningen ten behoeve van HR2006 voor de Hollandse Kust Rapportage Fase 1'(9P8603.A0/R0002/MVLED/SEP/Nijm), Technical report, Royal Haskoning. (Dutch)

Leffler, K. E. & Jay, D. A. (2009), 'Enhancing tidal harmonic analysis: Robust (hybrid L1/L2) solutions', *Continental Shelf Research* **29**(1), 78–88.

Lesser, G.; Roelvink, J.; van Kester, J. & Stelling, G. (2004), 'Development and validation of a three-dimensional morphological model', *Coastal Engineering* **51**(8-9), 883–915.

Lindström, M. (1979), 'Storm surge turbation', *Sedimentology* **26**(1), 115–124.

Malde, J. van (2003), *Historische Stormvloedstanden*, Aqua Systems International, Poeldijk. (Dutch)

McCall, R. (2008), 'The longshore dimension in dune overwash modelling: development, verification and validation of XBeach', Master's thesis, Delft University of Technology.

Moberg, A.; Bergström, H.; Ruiz Krigsman, J. & Svanered, O. (2002), 'Daily Air Temperature and Pressure Series for Stockholm (1756–1998)', *Climatic Change* **53**(1), 171–212.

Pawlowicz, R.; Beardsley, B. & Lentz, S. (2002), 'Classical tidal harmonic analysis including error estimates in MATLAB using T_TIDE', *Computers & Geosciences* **28**(8), 929–937.

Peña, A. & Gryning, S.-E. (2008), 'Charnock's Roughness Length Model and Non-dimensional Wind Profiles Over the Sea', *Boundary-Layer Meteorology* **128**(2), 191–203.

Philippart, M.; Dillingh, D. & Pwa, S. (1995), 'De basispeilen langs de Nederlandse kustDe ruimtelijke verdeling en overschrijdingslijnen'(RIKZ-95.008), Technical report, Rijksinstituut voor Kust en Zee/RIKZ. (Dutch)

Roelvink, J.; Reniers, A.; van Dongeren, A.; van Thiel de Vries, J.; R., M. & Lescinski, J. (accepted), 'Modeling storm impacts on beaches, dunes and barrier islands', *Coastal Engineering*.

Roelvink, J.; Van der Kaaij, T. & Ruessink, B. (2001), 'Calibration and verification of large-scale 2D/3D flow models, Phase I', Technical report, WL | Delft Hydraulics.

Steijn; R., Ormondt, M. van.; Onderwater, M. & Dongeren, A. van (2008), 'Veiligheidsaspecten project H&U Zeereep; Veiligheidsaspecten van mogelijke herstelscenario's van overslaggronden op de Nederlandse Waddeneilanden'(A1995), Technical report, Alkyon / WL|Delft Hydraulics. (Dutch)

Stockdon, H.; Holman, R.; Howd, P. & Sallenger, Jr., A. (2006), 'Empirical parameterization of setup, swash, and runup', *Coastal Engineering* **53**(7), 573–588.

Thiel de Vries, J.van; van Gent, M.; Walstra, D. & Reniers, A. (2008), 'Analysis of dune erosion processes in large-scale flume experiments', *Coastal Engineering* **55**(12), 1028–1040.

Vertegaal, C.; Arens, S.; Brugge, B.; Groenedaal, M.; ten Haaf, C. & Wondergem, H. (2003), 'Evaluatie "de Kerf" 1997-2002', Technical report, Vertegaal Ecologisch Advies en Onderzoek. (Dutch)

Vrijling, J. & Bruinsma, J. (1980), Hydraulic Boundary Conditions, *in* A. Paape; J. Stulp & W.A. Venis, eds.,'Hydraulic aspects of coastal structures: Developments in hydraulic engineering related to the design of the Oosterschelde Storm Surge Barrier in the Netherlands', Delft University Press, Delft, Netherlands, pp. 109–132.

Waghenaer, L. (1964), *Spieghel der zeevaert*, Van Leer, Amsterdam.

Weenink, M. (1957), 'A theory and method of calculation of wind effects on sea levels in a partly enclosed sea, with special application to the southern coast of the North Sea.', PhD thesis, Utrecht University.

Weerden, J. van; Janssen, J. & Vrijling, J. (1987), 'Effekt variatie opzetduren op de hoogwaterstanden in het Noordelijk Deltabekken'(DBW/RIZA nota 87.054), Technical report, Rijkswaterstaat. (Dutch)

Wieringa, J. (1996), 'Does representative wind information exist?', *Journal of Wind Engineering and Industrial Aerodynamics* **65**(1-3), 1–12.

Wieringa, J. & Rijkoort, P. (1983), *Windklimaat van Nederland*, Vol. 2, Staatsuitgeverij and Koninklijk Nederlands Meteorologisch Instituut, Den Haag and De Bilt. (Dutch)

Woodworth, P. L. (2006), 'The meteorological data of William Hutchinson and a Liverpool air pressure time series spanning 1768-1999', *International Journal of Climatology* **26**(12), 1713–1726.

Young, I. R. & Verhagen, L. A. (1996), 'The growth of fetch limited waves in water of finite depth. Part 1. Total energy and peak frequency', *Coastal Engineering* **29**(1-2), 47–78.

Glossary

Term	Description
AHN	Actueel Hoogtebestand Nederland; actual digital elevation model of the Netherlands
artificial dune	human-maintained foredune with minimum height of NAP + 11 m
blending height	height above which local obstacles do not influence wind speed; usually taken 60 m above earth surface
meso wind	wind speed at blending height
Monte Carlo method	method of probabilistic simulation / analysis which involves drawing a large number of random samples of all variables to calculate the reliability function
natural dune	open foredune in historical situation that is not maintained by human, but aeolian shaped with alternating large dunes and low entrances to dune valleys
NAP	Normaal Amsterdams Peil; Dutch vertical reference level
RD (grid)	Rijksdriehoek grid; official Dutch coordinate system

A XBeach parameter settings

This appendix gives an overview of the general settings (params.txt) used for the various XBeach simulations.

A.1 Calibration run: November 2007storm surge (1D / 2D)

Parameter	Value	Units	Description
Grid input			
nx	400 / 281	-	number of grid cells in x-direction
ny	2 / 292	-	number of grid cells in y-direction
vardx	1	-	option of variable grid size
xfile	*variable*	-	name of the variable grid size file in x-direction
yfile	*variable*	-	name of the variable grid size file in y-direction
xori	98299.30	m	x-origin in world coordinates
yori	502032.93	m	y-origin in world coordinates
alfa	-12.50	degrees	grid angle in world coordinates
depfile	*variable*	-	bathymetry file
posdwn	-1	-	depth definition positive up / down
General constants			
rho	1025	kg/m^3	mass density of water
g	9.81	m/s^2	gravitational acceleration
Wave discretisation			
thetamin	-180 / -100	degrees	lower directional limit (angle w.r.t. x-axis)
thetamax	180 / 20	degrees	upper directional limit (angle w.r.t. x-axis)
dtheta	360 / 15	degrees	directional resolution
Numerics input			
CFL	0.8	-	maximum courant number
eps	*variable*	m	threshold depth for drying and flooding
scheme	2[1]	-	numerical scheme for wave action balance
Boundary condition options			
tideloc	1	-	number of tidal time series (locations) to use
tidelen	235	-	length of tidal record
zs0file	wl10071108.txt	-	file containing tidal time series
instat	41	-	type of wave boundary condition
bcfile	*variable*	-	file containing wave boundary coefficients
back	1	-	bayside boundary condition (1 = wall)
left	1 / 0	-	left lateral boundary condition (1 = wall)
right	1 / 0	-	right lateral boundary condition (1 = wall)
Wave calculation options			
hmin	0.01	m	threshold water depth for concentration and return flow
wci	0	-	switch for wave current interaction
break	1	-	option breaker model (1 = roelvink)
gammax	*variable*	-	maximum ratio Hrms/hh
smax	-1	-	maximum shields value for overwash
Flow calculation options			
C	60	$m^{0.5}/s$	Chezy coefficient

1. *Some of the first runs where done with setting scheme = 1*

umin	0.1	m/s	threshold velocity
nuh	0.1	m^2/s	horizontal background viscosity
nuhfac	1	-	viscosity coefficient for roller induced turbulent horizontal viscosity
Time input			
tstart	0	s	start time of simulation
tint	1800	s	time interval output variables
tintm	1800	s	time interval output mean variables
tstop	135900	s	stop time simulation
Sediment transport calculation options			
dico	1	m^2/s	diffusion coefficient
D50	0.0002	m	D50 grain diameter of sediment
D90	0.00025	m	D90 grain diameter of sediment
Morphological calculation options			
morfac	5 / 10	-	morphological factor

A.2 November 1775 storm surge (1D/2D runs)

Parameter	Value	Units	Description
Grid input			
nx	453	-	number of grid cells in x-direction
ny	2 / 292	-	number of grid cells in y-direction
vardx	1	-	option of variable grid size
xfile	*variable*	-	name of the variable grid size file in x-direction
yfile	*variable*	-	name of the variable grid size file in y-direction
xori	98767	m	x-origin in world coordinates
yori	502653	m	y-origin in world coordinates
alfa	-12.50	degrees	grid angle in world coordinates
depfile	*variable*	-	bathymetry file
posdwn	-1	-	depth definition positive up / down
General constants			
rho	1025	kg/m^3	mass density of water
g	9.81	m/s^2	gravitational acceleration
Wave discretisation			
thetamin	-180 / -100	degrees	lower directional limit (angle w.r.t. x-axis)
thetamax	180 / 20	degrees	upper directional limit (angle w.r.t. x-axis)
dtheta	360 / 15	degrees	directional resolution
Numerics input			
CFL	0.7	-	maximum courant number
eps	0.001	m	threshold depth for drying and flooding
scheme	2[2]	-	numerical scheme for wave action balance
Boundary condition options			
order	2		order of wave steering at seaward boundary
front	1		seaward boundary condition
back	0	-	bayside boundary condition (0 = Neumann)
left	1 / 0	-	left lateral boundary condition (1 = wall)
right	1 / 0	-	right lateral boundary condition (1 = wall)
tideloc	1	-	number of tidal time series (locations) to use

2. *Some of the first runs where done with setting scheme = 1*

tidelen	*variable*	-	length of tidal record
zs0file	*variable*	-	file containing tidal time series
instat	41	-	type of wave boundary condition
bcfile	*variable*	-	file containing wave boundary coefficients
Wave calculation options			
break	1	-	option breaker model (1 = roelvink)
wci	0	-	switch for wave current interaction
roller	1	-	option roller model
gamma	0.55	-	breaker parameter in Baldock or Roelvink formulation
gammax	2	-	maximum ratio Hrms/hh
alpha	1		wave dissipation coefficient
n	10		power in Roelvink dissipation model
smax	1	-	maximum shields value for overwash
Flow calculation options			
nuh	0.1	m^2/s	horizontal background viscosity
nuhfac	1	-	viscosity coefficient for roller induced turbulent horizontal viscosity
hmin	0.05	m	threshold water depth for concentration and return flow
C	65	$m^{0.5}/s$	Chezy coefficient
umin	0.0	m/s	threshold velocity
hswitch	0.1	m	water depth at interface from wetslp to dryslp
Time input			
tstart	4800	s	start time of simulation
tintg	900	s	time interval output variables
tintm	1800	s	time interval output mean variables
tintp	10	s	time interval point output
tstop	*variable*	s	stop time simulation
taper	300	s	time to spin up wave boundary conditions
Sediment transport calculation options			
dico	1	m^2/s	diffusion coefficient
D50	0.00021	m	D50 grain diameter of sediment
D90	0.00028	m	D90 grain diameter of sediment
rhos	2650	kg/m^3	density of sediment
z0	0.006	m	zero flow velocity level in Soulsby van Rijn (1997) sediment concentration expression
facsl	1.6	-	bed slope factor
tsfac	0.1	-	max value for fall velocity
Morphological calculation options			
morfac	10	-	morphological factor
morstart	4800	s	start time of morphological updates
por	0.4	-	porosity
dryslp	1.0	-	critical avalanching slope above water
wetslp	0.3	-	critical avalanching slope under water
nspr	1	-	set directional spreading long waves (1 = bin all incoming long wave directions (instat 4+) in the centres of the short wave directional grid cells)
facua	1		

B BestFit results

BestFit® 1.01a is used to determine the best fitting distribution to the 200 $Z_{2\%}$ values of the 1D XBeach simulations. This is done for each one of the 6 profiles. Each data set is tested with 15 classes (bins) against 6 possible distributions:

- Erlang (a special case of the Gamma distribution)
- Gamma
- Lognormal
- Lognormal2 (a special case of the Lognormal distribution)
- Normal
- Weibull

As the lognormal and lognormal2 distributions almost use the same parameters, their test values are usually equal. This is considered in determining the best fit. The goodness-of-fit of each distribution is tested with all 3 available tests. The selection of the 'best fitting' distribution is based on a comparison and judgement of all 3 tests:

- χ^2-test
- Kolmogorov-Smirov test (K-S test)
- Anderson-Darling test (a modification of the K-S test that gives more weight to the tails of the distribution)

For all tests, lower values indicate better fits.

B.1 Profile 1

Function			χ^2-test		K-S test		A-D test	
Name	a	b	Value	Rank	Value	Rank	Value	Rank
Lognormal2	1.43	0.30	0.04649	1	0.029129	2	0.121436	1
Lognormal	4.39	1.35	0.04649	2	0.029129	3	0.121436	2
Erlang	10	0.44	0.048665	3	0.039221	4	0.347426	4
Gamma	10.84	0.41	0.054324	4	0.029014	1	0.218896	3
Weibull	3.32	4.85	0.140834	5	0.0751	6	1.986876	6
Normal	4.39	1.33	0.183551	6	0.061595	5	1.565897	5

B.2 Profile 2

Function			χ^2-test		K-S test		A-D test	
Name	a	b	Value	Rank	Value	Rank	Value	Rank
Lognormal	4.36	1.29	0.05256	1	0.037007	3	0.17672	1
Lognormal2	1.43	0.29	0.05256	2	0.037007	2	0.17672	2
Erlang	11	0.40	0.052807	3	0.03576	1	0.418259	4
Gamma	11.91	0.37	0.055923	4	0.038698	4	0.33223	3
Weibull	3.51	4.80	0.120771	5	0.071195	6	2.099586	6
Normal	4.36	1.26	0.131493	6	0.057207	5	1.709036	5

B.3 Profile 3

Function			χ^2-test		K-S test		A-D test	
Name	**a**	**b**	**Value**	**Rank**	**Value**	**Rank**	**Value**	**Rank**
Lognormal2	1.42	0.32	0.078623	1	0.046887	1	0.558185	1
Lognormal	4.35	1.45	0.078623	2	0.046887	2	0.558185	2
Erlang	9	0.48	0.079693	3	0.053305	4	0.705134	3
Gamma	9.28	0.47	0.081471	4	0.052175	3	0.721738	4
Weibull	3.14	4.83	0.128595	5	0.090517	6	2.235652	5
Normal	4.34	1.43	0.157985	6	0.086661	5	2.458662	6

B.4 Profile 4

Function			χ^2-test		K-S test		A-D test	
Name	**a**	**b**	**Value**	**Rank**	**Value**	**Rank**	**Value**	**Rank**
Erlang	14	0.31	0.32037	1	0.136023	3	2.476716	2
Gamma	14.20	0.30	0.320385	2	0.136185	4	2.476268	1
Lognormal2	1.42	0.27	0.331729	3	0.116532	1	2.903081	5
Lognormal	4.28	1.18	0.331729	4	0.116532	2	2.903081	4
Weibull	3.70	4.68	0.509746	5	0.159831	6	4.116171	6
Normal	4.28	1.14	0.528166	6	0.143513	5	2.531535	3

B.5 Profile 5

Function			χ^2-test		K-S test		A-D test	
Name	**a**	**b**	**Value**	**Rank**	**Value**	**Rank**	**Value**	**Rank**
Lognormal2	1.34	0.29	0.585834	1	0.151846	5	4.794592	3
Lognormal	3.98	1.20	0.585834	2	0.151846	4	4.794592	4
Gamma	10.64	0.37	0.62655	3	0.141545	2	4.526956	2
Erlang	10	0.40	0.628367	4	0.13239	1	4.427065	1
Normal	3.66	1.41	0.787715	5	0.21357	6	9.952883	6
Weibull	3.18	4.39	0.793219	6	0.148466	3	5.633109	5

B.6 Profile 6

Function			χ^2-test		K-S test		A-D test	
Name	**a**	**b**	**Value**	**Rank**	**Value**	**Rank**	**Value**	**Rank**
Gamma	13.37	0.32	0.155003	1	0.073859	2	0.589389	1
Erlang	13	0.33	0.1554	2	0.075779	3	0.615281	2
Lognormal2	1.41	0.28	0.171436	3	0.090915	5	0.778632	3
Lognormal	4.24	1.16	0.171436	4	0.090915	6	0.778632	4
Normal	4.24	1.16	0.215797	5	0.068091	1	1.197879	5
Weibull	3.69	4.65	0.236225	6	0.077058	4	2.070102	6

C Running XBeach on Deltares cluster

This section describes the two processes involved in running parallel (multiple processes) XBeach simulations on the Deltares computation cluster using MPI (Message Passing Interface): compiling a Linux executable from the XBeach source code and submitting a job file to the grid engine.

C.1 Compiling XBeach executable

1 Log on to the Linux development server.
2 Start a Terminal session (Applications > System Tools > Terminal).
3 Make a directory "checkouts":
`mkdir ~/checkouts`
4 Checkout the latest and greatest version of XBeach (enter your Deltares password if asked for):
`svn co https://repos.deltares.nl/repos/XBeach/trunk /checkouts/XBeach`
5 If you already have the local repository, but want to update it, use:
`svn update`
6 Go to the XBeach directory:
`cd ~/checkouts/XBeach`
7 Edit Makefile to use the Intel Fortran compiler:
`gedit Makefile`
8 On line 146, change "F90:=gfortran" to "F90:=ifort" (without quotation marks)
9 Save Makefile
10 Make sure version 10 of the Intel Fortran compiler is used (instead of version 8): `. /opt/intel/fc/10/bin/ifortvars.sh`
11 Delete all files not needed for compiling to get rid of files that could mess it up:
`make realclean`
12 Compile the parallel version:
`PATH=/opt/mpich2-1.0.7/bin:$PATH USEMPI=yes make install`
13 (optional) Copy the executable to your personal bin-folder:
`cd ~/bin`
`cp ~/checkouts/bin/xbeach.mpi .`

C.2 Run XBeach parallel version on the cluster

1 Place the XBeach simulation somewhere on a network drive (home or project share).
2 Log on to the cluster (h3 or h4) with SSH (secure shell). Under Windows, use the program PuTTy for that.
3 Make sure the Grid Engine environment is loaded:
`. /opt/sge/InitSGE`
4 Create the following job file (with a text editor):

```
#!/bin/sh

. /opt/sge/InitSGE
export PATH="/opt/mpich2/bin:$PATH"
echo "numslots: $DELTAQ_NumSlots"
```

```
echo "nodes: $DELTAQ_NodeList"
echo  $DELTAQ_NodeList  |  tr  '  '  '\n'  |  sed  's/.wldelft.nl//'  >
machines
echo "Machines file:"
cat machines
mpdboot -1 -n $DELTAQ_NumSlots -f machines
mpirun -np $DELTAQ_NumSlots ~/bin/xbeach.mpi
mpdallexit
```

Save the file as xbeach.sh.
The second last line should contain the path to xbeach.mpi. Edit this if you have placed it somewhere else.

5 Go to the XBeach simulation directory and start the simulation with:

on H3

```
qsub -pe spread N /path-to-job-file/xbeach.sh
```

on H4

```
qsub -pe distrib N /path-to-job-file/xbeach.sh
```

Where *N* is the number of parallel processes you want to start.